QUANTIFYING THE DISTRIBUTION OF FOREST FUNCTIONAL TYPES AND FOREST LEAF AREA INDEX IN THE ALPS

Dissertation
Zur Erlangung der Doktorwürde
an der Fakultät für
Biologie, Chemie und Geowissenschaften
der Universität Bayreuth

vorgelegt von
Albena Bobeva
aus Sofia, Bulgarien

Bayreuth, Oktober 2003

Die vorliegende Arbeit wurde von April 2001 bis Oktober 2003 am Lehrstuhl für Pflanzenökologie unter Leitung von Prof. Dr. J.D. Tenhunen angefertigt.

Vollständiger Abdruck der von der Fakultät für Biologie, Chemie und Geowissenschaften der Universität Bayreuth genehmigten Dissertation zur Erlangung des akademischen Grades eines Doktors der Naturwissenschaften (Dr. rer. nat.)

Promotionsgesuch eingereicht am: 21.10.2003
Tag des wissenschaftlichen Kolloquiums: 08.12.2003
Erster Gutachter: Prof. Dr. J.D. Tenhunen
Zweiter Gutachter: Prof. Dr. E. Parlow (Universität Basel)

CONTENTS

I. INTRODUCTION

1. Background

1.1. Land cover interpretation and classification

Land cover is one of the most important characteristics of the land surface, from both an environmental and a societal perspective. It is an important element of global environmental change processes; a key factor influencing earth system processes such as biogeochemical cycles, the annual cycles and spatial distribution of vegetation, vegetation biomass, and respiration; and in the next 100 years, is likely to be the most significant variable impacting biodiversity (Friedl M.A. et al., 1997; Dickinson R.E., 1995; Hall et al., 1995; Sellers and Schimel, 1993; Chapin et al., 2000; Foody G. M., 2002). Most ecosystem processes depend strongly on land cover and its attributes. The reality of global change, i.e., the accelerated changes in land cover, and in key biogeochemical processes that heavily depend on land cover, has increased interest in land cover characteristics and in the observation of spatial and temporal dynamics in land cover. Satellite observations have become the major source of obtaining data. The strengths of land cover classifications developed from satellite remotely-sensed data include large area coverage, repetitive coverage of earth's land surfaces, multispectral data acquisition, access to data related to past conditions, and the ability to consistently apply standardized classification techniques (Cihlar J. et. al., 2003a).

An important application of land-cover information (thematic maps) is the inference of parameters that influence biophysical processes and energy exchange between the atmosphere and the land surface, as required by regional and global-scale climate and ecosystem process models (Townshend et al., 1991). Examples of such parameters for climate modeling include leaf area index (LAI), surface resistance to evapotranspiration, canopy greenness fraction, vegetation density distribution, and fraction of photosynthetically-active radiation absorbed (FPAR) (Sellers, 1991a, 1991b). Examples of ecosystem process model parameters for which land cover type may serve as a surrogate include leaf photosynthetic capacity, canopy conductance, type of

photosynthetic system, and maximum photosynthetic rate (Running and Coughlan, 1988; Strahler A., 1996).

1.2. Leaf Area Index (LAI)

Leaf Area Index (LAI) defines an important structural property of a plant canopy, the number of equivalent layers of leaves the vegetation displays relative to unit ground area. Because LAI most directly quantifies plant canopy structure, it is related to a variety of canopy processes. Leaf area index is a key biophysical variable influencing land surface photosynthesis (Bonan et al., 1993), respiration, transpiration, leaf litterfall and energy balance (Running S. W., 1992). Hence, LAI is used by terrestrial models to quantify the above ecosystem processes. Mapped LAI values provide a description of the spatial pattern of forest structure and have served as inputs to functional models of ecosystem biogeochemistry (Running and Gower, 1991). Many ecosystem models have been developed to be sensitive to and driven by LAI (Running and Coughlan, 1988; Running and Hunt, 1993; Liu et al., 1997).

Leaf area index (LAI) is a quantitative measure of foliage density used for monitoring vegetation status (Cayrol et al., 2000; Waring and Running, 2000) and modelling fluxes of water (Band et al., 1991; Nouvellon et al., 2000), energy (Sellers et al., 1986; Bonan, 1995), and greenhouse gases (Liu et al., 1997; Nouvellon et al., 2000; Coops et. al., 2001; Frank, 2002) between the atmosphere and the land surface. Estimating LAI over large areas, however, is difficult. Direct measures of canopy structure are extremely labor-intensive, rendering their use beyond the stand level impractical (Fassnacht, 1997). Satellite remote sensing provides a unique way to obtain the distributions of LAI over large areas. LAI is "the single variable which may be derived from remote platforms that is of greatest importance for quantifying energy and mass exchange by plant canopies over landscapes" (Running, 1986).

LAI can be estimated using algorithms applied to satellite imagery, with ground-based measurements of LAI being required for calibration and validation. A variety of spectral vegetation indices derived from satellite remote sensing have been used to map leaf area index. LAI is one surface parameter that is routinely derived from remote sensing

measurements. Validation of LAI maps, however, is a daunting and challenging task and surface heterogeneity must be considered.

2. Current state of research

2.1. Studies on land cover classification and extrapolation

Remote sensing is an attractive source of thematic maps, such as those depicting land cover. With the help of other ancillary sources (digital elevation models, topographic maps, field surveys, etc.) remote sensing has been used successfully in mapping a range of land covers at a variety of spatial and temporal scales. Thematic mapping from remote sensing data is typically based on image classification. There are numerous studies related to land cover classification at various spatial scales (Loveland and Belward, 1997; DeFries et al., 1998; Hansen et al., 2000; Loveland et al., 1995; 2000; Cihlar et al., 1999, 2000; Cihlar J. et al., 2003a; Dorren L. et al., 2003; Marcus, 2003).

Different algorithms are available for land cover classification, each having its own limitations and applicability in different environments (Shrestha and Alfred, 2001). Widely used are minimum distance, parallelepiped and maximum likelihood (Richards, 1994). The most important of them is maximum likelihood classifier and it was used in numerous studies. (Keuchel et al., 2003; Shrestha and Alfred, 2001; Swain and Davis, 1978; Estes et al., 1983; Schowengerdt, 1983; Sabins, 1986; Lillesand and Kiefer, 2000; Jensen, 1996) In classification of multispectral data, the maximum likelihood classifier is considered to provide the best results, since it is based on the class mean and the variance-covariance matrix, where an unknown pixel is assigned to the most likely class.

Remote sensing data are almost essential in mapping land surface/cover, especially in mountain areas where accessibility is limited. There the supervised classification of land cover, however, is very difficult because of variations in the sun illumination angle. The spectral reflectance of vegetation varies with aspect and elevation gradient, with topographic effects having greatest influence in rugged mountain areas. Several studies show the advantages of topographic correction of reflection data based on digital elevation models (DEMs) for classification in steep mountainous terrain (Parlow, 1991; Parlow, 1996a; Imbery et al., 2001; Shrestha and Alfred, 2001; Itten et al., 1991, 1992a,

1992b, 1995; Dorren et al., 2003; Stolz et al., 1999). Applying remote sensing in mountainous areas not only provides its classical benefits in total, quick, accurate and relatively cheap coverage, but also it serves to promote new studies in inaccessible or difficult terrain. Otherwise, the most often applied methods for assessing structure in mountain forests are inventory methods, which are seldom used for spatial assessments over large areas (Bebi, et al., 2001).

Remotely sensed data have been widely used for assisting in vegetation mapping in the last few years and have proved an effective tool. They offer the possibility of extrapolating mapping results, especially in large and hardly accessible remote areas (Kalliola and Syrjänen, 1991;). Muller et al., 1999 express the importance of being able to extrapolate, or scale up, from relatively small, well-known sites, to broader regions.

2.2. Studies on mapping LAI using remote sensing data (Landsat satellite data)

Airborne and satellite remote sensing data have been used to estimate LAI based on relationships between remote sensing data and LAI measurements obtained from the field (White et al., 1997; Peddle et al., 1999; Peddle and Johnson, 2000; Johnson, 2000). Empirical models are important tools for relating field measured biophysical variables, such as LAI to remote sensing data. Empirical approaches are primarily based on relationships between LAI and vegetation indices (Tucker and Sellers, 1986; Peterson et. al, 1987;Verma et. al, 1993). Among the various vegetation indices, the Normalized Difference Vegetation Index (NDVI) and the Simple Ratio (SR) are most frequently used to derive LAI from remote sensing data. (Chen and Cihlar, 1996; Myneni et. al., 1994; Sellers et. al., 1993). NDVI and SR can be directly linked to biophysical parameters, such as leaf area index, amount of green leaf biomass, amount of photosynthetic material, etc. Studies have compared field LAI values with satellite sensor data at various spatial scales (Spanner et al., 1990; Curran et al., 1992; Chen et al. 2002; Gemmell F.M., 1995; Hall et al 2003) Remote sensing of LAI was first tested with Landsat TM data because the 30 m pixel size represents an area small enough to be directly measured on the ground. Numerous studies have been done to relate vegetation indices to LAI of coniferous forests (Wang, 2003; Chen and Cihlar, 1996; Running et. al. 1986; Nemani et.al. 1993;

Curran et.al. 1992), or of mixed and deciduous forests (Fassnacht et.al. 1997; Eklundh et.al. 2003; Chen et. al. 2002) using Landsat satellite data.

Different relationships have been derived (refer to appendix A). Considering the various regression models used to estimate LAI from vegetation indices as derived from Landsat data and reported in the literature, one can see that the regression models are highly site-specific. They depend on the climate, physiography, substrates, altitude and vegetation at investigated sites. They are also influenced by the differences in LAI field measurement methods and the atmospheric correction of the satellite image (Running et. al., 1986). A variety of methods exist for ground-based and remote estimation of LAI and this can lead to confusion and uncertainty regarding selection of methods, experimental design, and instrumentation (Hall, 2003). Most of methods for ground-based LAI measurements reported in the literature are based on allometry of simple physical dimensions, such as stem diameter at breast height vs. LAI, using species-specific or stand-specific relationships based on detailed destructive measurement of a sub-sample of leaves, branches, or whole individuals (Turner et al., 1999; Fassnacht et.al. 1997; Peterson et al., 1987; Curran et al., 1992; Running et al. 1986; Nemani et al., 1993; White, 1997). There is no uniform relationship between vegetation indices and field measured LAI for all investigated sites. The derived regression models can only be generalized to other regions with extreme care, and there are definite limitations in the geographic extent to which extrapolations may be carried out.

3. Aims of this study

The purpose of the preceding paragraphs was to emphasize the importance of land cover and LAI in ecosystem structure and functions. The necessity of obtaining spatial data, especially in mountain areas where accessibility is limited stimulate the use of satellite data for assisting classification of the land cover and vegetation interpretation in those regions. Therefore the main aims of the present investigation are to:

- classify land cover using Landsat data and to compare and validate the classification with CIR-based biotope maps from the Berchtesgaden National Park

- map LAI at 30m resolution using Landsat and forest inventory data in Berchtesgaden National Park

- describe ecosystem distribution and LAI variations along the elevation gradients within Berchtesgaden National Park

- develop an extrapolation potential for describing other test areas in the Alps where similar conditions exist (in this case in the Stubai and Ötz Valleys of Austria)

II. MATERIALS AND METHODS

1. Site description

1.1. National Park Berchtesgaden

The National Park Berchtesgaden occupies the south-eastern corner of Germany, comprising a small portion of the state of Bavaria and bordering Austria's province of Salzburg. The park was established in 1978 by a decree from the Bavarian government. It is the only alpine biosphere reserve in Germany and is situated between 12° 47' and 13°05' E and 47°27' and 47°45' N covering an area of 210 km^2 (Fig. 1).

Fig. 1: Location of National Park Berchtesgaden

Berchtesgaden National Park was declared a UNESCO Biosphere Reserve in 1990 and selected as an example of a nearly natural alpine ecosystem. The National Park is one of the oldest protected areas in the Alps and has a long tradition in research and application of Geographical Information Systems (GIS). All the maps shown for site and meteorological description of Berchtesgaden National Park are created within the project "Mapping Site Characteristics in the National Park Berchtesgaden", (Konnert V., 2001). The project was carried out between March 1, 1999 and June 30, 2001 in cooperation with the Technical University of Munich, Dept. of Ecology, the Faculty of Forest Science and Resource Management, Dept. of Geobotany (Prof. Dr. Anton Fischer), and the Administration of the National Park Berchtesgaden. The study area is a part of the Northern Limestone Alps, characterized by huge carbonate deposits of the mesozoic period. The landscape is composed of high mountains with steep and precipitous rock walls. The soil development in the national park Berchtesgaden varies as a mosaic. Rendzic soils occur frequently within the areas where dolomite decomposition occurs. Cambisol is the most frequently occurring soil type in the National Park. Cambic Podzol and Podzol are found over the radiolarian rocks. In some areas because of the influence of groundwater Stagnic Gleysol and Gley are present.

1.1.1. Climate

The study area is situated in the transition zone between atlantic and continental climatic influences. Due to the high altitude a typical mountain climate prevails. The altitude is between 601 m (Königsee) and 2713 m (the peak Watzmann) a.s.l. The average altitude is 1530 m. The altitudinal zone of 1500 to 1700 m includes the largest area of the park (Fig. 2). The most frequent expositions are those to the north. Expositions to the south (S, SSW, SSO) are least common, excepting level areas which consist mainly of the lake surfaces (Fig. 3).
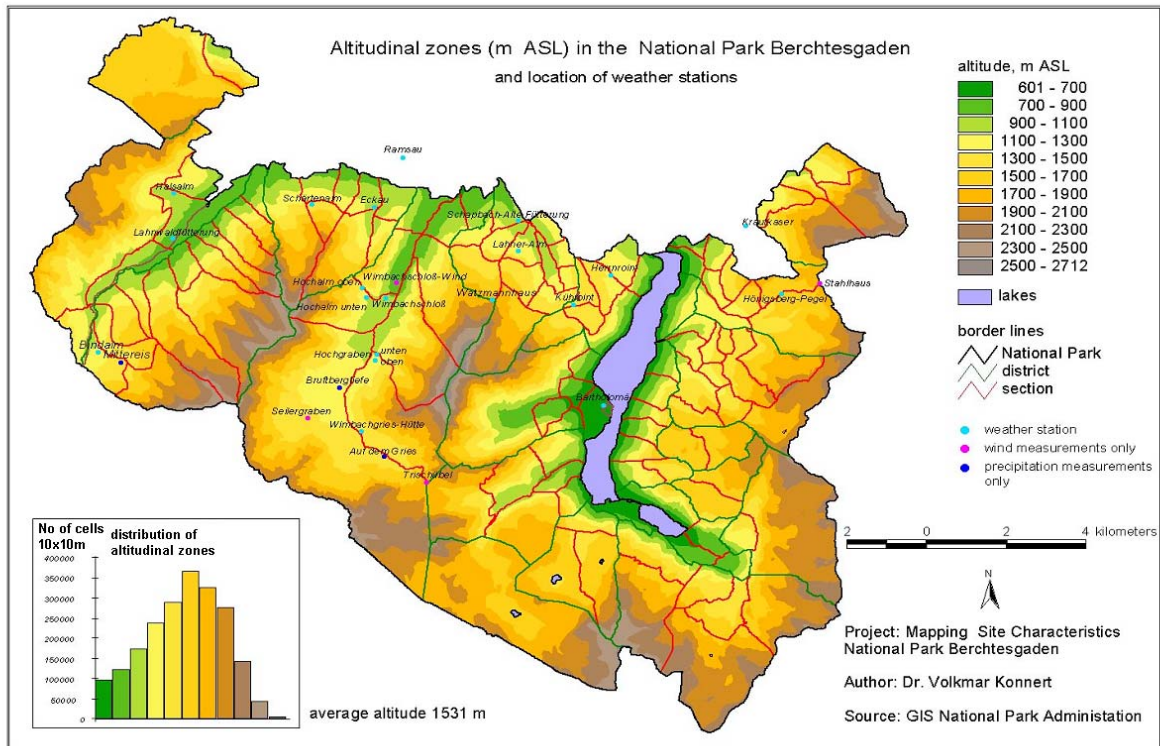
Fig. 2: Altitudinal zones in Berchtesgaden National Park (Konnert, 2001)
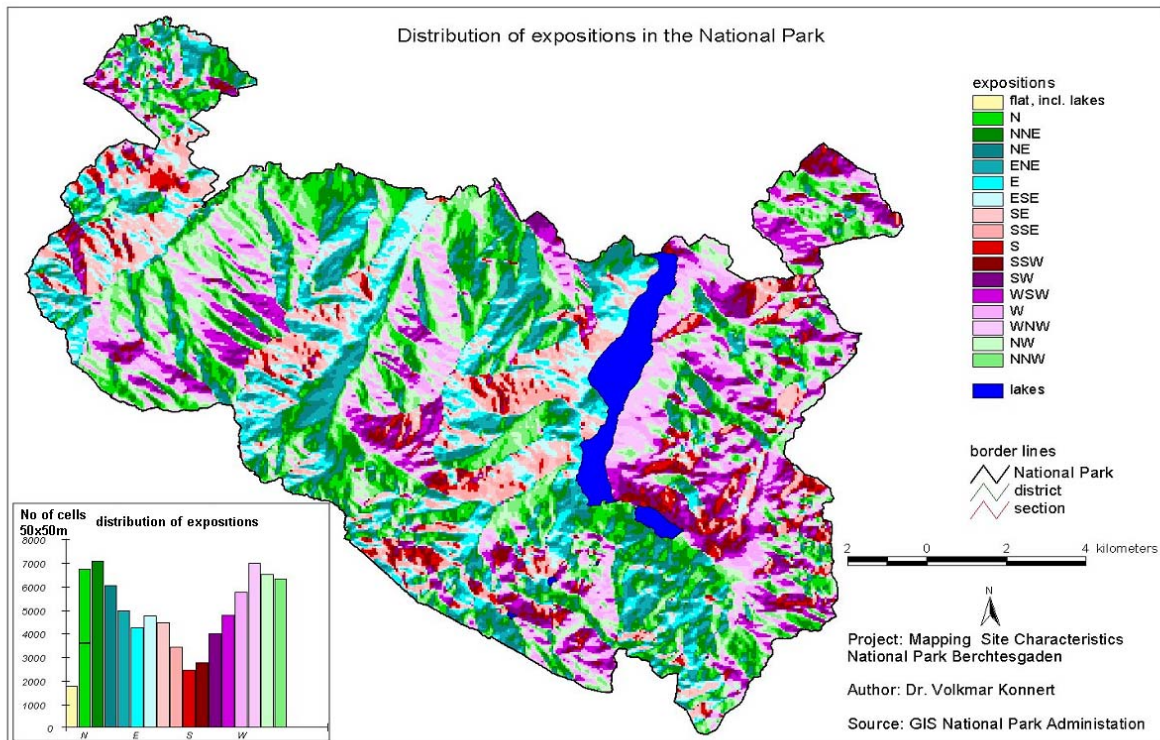
Fig. 3: Expositions in National Park Berchtesgaden (Konnert, 2001)

The relief energy of the alpine landscape of the National Park is very high. The steep, precipitous, and very precipitous slopes have much higher occurrence than other categories (Fig. 4). All existing meteorological data (temperature, precipitation and wind data) are derived from National Park network of weather stations. The mean annual temperatures range between +7°C (Königsee) and -2°C (peak Watzmann) depending on the altitude (Fig. 5). The distribution of the average temperature for months and year was calculated as a regression of the calculated average monthly or yearly temperatures of the weather stations and the parameters of the surrounding relief.

Mean value of annual precipitation is ca.1880 mm. It ranges between 1500 mm and 2200 mm (Fig. 6).
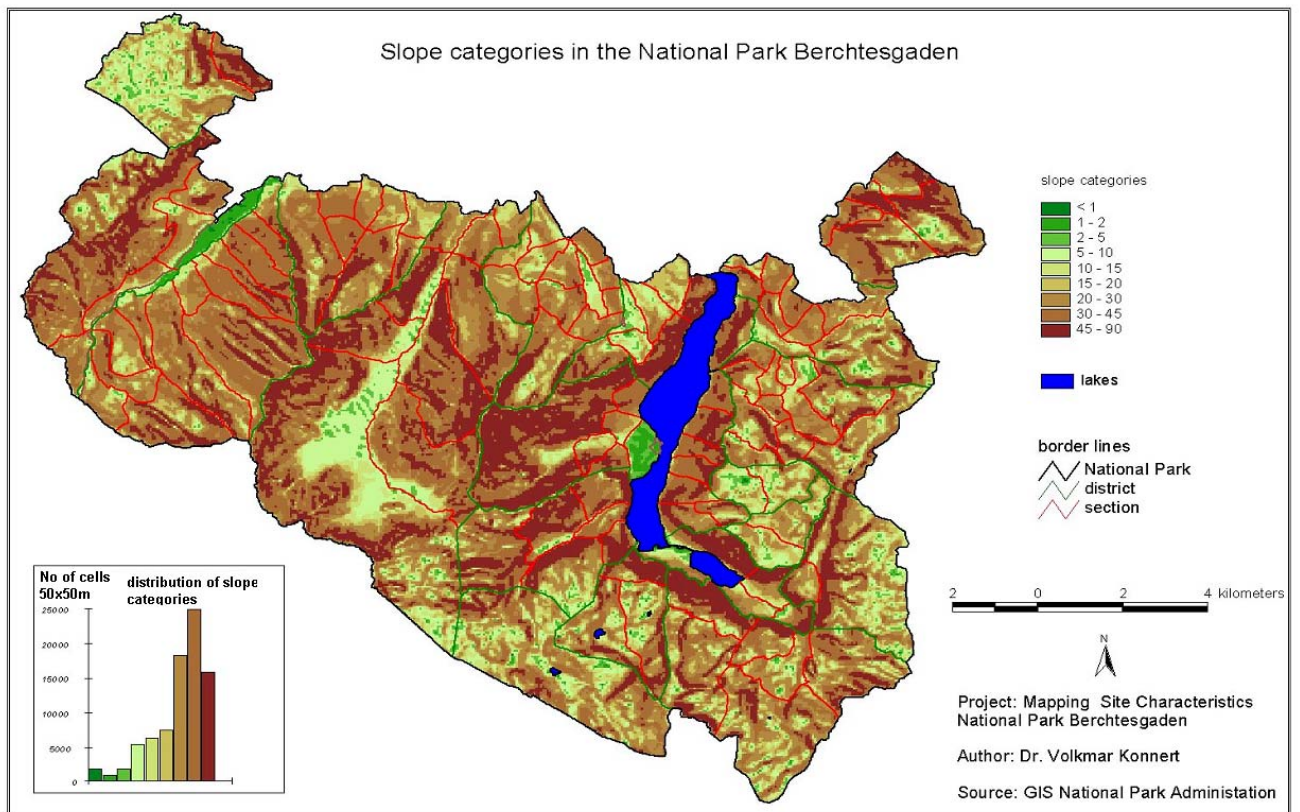
Fig. 4: Slope categories – Berchtesgaden National Park (Konnert, 2001)
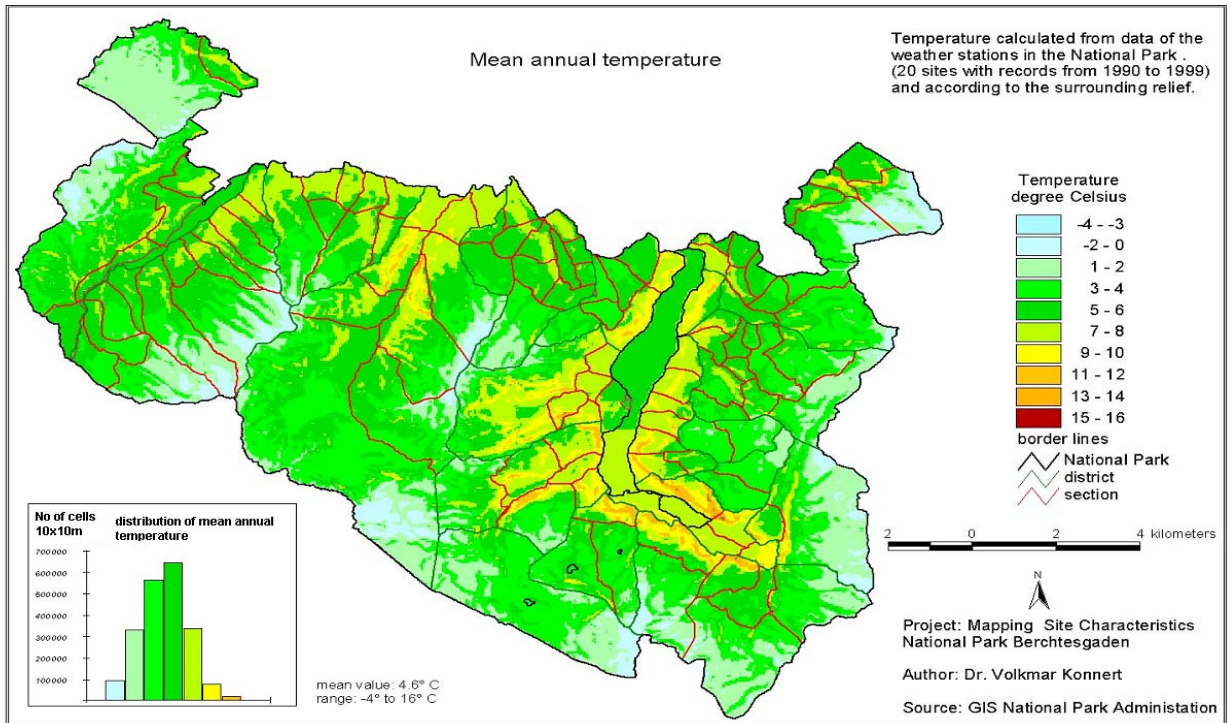
Fig. 5: Mean annual temperature (Konnert, 2001)
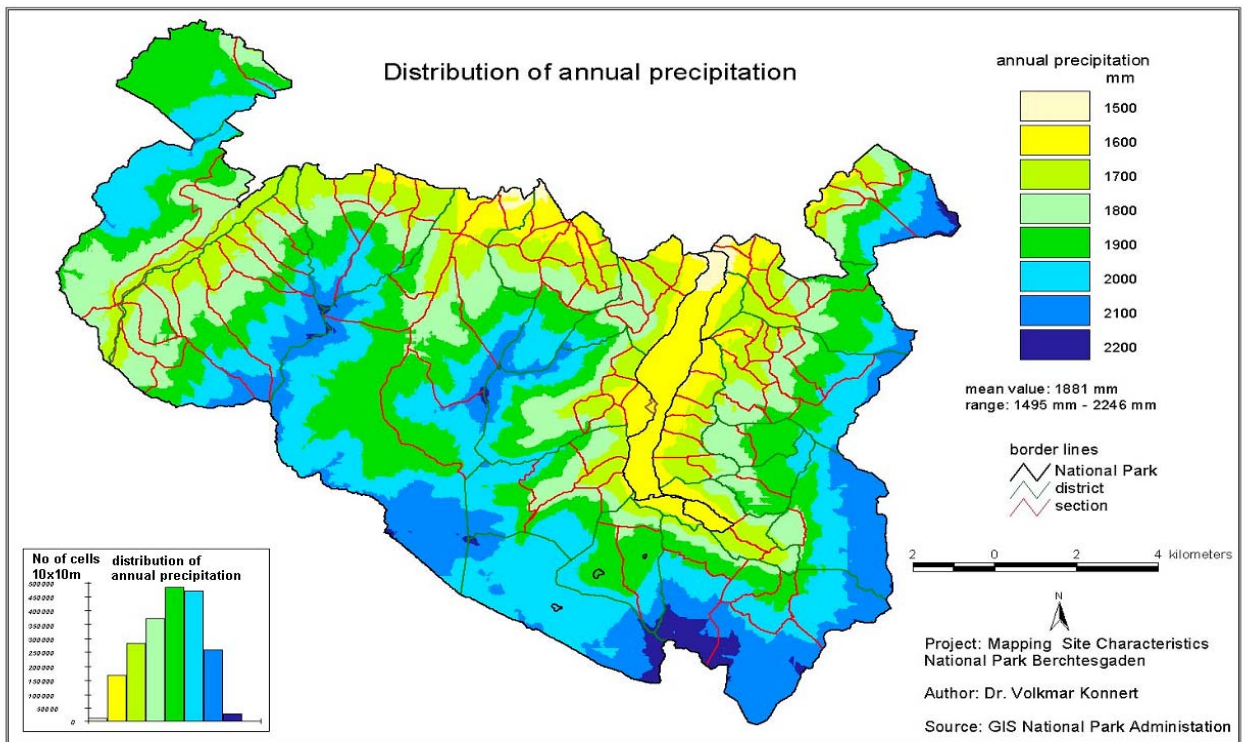
Fig. 6: Annual precipitation (Konnert, 2001)

1.1.2. Vegetation

This alpine region is characterized by a large number of diverse biotopes and vegetation zones from the lake "Königsee"(603 m) up to the peak areas of the "Watzmann" (2713 m) (Fig. 7). The highly variable climate leads to pronounced altitude zonation of the vegetation. Highly diverse forest communities have evolved due to immense differences in habitat conditions (more than 2000 m difference in altitude between peaks and valley floors).

Legend:
- Felsspalten- und Felsschuttgesellschaften
- Flachgründige alpine Rasen, Rasen- und Strauchgesellschaften der Schuttfelder
- Mittelgründige Kalk-Magerrasen
- Weiderasen (und Mähwiesen) (z. T. Brache)
- Hochstaudenfluren und Grünerlengebüsche
- Quellfluren, Sumpf- und Moorgesellschaften
- Alpenrosen- und Alpenrosen-Latschen-Gebüsche
- Grauerlen-Wälder
- Edellaubwälder und Hasel-Gebüsche
- Tannen-, Rotbuchen- und Tannenwälder der mittelmontanen Stufe
- Rotbuchen- und Tannen-Rotbuchen-Wälder der hochmontanen bis subalpinen Stufe
- Boreal-alpine Nadelwälder
- Sonstige Waldgesellschaften
- Stillgewässer
- Gletscher, Firnfelder
- keine Daten

Fig. 7: Vegetation map – National Park Berchtesgaden (after Storch, 1993)

Nearly a third of the vegetation sprouts on rock debris and in crevices. In the **submontane zone** (at 700 m a.s.l.) deciduous forests predominate. Beech forests (*Fagus sylvatica*) are well represented. *Acer pseudoplatanus* and *Fraxinus excelsior* are also found. Small areas are covered with *Ulmus glabra, Tilia platyphyllos* and *Alnus incana*. In most cases these species are distributed within the beech forests. **The montane zone** between 700 m a.s.l. and 1400 (1300) m a.s.l. is comprised of mixed forest – *Fagus sylvatica, Picea abies, Abies alba* and *Acer platanoides*. The portion of spruce forest increases on higher slopes. In many cases coniferous forest prevail, which is due to antropogenic impact and planting in past decades. In the northern part of the National Park, deciduous forest and silver fir (*Abies alba)* are missing. In the **subalpine zone** (1400 (1300) m a.s.l. – 2000 (1900) m a.s.l.) spruce-larch forests dominate – *Picea abies*

and *Larix decidua*. In some areas of the park, (Funtensee, Steinernes Meer, Blaueistal und Reiteralm) larch-alpine pine forests (*Larix decidua* with *Pinus cembra*) occur. The **alpine zone** (above 2000 (1900) m a.s.l.) is comprised of wind-dwarfed bushes and alpine meadows. *Pinus mugo, Alnus viridis* and *Rhododendron ferrugineum* are very common.

1.2. Stubai Valley

The Stubai Valley in Tirol (Austria) is a side valley of the Wipp-Valley in the Tyrolean Alps. The study area is situated at approx. 47° 07' N, 11° 17' E (Fig. 8).
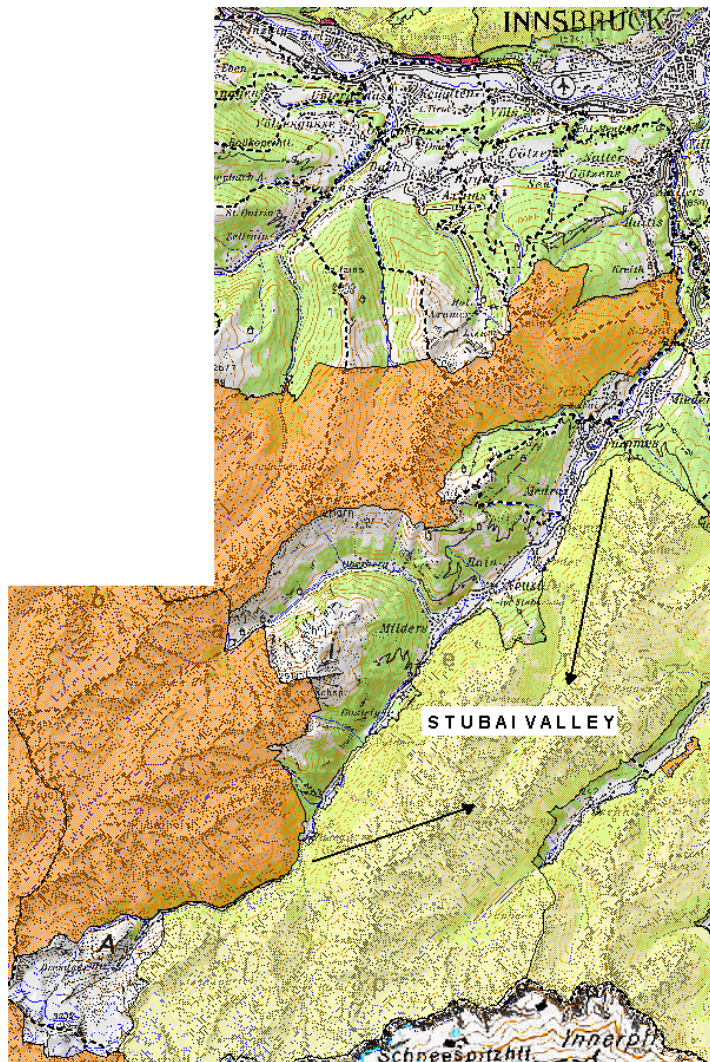
Fig. 8: Stubai Valley map (Land Tirol - www.tirol.gv.at)

1.2.1. Climate

The Stubai Valley study area is characterized by temperate continental inner alpine climate with frequent precipitation and heavy thunderstorms in the summer (Zeller V. et. al, 2000; 2001). About 50% of the annual precipitation is snow during the winter months (Cernusca A. et. al., 1999). Average air temperature and annual precipitation range from 6.3°C and 850 mm to 3.0°C and 1100 mm at the valley bottom and the treeline, respectively. Snow cover duration is approximately 100 days. The altitude is between 660 m and 3450 m. The altitudinal zones were classified (ENVI 3.4) according to the digital elevation model (DEM), which has been established trough the interpolation of digital contourlines (Fig. 9).
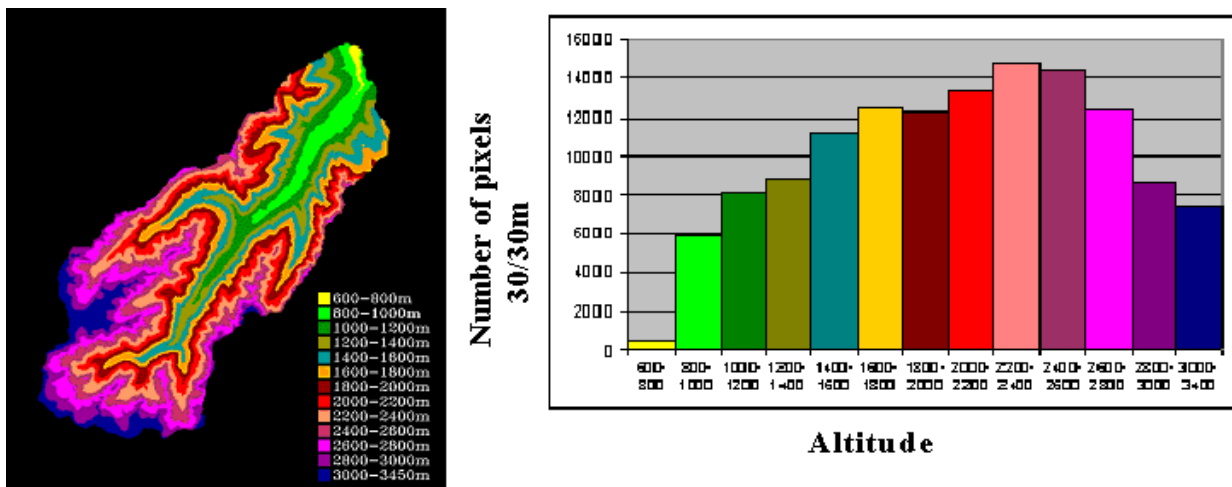
Fig. 9: Distribution of altitudinal zones in Stubai Valley (DEM obtained from Tyrolean State Government, modified by Colgan A., GLOWA DANUBE Project)

Slope for the study area was calculated using the existing Digital Elevation model. The slope map was divided further into 6 categories. The number of pixels is shown (Fig. 10).
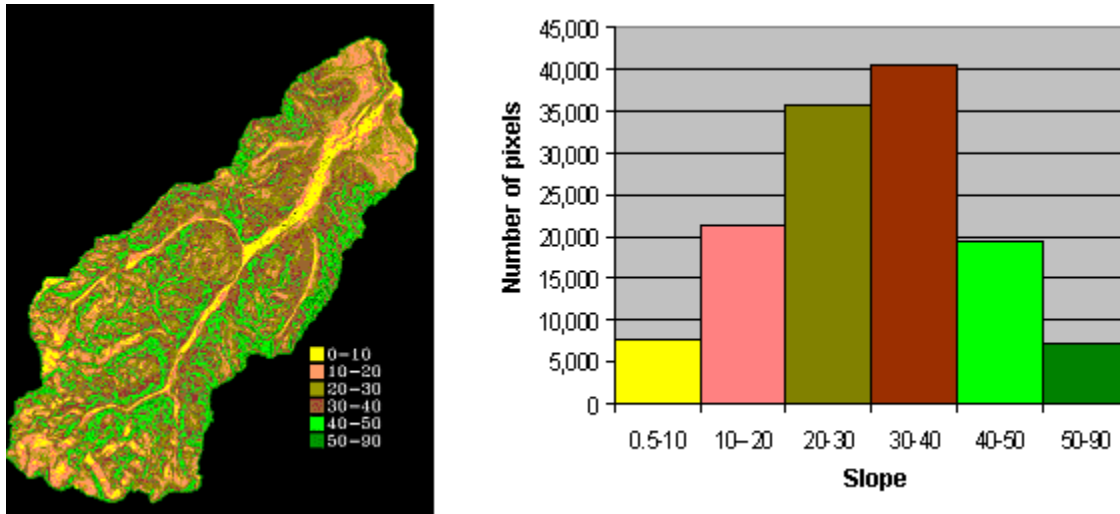
Fig. 10: Distribution of slope categories–Stubai Valley (derived from DEM in Fig. 9)

The 360°- degree exposition map was separated into 8 categories and each of them has a width of 45° (Fig. 11).
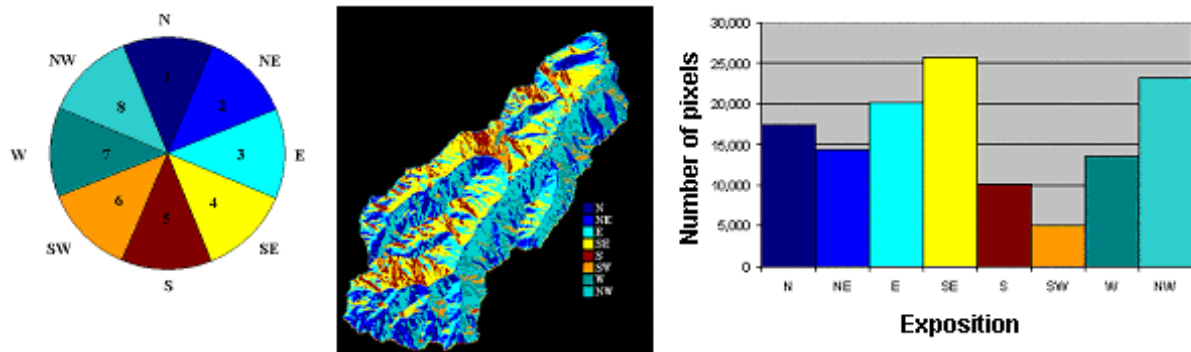
Fig. 11: Aspect separated into 8 categories and distribution of expositions – Stubai Valley (derived from DEM in Fig. 9)

1.2.2. Vegetation

Vegetation in the Stubai Valley includes alpine grasslands and subalpine coniferous forests at the highest levels, and cultivated areas at the bottom of the valley. The

vegetation can be described with following categories (ECOMONT project, Cernusca A. et al., 1999):

- Intensively managed hay meadow
- Lightly managed hay meadow
- Intensively managed pasture
- Lightly managed pasture
- Forest

Intensively managed hay meadow

The characteristic plant community of these hay meadows is *Trisetetum flavescentis*, with the dominant species *Alchemilla vulgaris, Dactylis glomerata, Leontodon hispidus, Plantago lanceolata, Geranium sylvaticum,* etc. These types of meadows are located below the alpine huts at 1850 m a.s.l.

Lightly managed hay meadow

Sieversio-Nardetum strictae is the prevailing plant community. Species typical for intensively used hay meadows are also present.

Intensively managed pasture

The pasture ranges from 1900 to 2000 m a.s.l. *Seslerio-Caricetum* is adjacent to the pasture. Dominant species are *Alchemilla millefolium, Plantago media, Ranunculus montanus, Lotus corniculatus,* etc.

Lightly managed pasture

The proportion of forage plants (*Alchemilla millefolium, Lotus corniculatus, Trifolium pratense,* etc.) has decreased. Dominant plant species such as *Calluna vulgaris, Carex montana, Sesleria varia, etc.)* are present.

Forest

The dominant trees are spruce (*Picea abies)*, interspersed with *Larix decidua* and *Pinus sylvestris.* Mixed and deciduous forests are not well represented. They cover a small part of the investigated area. Some broad-leaved trees such as *Sorbus aucuparia, Salix sp.* and *Alnus viridis* are found. A land use (ground truth) map, which includes a vegetation description for part of the region, was created. It will be discussed in the chapter IV.

1.3. Ötz Valley

The Ötz Valley is situated in the Central Alps (about 46.8 degree north latitude, 10.70 degrees east longitude) at the border between Switzerland, Italy and Austria (Fig. 12).
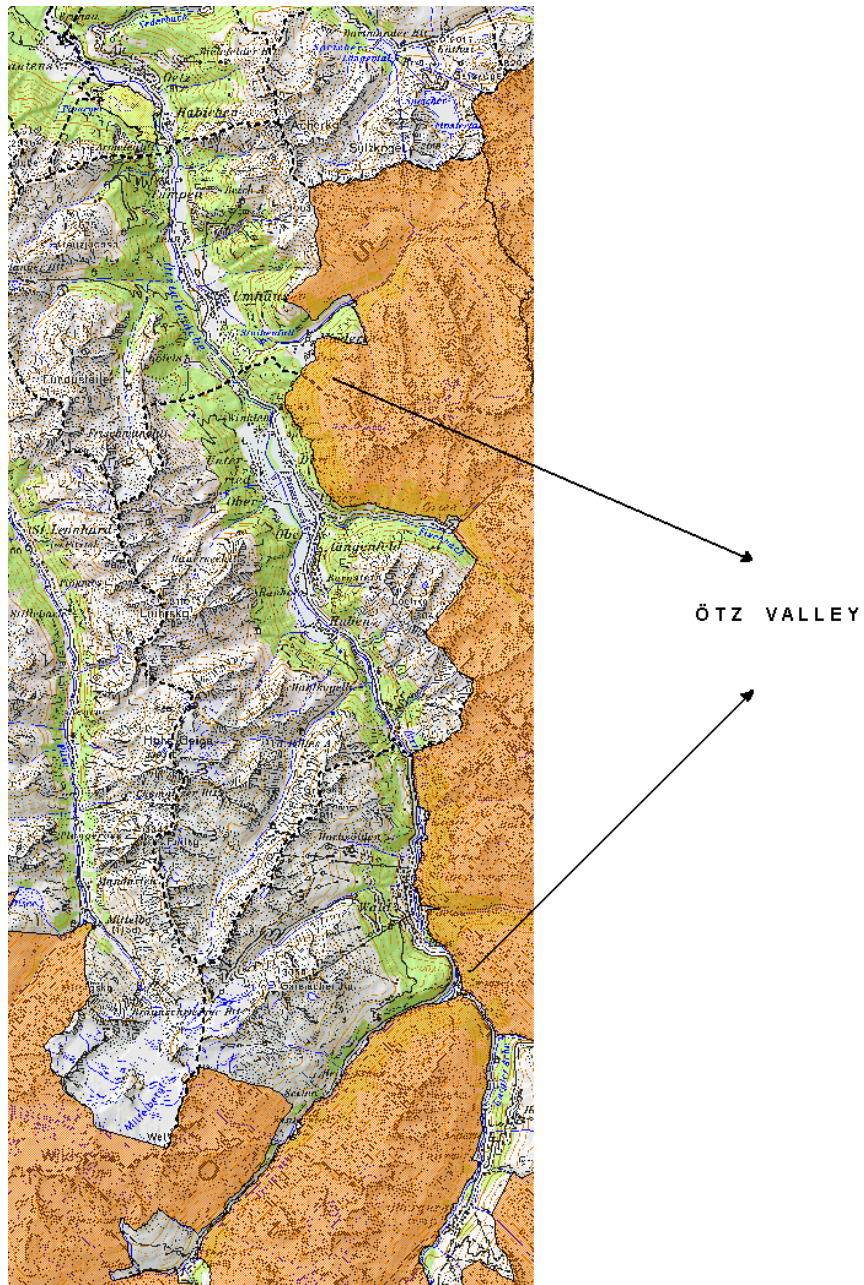
ÖTZ VALLEY

Fig.12: Ötz Valley map (Land Tirol - www.tirol.gv.at)

1.3.1. Climate

The Ötz valley is an inner alpine dry valley with an average precipitation of 700 to 800 mm a year, concentrated over few days. The precipitation increases with elevation, but is not as much as occurs in the valleys further to the east in Tyrol, where the average is ca. 1000-1500 mm occurring on 110 to 150 days. An additional reason for the lack of snow in winter is the location in a North-South-valley, which is responsible for the occurrence of the warm wind known as "foehn" (Pfeffer K. et al, 2000).

The altitude is between 660 m and 3450 m. The altitudinal zones were classified (ENVI 3.4) according to the DEM, which was obtained by the interpolation of digital contourlines (Fig. 13).
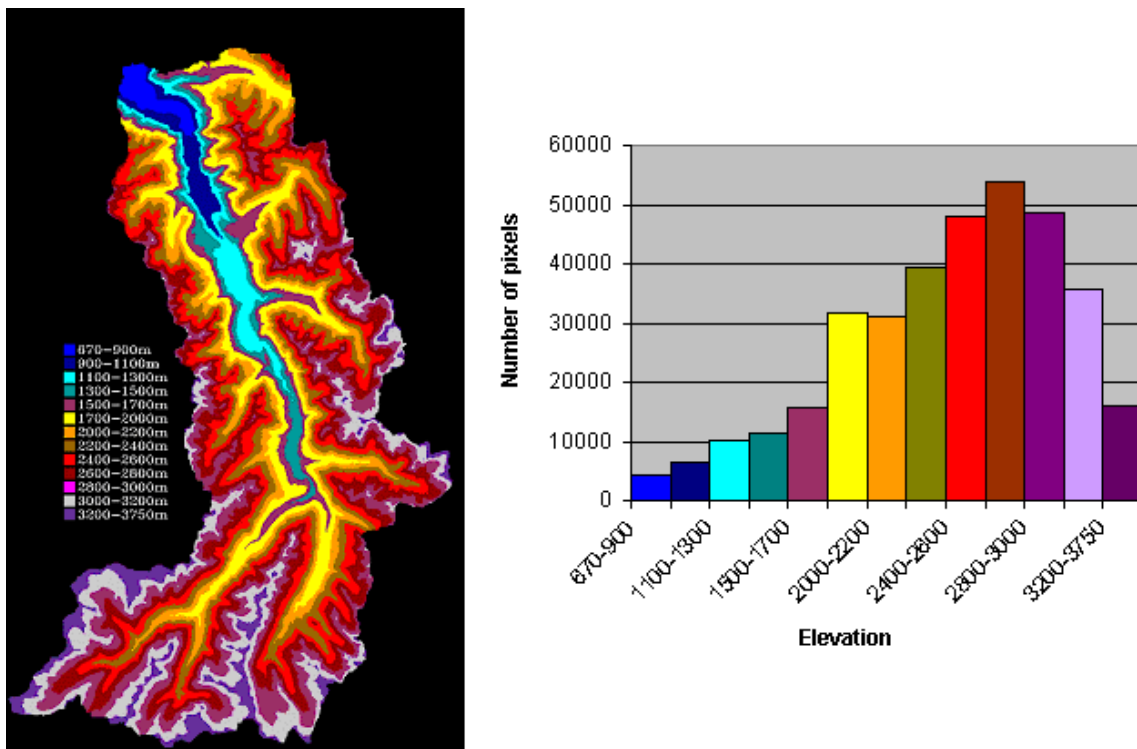
Fig. 13: Distribution of altitudinal zones in Ötz Valley (DEM obtained from Tyrolean State Government, modified by Colgan A., GLOWA DANUBE Project)

Slope for the study area was calculated using the existing digital elevation model. The slope map was divided further into 6 categories. The number of pixels is shown (Fig. 14).
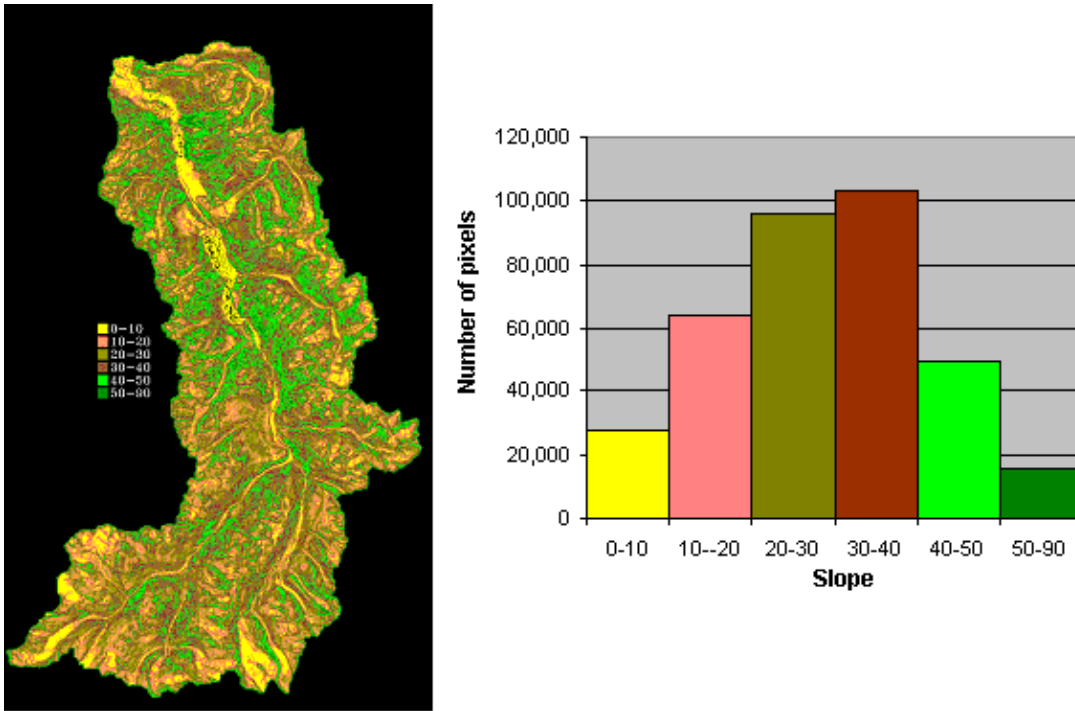
Fig. 14: Distribution of slope categories – Ötz Valley (derived from DEM in Fig. 13)

The 360°- degree exposition map was separated into 8 categories and each of them has a width of 45° (Fig. 15).
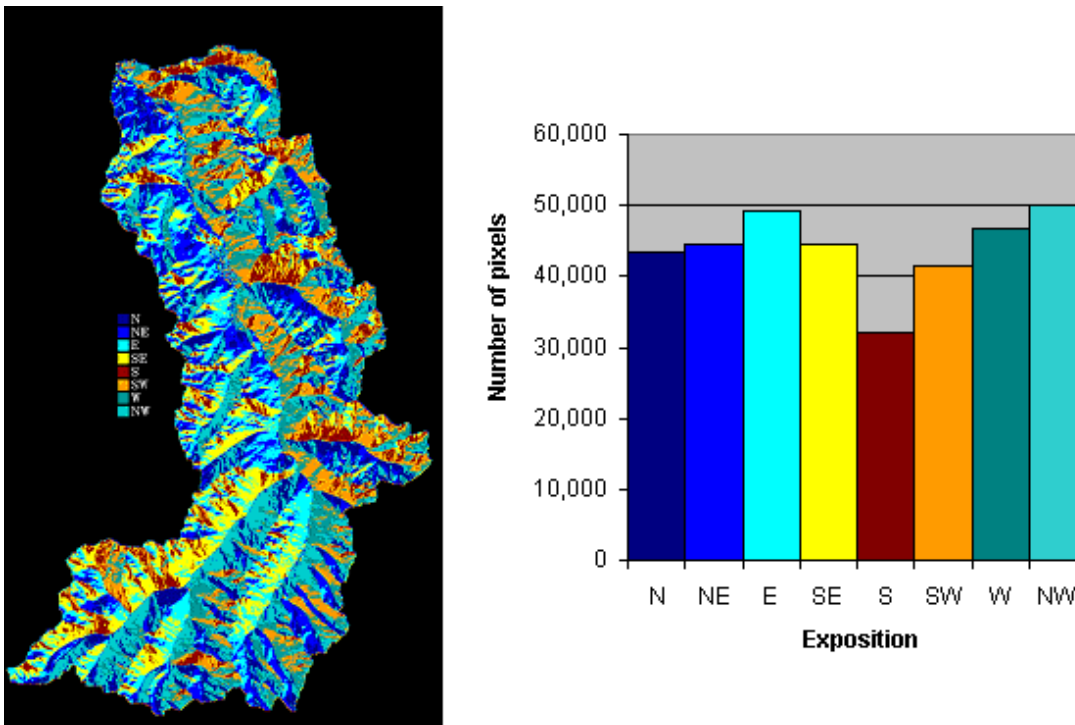
Fig. 15: Distribution of expositions – Ötz Valley (derived from DEM in Fig. 13)

1.3.2. Vegetation

In Ötz Valley as well as in Stubai Valley, the altitudinal zonation of the vegetation is pronounced. In the **submontane** and **montane** zones the forest mainly consists of spruce and larch. Coniferous forests are dominant in both valleys. Mixed forests as well as deciduous forests cover only small patches in the valleys. In the upper **subalpine** and **alpine** zone, dwarf mountain pine *Pinus mugo* is dominant. In the area above timberline, dwarf shrubs *(Rhododendron ferrugineum, Vaccinium myrtillus* and *Loiseleuria procumbens*), alpine grasslands (*Carex curvula, Elyna myosuroides*), moss and some pioneer vegetation are present (Kilian et. al, 1994).

2. Data collection and description

2.1. Collection and processing of field data

2.1.1. Alpine habitat mapping – National Park Berchtesgaden

Within the framework of the Project "Alpine Habitat Diversity–HABITALP–INTERREG IIIB Alpine Space Program", the administration of the National Park Berchtesgaden decided to monitor the entire area of the National Park and its pre-field. Color infrared photos were considered to provide the best method for vegetation interpretation of the area and for classification of the land cover. They have been used for clear differentiation of the biotope types in the National Park. The periods of flyovers were in July or August during the vegetation growth period in the years 1980, 1990 and 1997. The mapscale of the original aerial photos is 1:11000. The first interpretation key was developed by the researchers of the MaB 6 (Man and Biosphere)-Project 'Ecosystem Research Berchtesgaden' in the year 1984/85 (Kerner et al., 1991). Having established a GIS based on interpretation of aerial photographs at the beginning of the 80s, the National Park has carried out two update interpretations based on CIR-images from 1990 and 1997. The update of the database was realized by the Center for Landscape Informatics (ILI GIS Services, Freising) (Kias et al., 1994, 1996, 1999). At that time, a new interpretation key for CIR-photos was developed by a working team of nature conservation of the German "Landesämter" und "Landesumweltämter" (Bundesamt für Naturschutz, Bonn (HRSG), 1995). This interpretation key was used for the new CIR-photos from 1997, but the old interpretation key was used to draw a comparison between the CIR-photos of both dates (Franz H., 2000). For covering the entire area of the National Park, all received aerial images are merged during the process called mosaicking. The entire image was georeferenced in ArcInfo program (ESRI GIS and Mapping Software) and further tested with field observations using geographical positioning systems (GPS). Interpretation of the data constructing a biotope map was carried out using an interpretation key which was obtained according to the brightness, texture and surface, shadows, stereoscopic

effect, type of vegetation, etc. A summary of the hierarchical interpretation key, which covers 153 biotope types in the National Park is summarized in Table 1.

Table 1: Abstract of the hierarchical interpretation key

MERKMAL 1 Biotop- bzw. Nutzungstyp 4stelliger Code	MERKMAL 2 Art - Gattung - Ausprägung 3stelliger Code	MERKMAL 3 Bedeckung Beschirmung 1stelliger Code
5720 Schuttflur mit Bewuchs		
	erste Stelle des 3stelligen Codes: Rasenanteil	
	0.. Rasenanteil, Verheidung: Keine Aussage, nicht erkennbar **1..** Rasenanteil, Verheidung: Keine **2..** Rasenanteil, Verheidung: Vereinzelt (1-10%) **3..** Rasenanteil, Verheidung: Beigemischt (10 - 40%) *Rasen- / Verheidungsanteil über 40%: anderer Biotoptyp*	**0..** Keine Aussage, nicht erkennbar **1..** Schutt- und Blockhalde (flächig, plan) **2..** Schuttkegel (inkl. Murkegel) **3..** Moräne **4..** Bergsturzablagerung **5..** Blockgletscher
	zweite Stelle des 3stelligen Codes: Gebüschanteil	
	0. Gebüschanteil: Keine Aussage, nicht erkennbar**.** **1.** Gebüschanteil: Keiner **2.** Gebüschanteil: Laubgebüsch (dominant) -vereinzelt (1- 10%) **3.** Gebüschanteil: Laubgebüsch (dominant) -beigemischt (10 - 40%) **5.** Gebüschanteil: Nadelgebüsch (dominant) -vereinzelt (1- 10%) **6.** Gebüschanteil: Nadelgebüsch (dominant) -beigemischt (10 - 40%) *Gebüschanteil über 40%: anderer Biotoptyp*	**0** Keine Aussage, nicht erkennbar **1** Schutt- und Blockhalde (flächig, plan) **2** Schuttkegel (inkl. Murkegel) **3** Moräne **4** Bergsturzablagerung **5** Blockgletscher
	dritte Stelle des 3stelligen Codes: Rasenanteil	
	0 Baumanteil: Keine Aussage, nicht erkennbar **1** Baumanteil: Keiner **2** Baumanteil: Laubgehölz (dominant) -vereinzelt (1- 10%) **3** Baumanteil: Laubgehölz (dominant) -beigemischt (10 - 30%) **5** Baumanteil: Nadelgehölz (dominant) -Vereinzelt (1 - 10%) **6** Baumanteil: Nadelgehölz (dominant) -beigemischt (10- 30%) *Baumanteil über 30%: Wald (7000)*	**0** Keine Aussage, nicht erkennbar **1** Schutt- und Blockhalde (flächig, plan) **2** Schuttkegel (inkl. Murkegel) **3** Moräne **4** Bergsturzablagerung **5** Blockgletscher

For mapping of units that are need to cover a complete area, more or less homogeneous polygons that represent the above-stated specific criteria are identified. To each polygon, one or more specific features were assigned and the entire area was classified into more than 150 land cover classes. The CIR biotope map consists of 7081 polygons (Kias, et al., 1999) (Fig. 16).

Fig. 16: Deciduous forest - St. Bartholomä (left) and Spruce forest – Saalachsee (right) and homogeneous polygons for the test sites (Kias et al., 1999)

After interpretation and classification based on digitized ground truth polygons as mentioned above, the biotope types map was carried out. The following example shows land cover interpretation and classification of the northern part of the lake Königsee (Fig. 17).
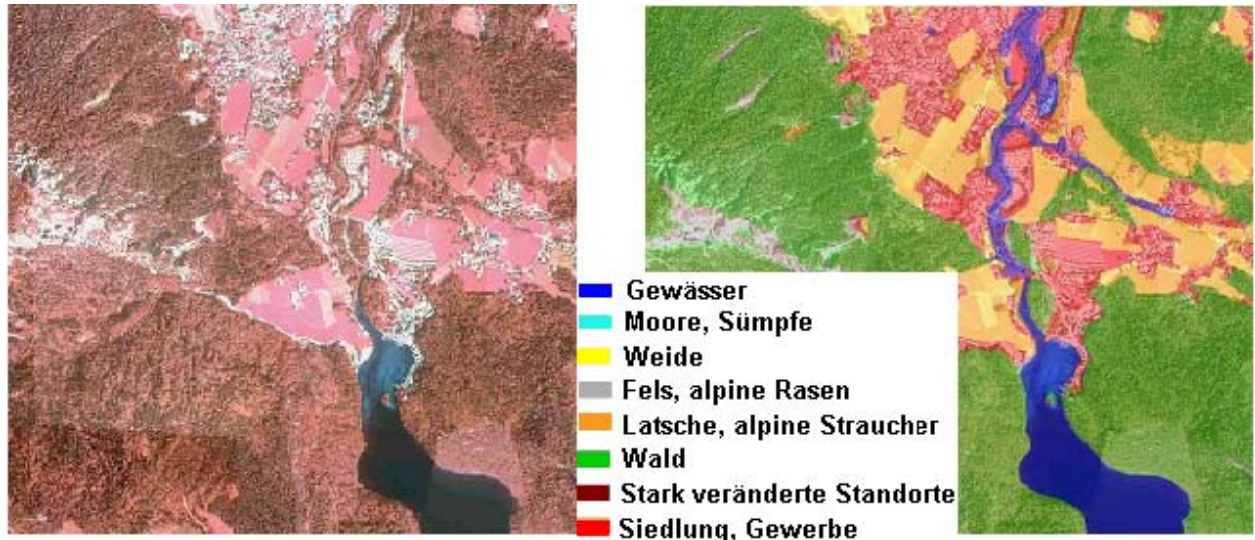
Fig. 17: Biotope types at the northern end of the lake Königsee (National Park Berchtesgaden archive)
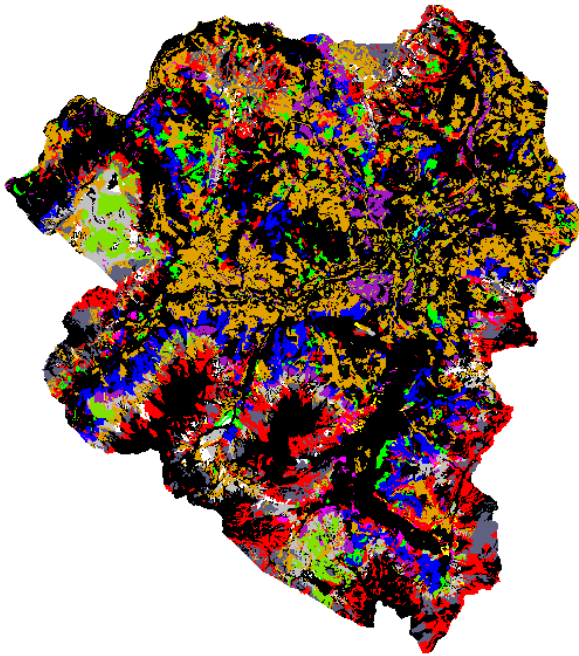
The biotope map with 153 classes (biotope types) was used as a ground truth map for comparison with remote sensing based supervised classification (Fig. 18). The description of biotope types is given in Appendix B. The discussed maps where used as a reference data for validation of the remote sensing classification results. Combining ground truth or other ancillary information with remote sensing derived information leads to better results in interpretation of the landscape and monitoring of forest functions.

Fig. 18: Biotope types in National Park Berchtesgaden and in the pre-field part of the park

2.1.2. Forest inventory data

Within the framework of the projects „Mapping Site Characteristics in the National Park Berchtesgaden" (carried out between March 1, 1999 and June 30, 2001 in cooperation with the Technical University of Munich, Dept. of Ecology, the Faculty of Forest Science and Resource Management, Dept. of Geobotany (Prof. Dr. Anton Fischer), and the Administration of the National Park Berchtesgaden) and „Waldentwicklung im Nationalpark Berchtesgaden von 1983 and 1997" (Institute for Forest Growth at the Albert-Ludwigs-University in Freiburg (Dr. Volkmar Konnert)), a forest inventory database was created. The forest-inventory data were initially gathered in 1983/84. The existing sample network created in 1983/84 was re-measured during the period 1995/1997 (April to October each year) in order to obtain information on the development of the forests within the National Park. The inventory database was used for correlation with remote sensing derived information. The inventory was carried out using the angle-counting method (as in the first inventory), as well as by using a method of concentric circles (method applied by the Bavarian State Forest Administration).

Over the territory of the National Park Berchtesgaden a raster grid with 200/200m squared cells was created (Fig. 19).
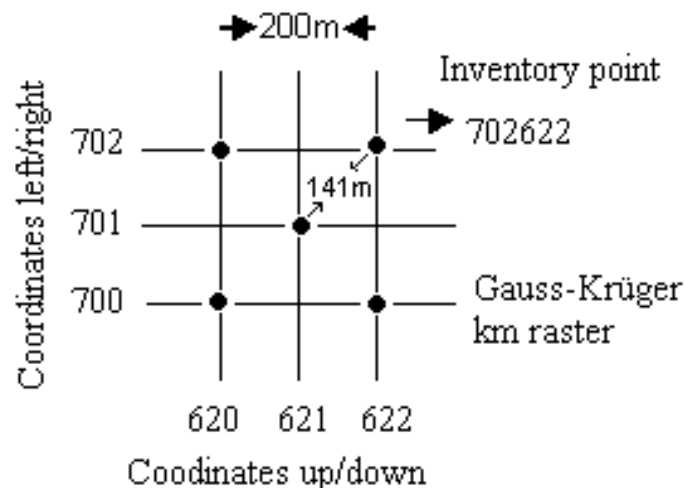

Fig. 19: Raster grid – forest inventory data

In the first forest inventory, 39952 trees were examined. This number is defined as 100 %. 90.3 % of these trees were measured during the second inventory, 9.7 % disappeared, 11.2 % had newly established. Compared to the first inventory, 101.5 % of the trees were studied in the second inventory. Nearly 4200 inventory points were monitored. The distance was 141 m between the inventory points. The points were marked with magnets during the first series of forest monitoring measurements. For each of the forest stands (grid cell) a number of stand parameters was measured - stand age, tree height, stand density, soil depth, DBH (diameter at breast height) etc. The ground plots in which stand parameters are measured are generally 50, 150 and 500m^2 in size, depending on the DBH of trees to be measured (Table 2). Then all the data sampled in an individual circle are recalculated for 1ha. (Konnert, 2000).

Table 2: Plot sizes according to DBH

DBH cm	Plot size m^2
0-5	25
6-11	50
12-19	150
>=20	500

The diameter at breast height was measured for all the trees falling into the ground plot (concentric circle) at 1.3m above ground level. DBH was separated in different classes. Stand age was measured with the counting of year rings on cores taken from the tees. Very old trees predominate clearly in all measured stands.

According to age, all trees were grouped into age classes of every 20 years. Tree height was measured in every ground plot with Suunto altimeter (SUUNTO, CA, USA). Canopy density was estimated in every 500 m^2 circle to one tenth of ground cover. Forest stand data are stored in an ArcInfo Geographic Information System (GIS) database. Stand summary information, as well as individual plot and tree data are stored. The data are available in raster format, which is very useful for further correlation with remote sensing data. This allows interactive exchange with multiple types of data.

By analyzing diverse data sets together, it is possible to extract better and more accurate information in a synergistic manner than by using a single data source alone.

2. 2. Collection and processing of remote sensing data

The second part of this study concerns the use of satellite images as a tool for forest monitoring. Studies in the field (ground truth investigations) provide detailed measurements over relatively small areas at different times. Remote sensing data provide synchronous measurement of very large areas but with reduced potential for local details. (Kerr and Ostrovsky, 2003). Combining remote sensing and ecological measurements by defining a nested set of test sites to be sampled with the use of ground truth investigations lead to spatially integrated measures of ecosystem structure and functions. Landsat Thematic Mapper data are frequently used for land cover and forest mapping, Leaf Area Index (LAI) derivation and prediction, etc. Landsat data are excellent for providing regional overviews of forests and for monitoring changes in forest conditions. In this study it is important to supplement Landsat data with ancillary spatial data, as from the digital elevation model and forest inventory, in order to obtain the desired output or product.

2.2.1. Landsat data characteristic and Remote Sensing of vegetation

<u>Landsat data – brief description</u>

A Landsat Thematic Mapper 5 image was used in this case study – path 192 and row 27 was acquired on September 14, 1999 under clear sky conditions. For the investigation of the test area Ötz Valley (Austria) a Landsat 7 ETM+ - path 193 and row 27, scene was used (Table 3). It was obtained on September 13, 1999. Both scenes are Level 1 System corrected – 1G level. They are radiometrically and geometrically corrected to user-specified parameters, including output map projection, image orientation - UTM and WGS84, and resampling nearest neighbour algorithm (EURIMAGE, 2001).

Table 3: Landsat 5 TM and Landsat 7 ETM+ bands spectral range and spatial resolution

Landsat 5 TM characteristic			Landsat 7 ETM+ characteristic		
Band number	Spectral Range (μ)	Ground resolution (m)	Band number	Spectral Range (μ)	Ground resolution (m)
1	0.45 - 0.52 (blue)	30	1	0.45-0.52 (blue)	30
2	0.52 - 0.60 (green)	30	2	0.52-0.60 (green)	30
3	0.63 - 0.69 (red)	30	3	0.63-0.69 (red)	30
4	0.76 - 0.90 (NIR)	30	4	0.76-0.90 (NIR)	30
5	1.55 - 1.75 (SWIR)	30	5	1.55-1.75 (SWIR)	30
6	10.4 - 12.4 (Thermal IR)	120	6	10.4-12.5 (Thermal IR)	60
7	2.08 - 2.35 (SWIR)	30	7	2.09-2.35 (SWIR)	30
			8	0.522-0.90 (Panchromatic)	15

Landsat data were selected for this study because the available spatial resolution of 30 m is appropriate for correlation with forest stand data. The ability of Landsat to acquire spectral information in seven satellite bands, ranging from the visible part of the spectrum to the mid-infrared part of the spectrum (thermal band is also included) allows detailed investigation of vegetation spectral response, definition of spectral vegetation indices for regression with biophysical variables and supervised (or unsupervised) classification of the vegetation types (or land cover) (Table 4).

Table 4: Landsat Thematic Mapper bands, their spectral ranges, and principal remote sensing applications for earth research (Lillesand and Kiefer, 2000)

Landsat bands	Principal applications
1	Designed for water body penetration, making it useful for coastal water mapping. Also useful for soil/vegetation discrimination, forest type mapping, and cultural feature identification
2	Designed to measure green reflectance peak of vegetation for vegetation discrimination and vigor assessment. Also useful for cultural feature identification
3	Designed to sense in a chlorophyll absorption region aiding in plant species differentiation. Also useful for cultural feature identification
4	Useful for determining vegetation types, vigor, and biomass content, for delineating water bodies, and for soil moisture discrimination
5	Indicative of vegetation moisture content and soil moisture. Also useful for differentiation of snow from clouds.
6	Useful in vegetation stress analysis, soil moisture discrimination, and thermal mapping applications
7	Useful for discrimination of mineral and rock types. Also sensitive to vegetation moisture content.

Remote Sensing of vegetation

Spectral signatures of vegetation have shown that Landsat bands are useful in monitoring natural vegetation trends. Leaf Area Index (LAI) and Green Vegetation projected cover are considered as biophysical indicators for forest structure and function, which can be inferred from spectral reflectances (Fig. 20 and Fig. 21).
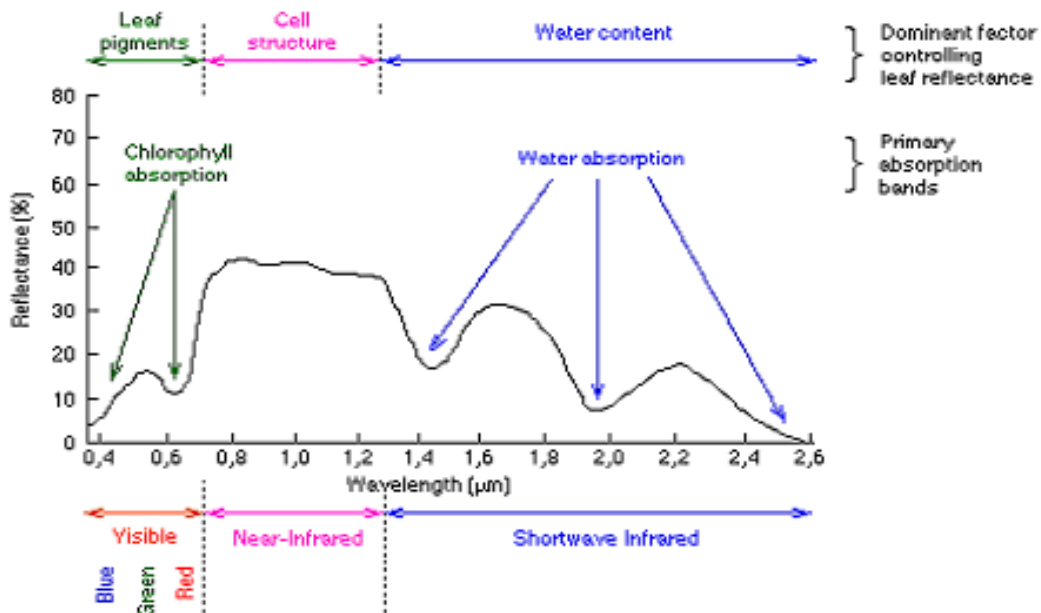
Fig. 20: Typical spectral response characteristics of green vegetation (after Hoffer, 1978)

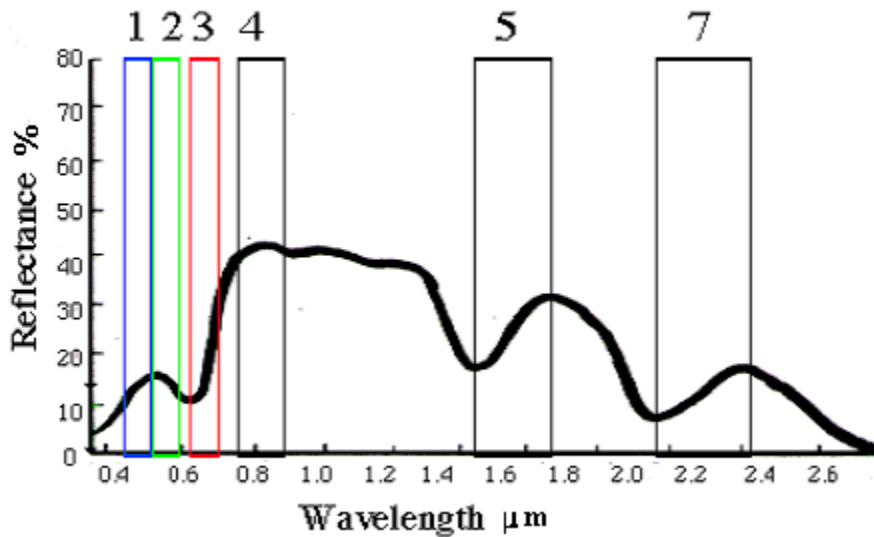**Fig. 21: Typical spectral response characteristics of green vegetation (after Hoffer, 1978) and Landsat TM bands**

Landsat visible red band 3 is sensitive to chlorophyll absorption. It is highly reflective for most soils, hence it is appropriate for discerning between vegetation and soil (Wulder M.A. 1998). The internal structure of healthy leaves acts as a diffuse reflector of near-

infrared (band 4) wavelengths. The middle-infrared energy is strongly absorbed by water in vegetation. Landsat band 5 measures the changes in leaf-tissue water content (as reflectance is found to decrease as water content decreases) which may be related to differences between plant species or vigor (Avery and Berlin, 1992). Green vegetation has a reflectance of less than 20% in the 0.5 to 0.7 μm spectral interval, but about 60% in the 0.7 to 1.3 μm range.

All of these spectral patterns are used for vegetation discrimination and interpretation – derivation of forest masks, LAI correlations and extrapolation procedures. From the TM data a number of different transformations (Table 1) were used in the analysis. For supervised classification in this study, all Landsat bands were used except the temperature band 6 because of its resolution of 60/120m. For correlations with LAI or vegetation density, the most important bands are band 3 and 4.

2.2.2. Image preprocessing

Georeferencing

To enable relating remote sensing and GIS data, both data sets were geometrically transformed to real world coordinates using UTM projection and WGS84 datum. Image to image registration (ENVI 3.4.) was further used for coregistering the data. The RMS accuracy was 0.05 pixels utilizing more than 150 ground control points and nearest-neighbor resampling technique. The procedure was used for all the test sites (Berchtesgaden, Stubai and Ötz Valleys) in order to reference satellite images to match base image geometry („ground truth maps", DEM).

Atmospheric correction

Atmospheric correction involved suppressing the effect of atmospheric scattering using a modified dark object subtraction technique of Chavez P.S. (1988). It is an empirical approach based on the histograms of the bands and only accounts for atmospheric scattering (rayleigh scattering). The correction is applied by subtracting the minimum observed value, determined for each specific band, from all pixel values in each respective band. Initially the minimum response in each band in the image was extracted

assuming that without atmospheric scattering the minimum radiance of these features would be zero. Radiances measured at the satellites are almost always greater than zero. This is because even if we had a 'dark object' in our scene (like a deep, calm lake), we will still measure some scattering from the atmosphere between the satellite and the dark object. For each band, all of the pixel values were shifted by the amount of the lowest pixel value (Table 5). Thus, if pixel value in one band ranged from 7 to 219, we shift them all down by 7, so that the resulting band has pixel value ranging from 0 to 213 (Fig. 22 and Fig. 23).
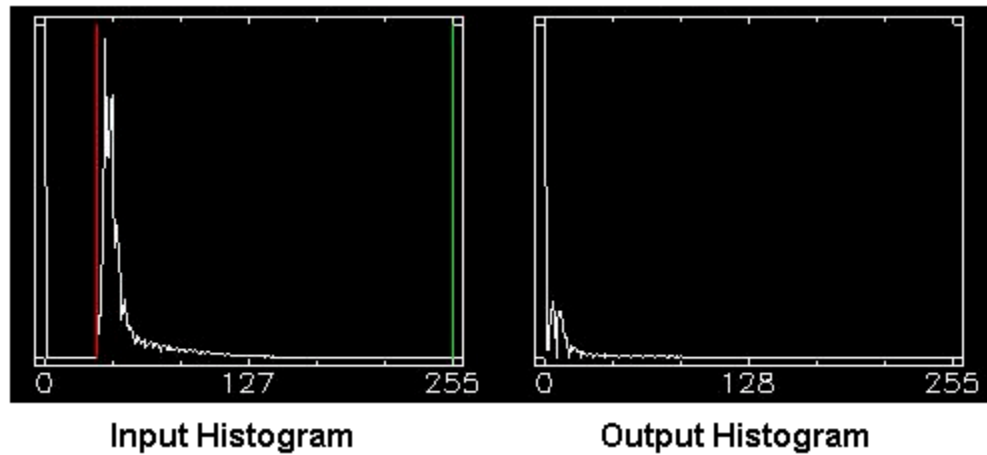
Fig. 22: Subtraction of the minimum band value - histogram of band 1 Landsat TM
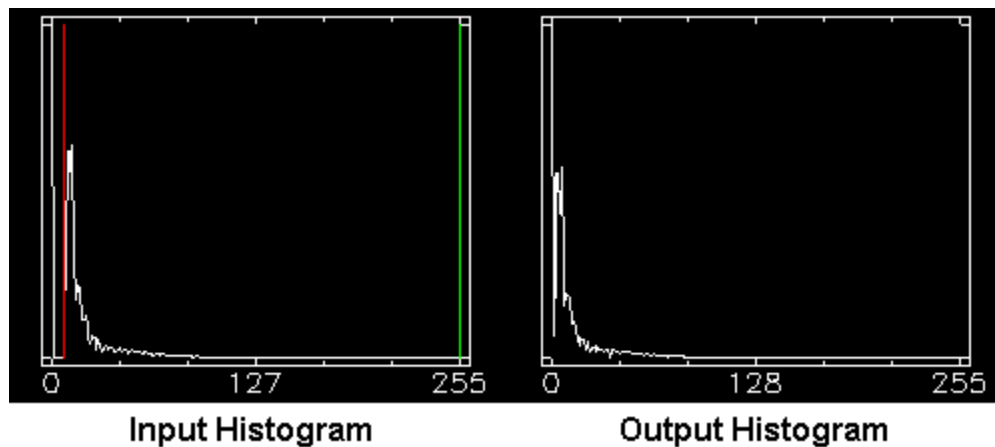
Fig. 23: Subtraction of the minimum band value - histogram of band 3 Landsat TM

Table 5: Minimum band values obtained in histograms of the Landsat scene of National Park Berchtesgaden

Landsat TM bands	Band minimum (DN)
1	33
2	9
3	7
4	6
5	3
7	1

Since scattering is wavelength dependent the minimum values vary from band to band (Table 5). This value is subtracted from the histogram in each band where the slope of the histogram begins to increase dramatically.
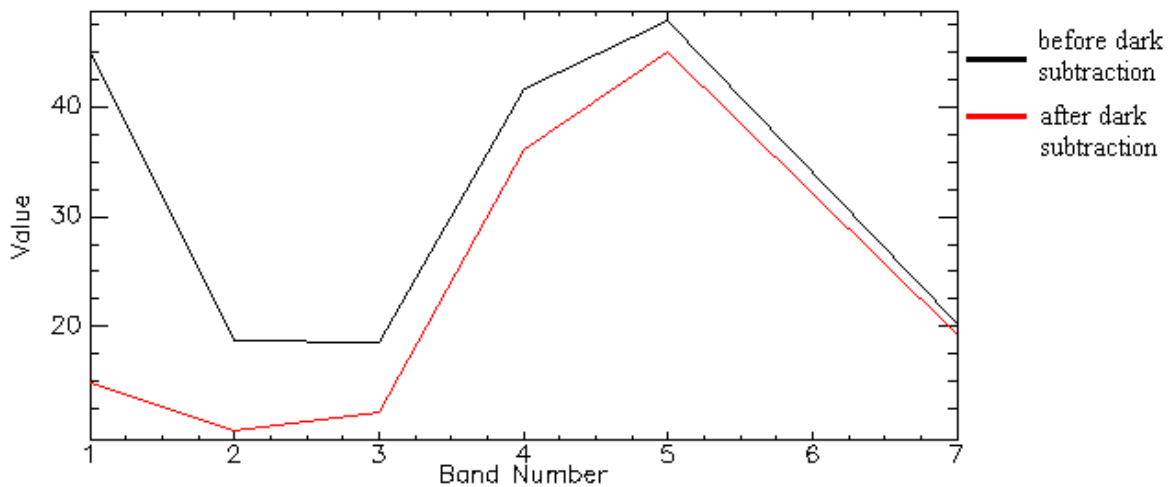
Fig. 24: Reducing the effect of atmospheric scattering –mean band values before and after dark subtraction method is applied

The atmospheric correction caused changes in vegetation ratio images such as NDVI and SR used in this study for correlation with ground truth data such as LAI, vegetation density, etc. Vegetation, which has positive NDVI values (above 0.2-0.3) after atmospheric correction receive higher NDVI values as seen from Fig. 25.
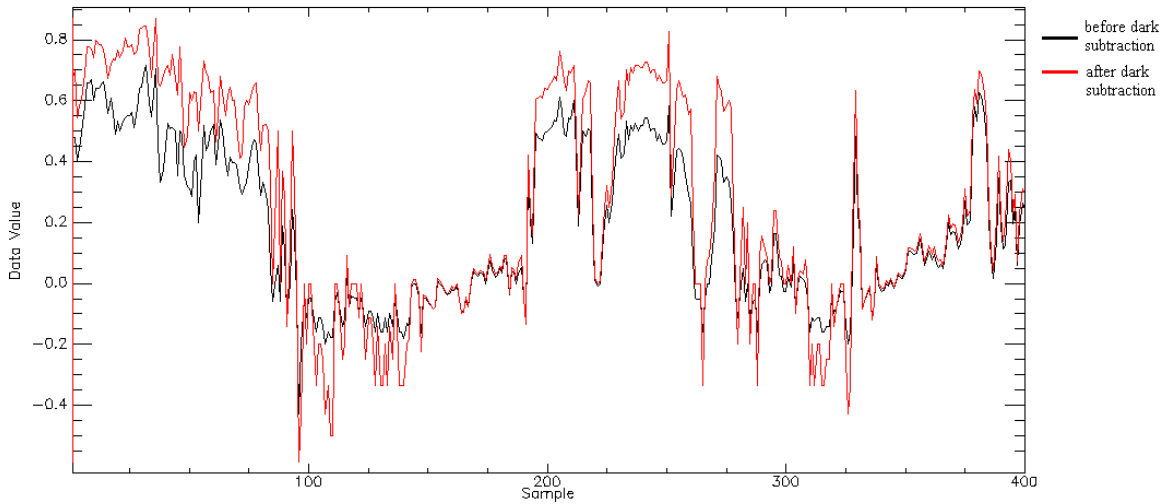
Fig. 25: Effect of atmospheric correction on NDVI values – horizontal profile

The atmospheric correction showed the expected changes in reflectance such as minimizing additive effect due to Rayleigh and aerosol scattering, especially in the visible bands, where this effect is stronger than in the infrared bands (as also found in other studies) (Liang, S et al., 2001) (Fig. 24). Different scenes can be better compared after atmospheric correction. Changes observed will be due to changes on the earth's surface and not due to different atmospheric condition.

Topographic correction

The correction of topography-induced illumination effects in mountain areas is an important and imperative step in data preprocessing to get better classification results and to use the satellite data in the fields of environmental research and monitoring. (Parlow, 1996a). It allows to suppress the shadow effects due to relief. An object lying in shadow receives and reflects less radiation than the same object on the sunny side. Therefore the same objects despite their equal reflectance display varying values according to their position to the sun. (Parlow, 1996a, Parlow, 1996b, Itten et al., 1992a) Then ridges or valleys may be over- or under-emphasized depending on their orientation.

In this study, the SWIM (Short Wave Irradiance Model, Parlow, 1991, 1996a) was used for topographic correction of the Landsat data. It is a physically-based and distributed radiation model for clear sky conditions to compute solar irradiance (direct and diffuse)

under the assumption of a standard atmosphere and on the basis of a digital elevation model (DEM) (Parlow, 1996a). The standard atmosphere is automatically adjusted according to the time of the year and latitude (summer – winter, tropical – midlatitudinal – polar). Altitudinal effects, path length and transmissivity are also considered (Parlow, 1996a) (Fig. 26).
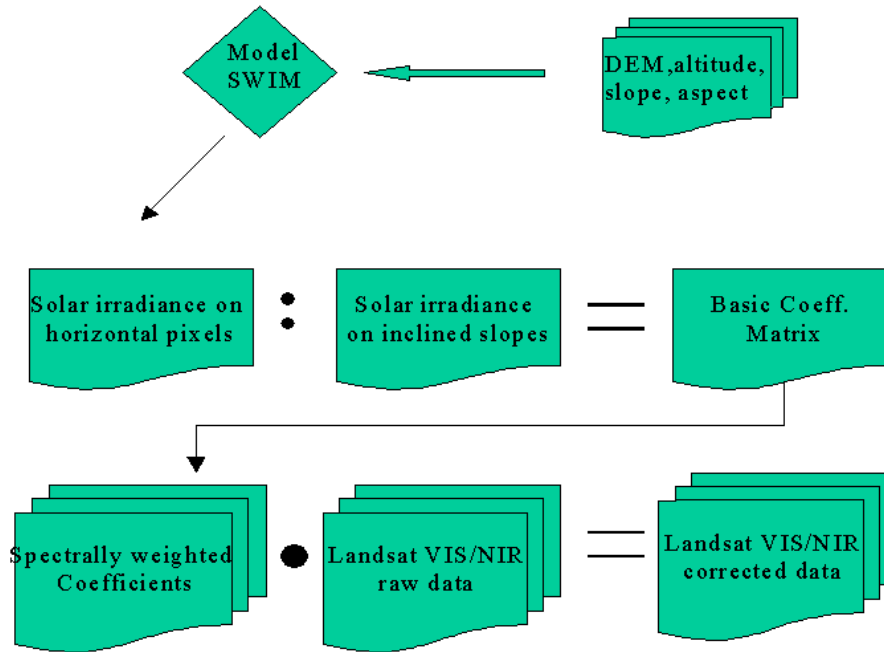
Fig. 26: The SWIM model conception (Parlow, 1996a)

The solar irradiance for the time of satellite overpass was computed for the territory of National Park Berchtesgaden. The irradiance on horizontal surfaces at different altitudes (I_{hori}) and the irradiance on inclined surfaces (I_{incl}) were calculated. For any horizontal surface the ratio (I_{hori})/ (I_{incl}) = 1. Surfaces exposed to the sun receive more radiation than horizontal surfaces (I_{hori})/ (I_{incl})< 1. On shaded slopes the ratio is > 1. The basic coefficient matrix was calculated, which is the ratio between solar irradiance on horizontal pixels and solar irradiance on inclined slopes (Table 6). In the following table an example of basic coefficient matrix calculation is given.

Table 6: Calculation of basic coefficient matrix

Shaded pixels		
Solar irradiance on horizontal pixels (W/m^2)	**Solar irradiance on inclined slopes (W/m^2)**	Basic coefficients
616	563	1.09
626	438	1.42
618	451	1.37
612	352	1.73
638	176	3.6
637	251	2.53
618	507	1.21
622	497	1.25
622	417	1.49
626	294	2.12
Sun exposed pixels		
627	734	0.85
613	837	0.73
640	796	0.8
629	744	0.84
646	804	0.8
644	942	0.68
621	903	0.69
617	813	0.76
622	830	0.74
658	727	0.91
Horizontal pixels (for example lake Königsee)		
607	607	1-neutral

The ratio leads to a basic information of how the different locations (satellite pixels) must be treated (reducing or increasing the observed reflectance to adjust for variation in radiation received), but it does not consider the different scattering that occurs with reflectance of different Landsat bands. Therefore, band specific correction coefficients (weighting factors) must be used to gather with $(I_{hori})/(I_{incl})$. These weighting factors were used as scalars and multiplied pixel by pixel with the satellite data. They were worked out especially for mountainous terrain by Parlow (1996a) (Table 7).

To calculate spectrally weighting scalars from the basic coefficient matrix, the proportion of diffuse/direct radiation was used. In Landsat TM band 1 and 2 the proportion of diffuse radiation has its maximum, so the factors are closer to 1 (less adjustment of the image is needed). For these bands, the weighting factor is smaller than for TM-bands 3, 4, 5 and 7. The following formula and weighting factors were used for calculation of the spectral coefficients (Parlow, 1991, 1996a,).

Table 7: Band specific weighting factors (after Parlow, 1996a)

Landsat bands	Factor f
1	0.2
2	0.33
3	0.5
4	0.5
5	0.5
7	0.5

$$\textbf{Coeff}_{\textbf{spectral}} = \textbf{f} \cdot \textbf{Coeff}_{\textbf{basic}} - \textbf{f} + \textbf{1}$$

f - spectral weighting factor

After topographic correction, shadow effects on northern and northwestern slopes are minimized and the very bright radiance on southern and southeastern slopes is reduced (Fig. 27).
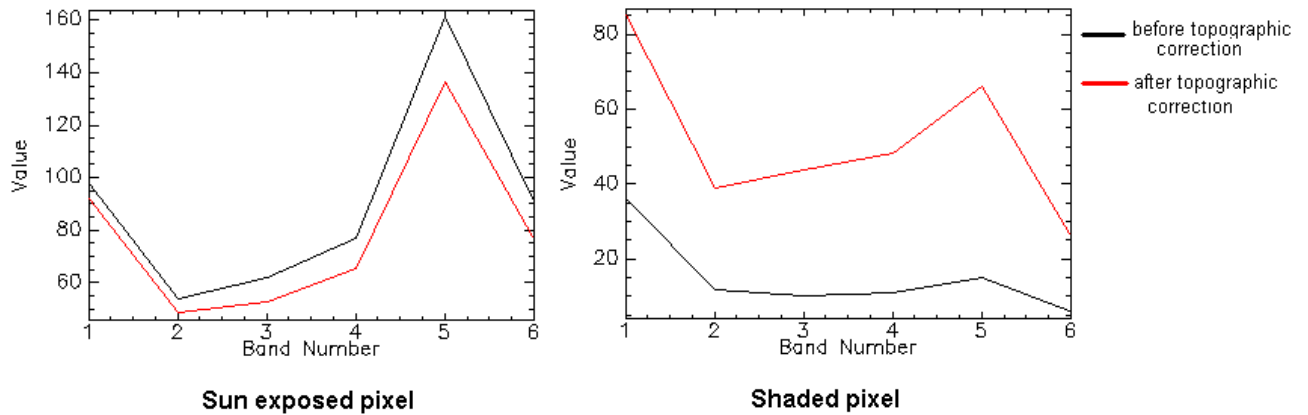
Fig. 27: Topographic correction effect

2.2.3. Vegetation indices – derivation and description

Much attention in the remote sensing of green vegetation is focused on the strong reflectance contrast between the visible (RED) and the near infrared (NIR) which is often referred to as the "red edge". For green vegetation there is a significant difference in reflectance and absorption of electromagnetic radiation when going from visible to near or mid infrared wavelengths. Vegetation differs from other land surfaces because it tends to absorb strongly the red wavelengths of electromagnetic spectrum and reflect in the near-infrared part. Vegetation indices are a measure of the difference in the reflectance in these wavelength ranges. These ratios and indices are indicative of the quantity and quality of vegetation (Tueller, 1989). All of these vegetation indices are dependent on the presence of the red edge feature. If the red reflectance is plotted against the near-infrared reflectance for a variety of surfaces, a triangular shaped distribution is found in the resulting values (Fig. 28).
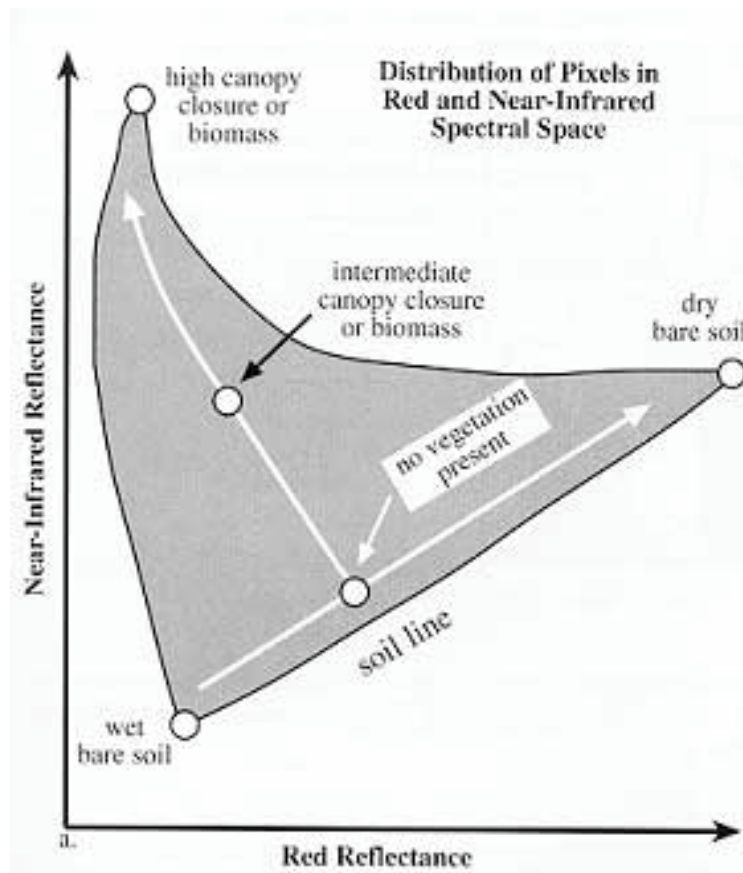
Fig. 28: Distribution of reflectance values in a remote sensing image in the red and near-infrared regions

The greater the biomass and/or canopy closure in an ecosystem, the greater the near-infrared reflectance and the lower the red reflectance. The soil line represents areas on the ground that do not have significant vegetation cover but vary in reflectance based upon whether the soil is wet or dry. Areas where vegetation is present will be found somewhere above the soil line (Jensen J.R., 2000).

One way of characterizing this relationship with a single variable is by dividing the near-infrared reflectance by the red reflectance (NIR/RED). The larger this ratio, the more photosynthetically active vegetation is present. With aircraft and satellite digital sensors, we acquire brightness or reflectance data in separate regions of the electromagnetic spectrum. This allows us to create a NIR/RED ratio image simply by dividing the NIR image by the Red image. The resulting vegetation index is often called Simple Ratio (SR). From Landsat TM or ETM+ data it is calculated as:

$$SR = Band\ 4\ /\ Band\ 3$$

Because these ratio values vary considerably from one region to another, a way of normalizing the ratio was established called the Normalized Difference Vegetation Index or NDVI. It is the most widely used vegetation index. The NDVI transformation is computed as the ratio of the measured intensities in the red (RED) and near infrared (NIR) spectral bands using the following formula:

$$NDVI = (NIR - RED)\ /\ (NIR + RED)$$

The Thematic Mapper (TM and Enhanced Thematic Mapper Plus (ETM+) bands 3 and 4) provide RED and NIR measurements and therefore can be used to generate NDVI data sets with the following formula:

$$NDVI = (Band\ 4 - Band\ 3)\ /\ (Band\ 4 + Band\ 3)$$

By normalizing the difference in this way, the values can be scaled between a value of minus 1.0 to 1.0. Vegetated areas will typically have values greater than zero and negative values indicate non-vegetated surface features such as water, barren soil, ice, snow, or clouds. Values >0.5 indicate dense vegetation.

Vegetation indices and especially NDVI have proved to have an extremely wide range of applications. The resulting indices are sensitive to the presence of vegetation on the Earth's land surface and can be used to address issues of vegetation type, amount, and condition. Numerous studies have explored the relationship between remotely sensed vegetation indices and field measured estimates (as present in this study) of vegetation amount: aboveground biomass, leaf area, canopy closure, etc. NDVI and SR can be directly linked to biophysical parameters, such as leaf area index, amount of green leaf biomass, amount of photosynthetic material, etc.

As well, NDVI normalizes the external influences of sun angle, viewing angle and atmospheric absorption effects. Atmospheric effects such as scattering act to increase the

reflectance values in band TM3 with respect to band TM4 and reduce the computed vegetation indices. Therefore atmospheric correction of the sensor data must be made (refer to image preprocessing).

Differences in canopy roughness at the scale of meters affect the study of forests. These meter-sized shadows are not visible in the Landsat imagery, for which sensor resolution is 30x30m. Band ratios (NDVI, SR) tends to remove such variations in overall brightness (Jensen J.R., 1996). Thus resulting NDVI and SR values should not be affected by small shadows (Aber J., et al., 2002).

2.2.4. Supervised classification methodology and accuracy assessment

Supervised classification methodology

Supervised classification is a probabilistic method able to arrange the pixels in different user defined classes. Classification is a process in which all the pixels in an image that have similar spectral signatures are identified. (Lillesand and Kiefer, 2000). The strategy is to identify homogeneous, representative samples, which represent various features or land cover classes of interest. These samples are called *training areas*. The selection of appropriate training areas is based on field observations and ideally supported by reliable ancillary sources, such as aerial photos, maps, or other ground truth data (Fig. 29).
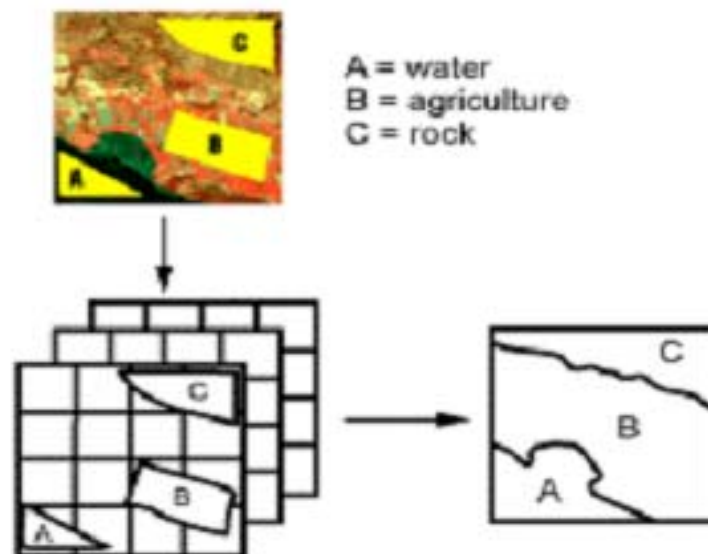

Fig. 29: Identification of "test areas" on the satellite scene

Training areas are located on the digital image using references to ground truth data and infrared aerial photographs of the area. Polygons are drawn on the digital image representing the training areas – *on-screen digitizing*. Generally a vector layer is digitized over the raster scene. The vector layer consists of various polygons overlaying different land cover types (Fig. 29). The more training areas that are available, the higher the overall accuracy will be for the classified image. Test sites are used for getting spectral signatures for the outlined areas. The most homogeneous and representative areas for different land cover features are compared for spectral characteristics and differences using scattergrams. Digital image classification uses the spectral information represented by the digital numbers in one or more spectral satellite bands, and attempts to classify each individual pixel based on this spectral information. In either case, the objective is to assign all pixels in the image to particular classes or themes (e.g. water, coniferous forest, deciduous forest, etc.). The resulting classified image is comprised of a mosaic of pixels, each of which belongs to a particular theme, and is essentially a thematic map of the original image (Yamagata, 1997).

Accuracy assessment

Accuracy assessment is the procedure used to quantify the reliability of a classified image. The accuracy of spatial data has been defined by the United States Geological Survey as: "The closeness of results of observations, computations, or estimates to the true values or the values accepted as being true". The accuracy of a classified image refers to the extent to which it agrees with a set of reference data (ground truth map). Most quantitative methods to assess classification accuracy involve an error matrix built from the two data sets (i.e., remotely sensed map classification and the reference data) (Maingi, et. al 2002). In other words accuracy is the degree (often as a percentage) of correspondence between observation and reality.

An error (confusion) matrix is a square array of numbers organized in rows and columns which express the number of sample pixels assigned to a particular category relative to the actual category as indicated by reference data (Congalton, 1996, 1999a, 1999b). The overall accuracy is calculated by summing the number of pixels classified correctly and dividing by the total number of pixels. A Random sampling method was employed to

estimate classification accuracy in this study. For an accuracy assessment of vegetation classification, random samples are drawn for each vegetation class separately. (Congalton, 1999) A direct comparison at each pixel of the aerial photo-interpreted land cover with the corresponding map label (pixel-to-pixel comparison) is a restrictive protocol for defining agreement. It reflects a "conservative bias" (Verbyla and Hammond, 1995) due to the confounding of true classification error with errors attributable to misregistration (positional errors) or the difference between polygon minimum mapping unit area and pixel size of the classified image (inability to confidently photo-interpret a sample unit). The results of this comparison are also affected by temporal differences between Landsat TM data and aerial photo acquisition (Zhu, et al., 1998).

A widely used, acceptable accuracy is 85%, which is strived for in the land cover/use classification adopted by the U.S. Geological Survey. The kappa coefficient of agreement (k) is another measure of the accuracy of the classification (Rosenfield and Fitzpatrick-Lins, 1986). In contrast to the overall accuracy described above this coefficient utilizes all elements from the confusion matrix. It is based on the difference between the actual agreement in the error matrix (i.e. the agreement between the remote sensing classification and the reference data as indicated by the major diagonal) and the chance agreement indicated by the row and columns totals.

$$\hat{\kappa} = \frac{N \sum_{i=1}^{r} x_{ii} - \sum_{i=1}^{r} (x_{i+} \cdot x_{+i})}{N^2 - \sum_{i=1}^{r} (x_{i+} \cdot x_{+i})}$$

r = number of rows in the confusion matrix

x_{ii} = the number of observations in row i and column i (on the major diagonal)

x_{i+} = total of observations in row i

x_{+i} = total of observations in column i

N = total number of observations included in the matrix (Lillesand and Kiefer, 2000)

The Kappa coefficient lies typically on a scale between 0 and 1, where the latter indicates complete agreement. Kappa values are also characterized into 3 groupings: a value greater than 0.80 represents strong agreement, a value between 0.40 and 0.80 represents moderate agreement, and a value below 0.40 represents poor agreement (Congalton, 1996).

III. LAND COVER CLASSIFICATION AND VEGETATION INTERPRETATION IN NATIONAL PARK BERCHTESGADEN

1. Summary

The interpretation of vegetation in National Park Berchtesgaden consists in classification and mapping the vegetation in the park and determination of forest types. The image classification procedure synthesizes satellite data with field data and other ancillary data derived from Geographic Information System (GIS - ArcInfo) coverage. Supervised classification describes the physiographical characteristics of the study region, which ranges from bare rocks to forests. It refers to the maximum likelihood statistical algorithm used to sort and group data into discrete classes, which can be uniquely identified. Ground truth data were used to improve the classification and for assessing accuracy of the results. They provide samples of ground objects with known qualities and known class membership and these are used as training sites in the classification procedure.

2. Results

2.1. Using Landsat TM data for supervised classification of the land cover in National Park Berchtesgaden

For interpretation and mapping of vegetation in the National Park Berchtesgaden, Landsat TM data were used. Spectral vegetation signatures were derived from remote sensing data and supervised classification was applied. Data processing was performed in the ENVI 3.4 (The Environment of Visualizing Images) software package (Fig. 30).
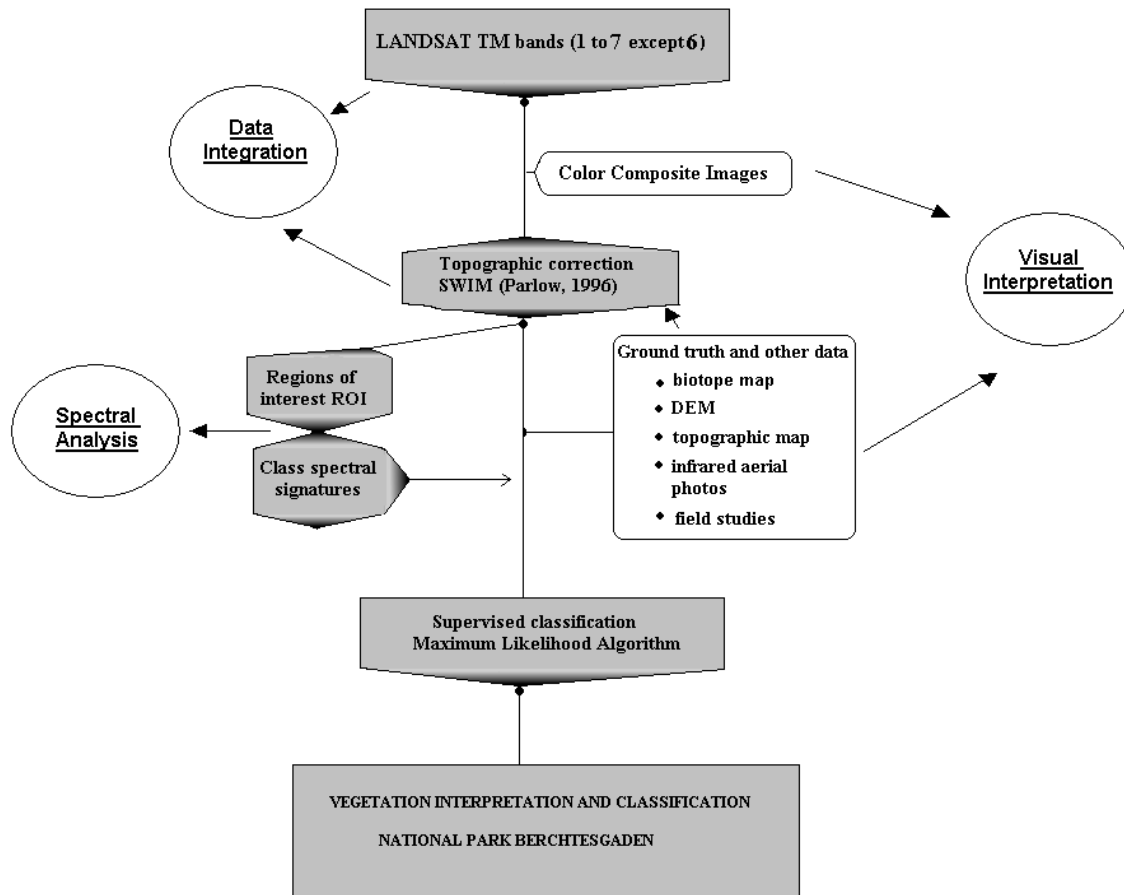
Fig. 30: The workflow in the Classification Procedure

Three general methods have been used to interpret and extract information from the Landsat TM scene and to generate a supervised classification (Singhroy, 1992).

1. <u>Visual interpretation</u> - based on features of tone (color), pattern, shape, texture, etc. of the satellite image

2. <u>Data integration</u> - merging of Landsat TM scene with other types of data, such as the digital elevation model (DEM), biotope type map, etc.

3. <u>Spectral analysis</u> - identification of surface objects on the basis of their spectral signatures

As a preliminary step and in order to improve the spectral classification accuracy, a DEM and derived slope and aspect images (refer to Chapter II) are used for topographic correction of the Landsat scene via the short wave irradiance model (SWIM) (Parlow, 1996a). Utilization of the DEM with the Landsat data reduced the shadow effect by

decreasing the brightness values of surfaces facing the sun and increasing values of surfaces facing away from the sun. The corrected values of different slope and aspect categories were moved forward the values that would occur on a horizontal surface. Topographic correction, especially in mountain areas is an important and imperative step in satellite data preprocessing to get better classification results and to use the satellite data in the fields of environmental research and monitoring.

Supervised classification consists of three main steps (Fig. 31):

1. *Training* – identifying homogeneous information classes
2. *Classification* – automatic categorization (using a classification algorithm – in this case maximum likelihood)
3. *Output* - digital map
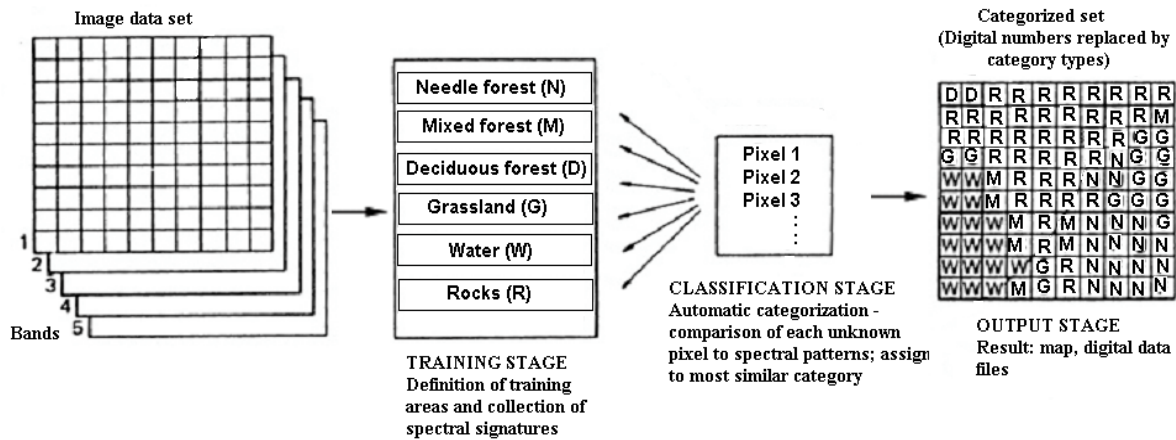
Fig. 31: Main steps in supervised classification

2.1.1. Identification of training areas (Regions of interest (ROI))

The first step in classification is the definition of homogeneous representative samples of the different surface cover types of interest. For creation of training areas (Regions of interest (ENVI)), a number of color composite images were compared (Fig. 32). An appropriate combination of bands is selected for better recognition of specific surface features and defining boundaries between different classes.
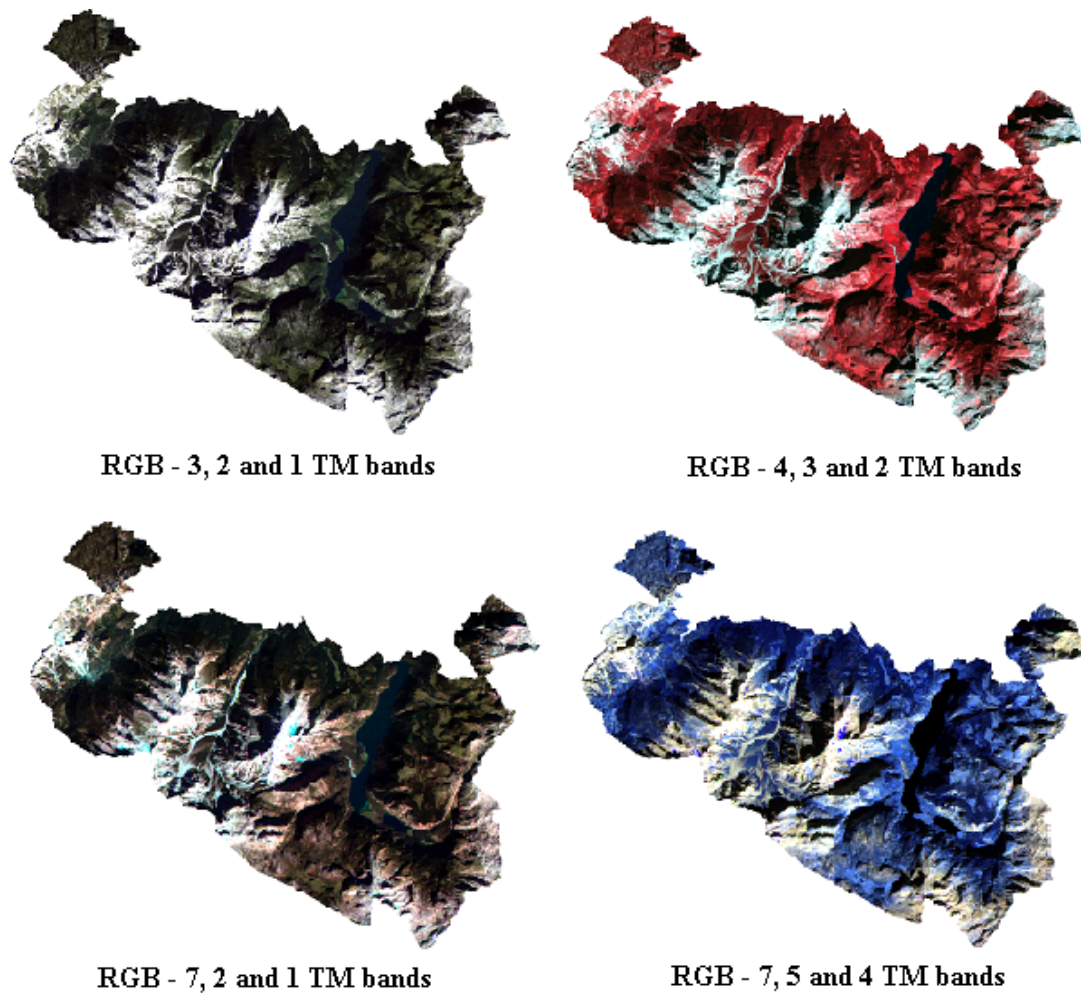
Fig. 32: Color composite images - visual interpretation

Color composite image (3, 2 and 1 TM bands - upper left corner, Fig. 32) is a "natural color" composite that simulates normal color appearance of the scene. This image is based entirely on reflected solar radiation in the visible portion of the electromagnetic spectrum. The rocks are depicted in white, water is dark blue and vegetated areas are shown in very dark green and shades of brown. A near infrared composite (4, 3 and 2 TM bands – upper right corner, Fig. 32) eliminates the visible blue band and uses a near infrared (NIR) band to produce the image. Vegetation has a very high reflectance in the NIR band (4), since energy at this wavelength is reflected. Thus, in a 4/3/2-NIR composite image, vegetation is depicted as varying shades of red. Since different types of vegetation have different levels of chlorophyll in their leaves, each type of plant has its

own shade of red. This makes a 4/3/2 composite very useful in determining the extent of vegetation and in classifying different vegetation types. In a composite image of visible and mid-infrared bands (7, 2 and 1 TM bands – lower left corner, Fig. 32) visible bands penetrate water and show suspended sediment in surface water. Snow is shown in cyan-blue color and is well differentiated from the rocks. In infrared false-color composite (7, 5 and 4 TM bands – lower right corner, Fig. 32), band 4, which is strongly reflective in the case of healthy vegetation, appears in blue so that areas on the images colored blue correspond to vegetated ground surface. In the color composite image (5, 4 and 3 TM bands, Fig. 33) the vegetation is in green color, rocks are in pink color, water - black color, snow – cyan color. This image is suitable for recognition of vegetation and its features and helps by visual interpretation of the image.

All of these images are helpful for best recognition of surface features and for obtaining precise training areas (Fig. 33).
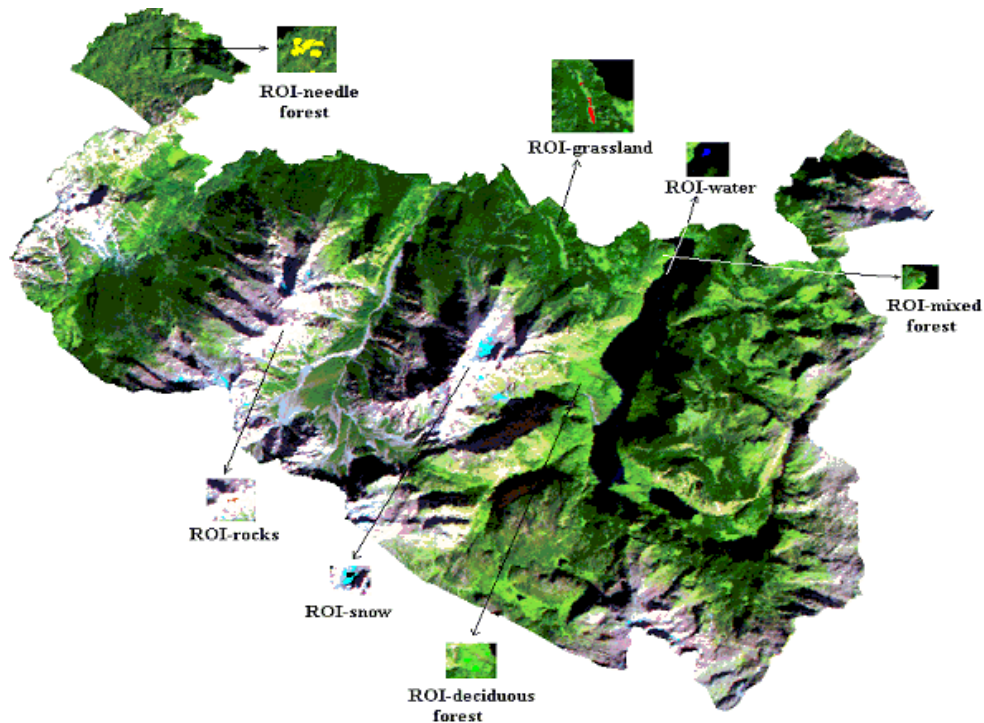
Fig. 33: Color Composite Image (5, 4 and 3 bands) and creation of Regions of interest

In general, these images allow an easy differentiation between vegetated and non-vegetated areas and to discern forested area and grassland. For differentiation between

class *rocks* and *snow* 7/2/1 color composite is very useful. The most important images for vegetation differentiation, were the 5/4/3 and 4/3/2 composites. *Water* was identified via the 3/2/1 color composite image.

Training areas were delineated through described color composites of multi-spectral Landsat data. The selection of the training areas was based on the above mentioned interpretation of color composite images and on the a priori knowledge derived from other reliable ancillary sources – digital elevation model (DEM), aerial photos, thematic maps (vegetation and biotope map - previously established from infrared aerial photointerpretation (CIR-biotope map in the National Park)) or field observations. In order to include information along elevation gradient, the digital elevation model (NP Berchtesgaden) was used. First the DEM was co-registered to the remote sensing scene, which was further draped over the DEM. A perspective view of the landscape with color-coding from Landsat image is shown in Fig. 34.
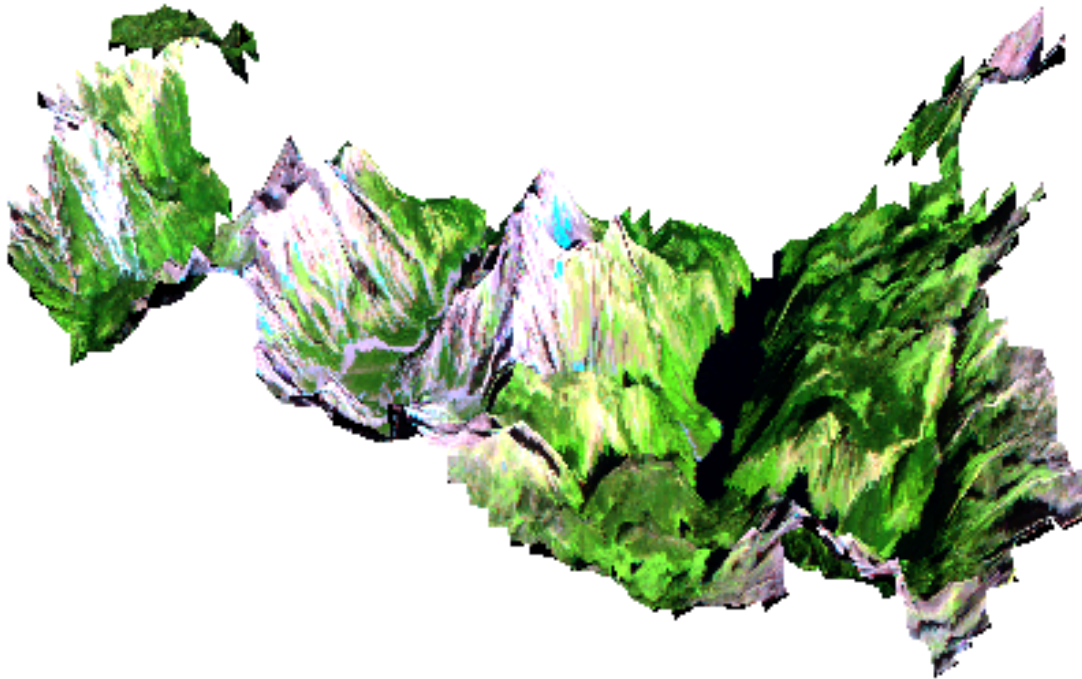
Fig. 34: Perspective view of the landscape – color coding from Landsat TM scene

Infrared aerial photos and field observations are also used as other ancillary sources for recognition of training areas (Fig. 35). All the training areas selected are with known characteristics and class membership.

Infrared aerial photo

Satellite image
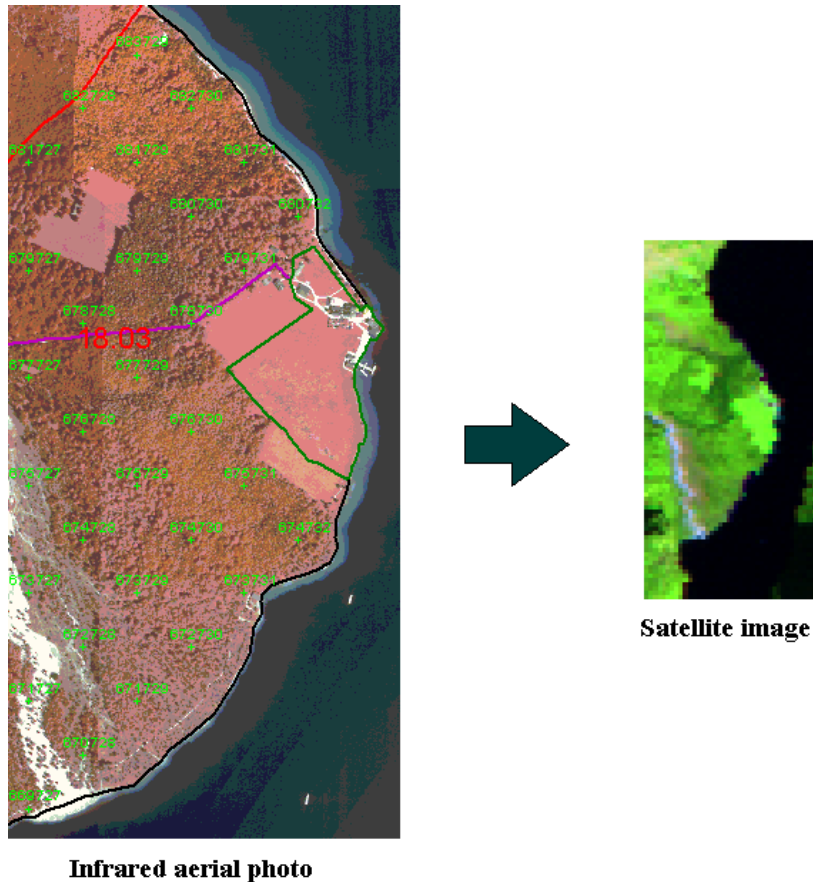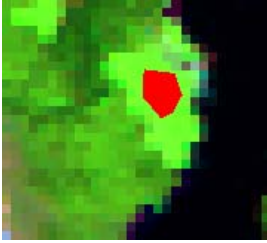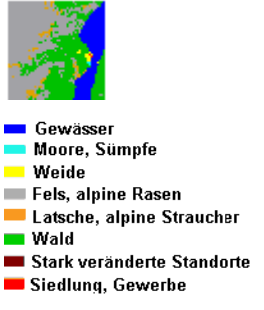
Fig. 35: Using infrared aerial photos as ancillary source in vegetation interpretation

The ground truth biotope map was used as a reference test information. Training sites represent each known land cover category that appears fairly homogeneous on the image. They are located with polygonal boundaries drown on the image display to identify the classes (Fig. 33). The training areas selected were widely distributed over the whole scene. Training sites are used to classify all of the pixels within the image into one of the defined land cover classes (Table 8).

Table 8: Selection of training areas

Training areas	Color composites	Aerial photos	Biotope map	DEM
Class (e.g. ROI - grassland)	543, 321, 432, 754		Gewässer / Moore, Sümpfe / Weide / Fels, alpine Rasen / Latsche, alpine Straucher / Wald / Stark veränderte Standorte / Siedlung, Gewerbe	Elevation 605–611 m

The selection of the training areas was based on the interpretation of a set of color composite images and on the a *priori* knowledge for the investigated region.

Once the training sites are developed the reflectance values are plotted as a function of the band sequence (increasing with wavelength) to derive spectral signatures from the specified regions of interest. For every object class a spectral signature (spectral response) in bands 1 to 7 (except 6) Landsat TM was derived. (Fig. 36)
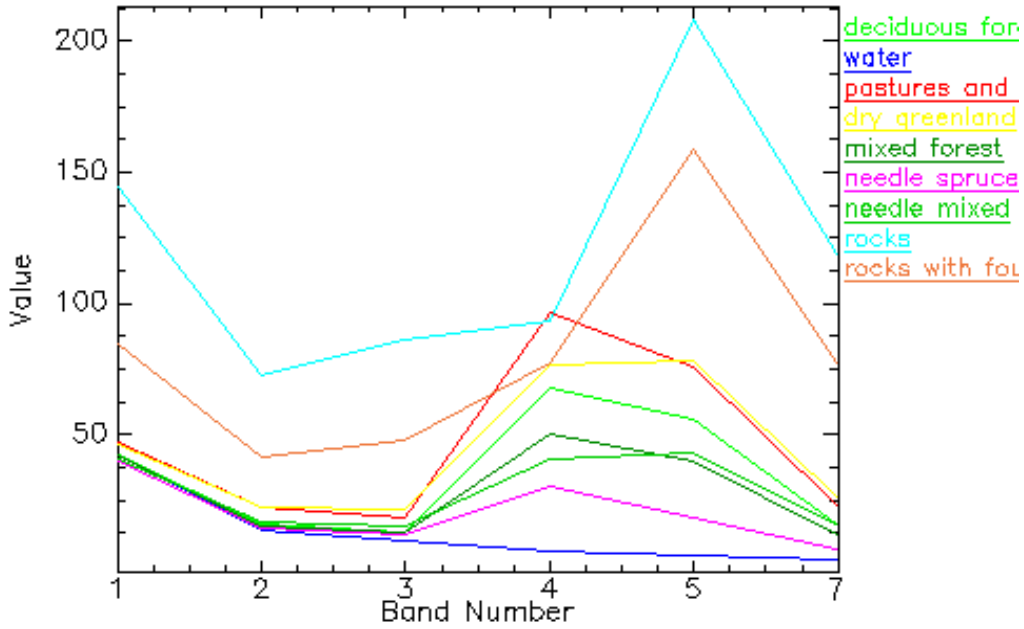
Fig. 36: Class spectral responses – mean values The band 6 (the temperature Landsat band) was excluded from topographic correction, respectively from classification

The vegetation shows its typical spectral response – lower reflectance in band 3; higher reflectance in band near infrared band 4 (refer to Chapter II). Land cover type *rocks* shows the higher reflectance in all bands and *water* (as a very dark object) shows the lowest. Mixed forests show spectral response between deciduous and needleleaf forest (Fig. 36).

2.1.2. Classification

The second basic step in classification is identification of similar objects to the training sites according to spectral characteristics. Each pixel is compared with the various signatures of training objects until all pixels in the scene are identified via the maximum likelihood algorithm. Applications of maximum likelihood classification are well established in the literature of remote sensing (Swain and Davis, 1978; Estes et al., 1983; Schowengerdt, 1983; Sabins, 1986; Lillesand and Kiefer, 2000; Jensen, 1996) (Fig. 37).
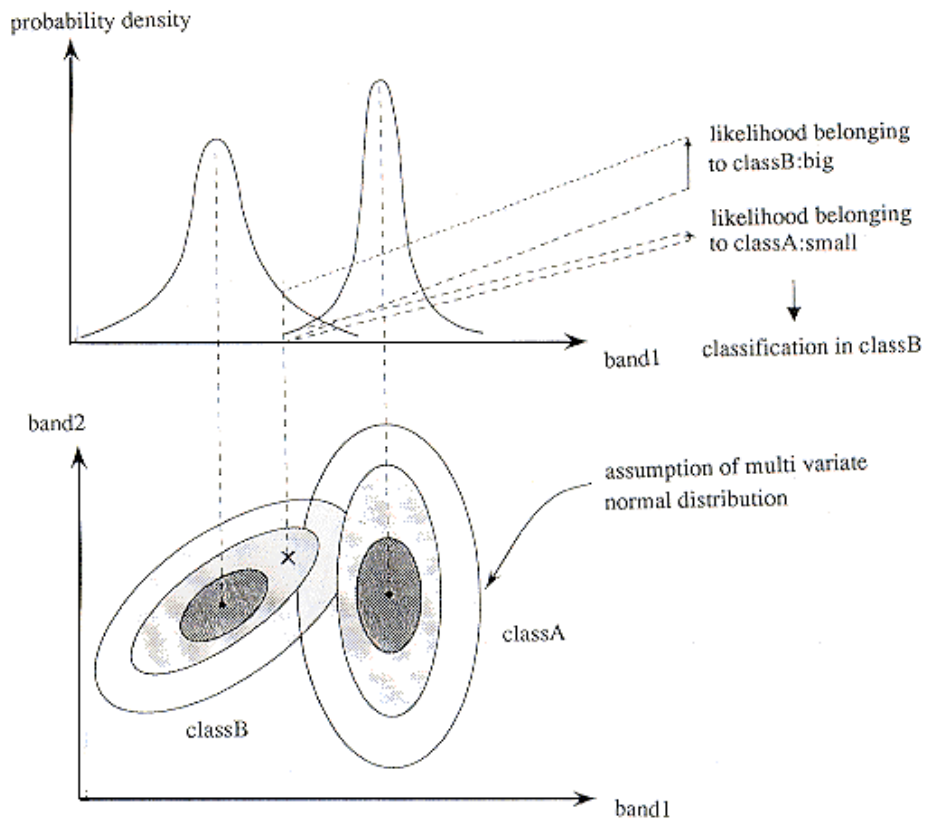
Fig. 37: Concept of maximum likelihood algorithm

The maximum likelihood algorithm assumes that the statistics for each class in each band are normally distributed and calculates the probability that a given pixel belongs to a specific class. Each pixel is assigned to the class that has the highest probability. The full maximum likelihood classifier uses the Gaussian threshold stored in each class signature to determine if a given pixel falls within the class or not. The threshold is the radius (in standard deviation units) of a hyperellipse surrounding the mean of the class in feature space (Lillesand and Kiefer, 2000). If the pixel falls inside the hyperellipse, it was assigned to the class. The class bias is used to resolve overlap between classes, and weighted one class in favor of another. If the pixel did not fall inside any class, it was assigned to the class (0) (unclassified). As an output seven land cover classes were derived and a classification map (Fig. 38) was generated. The spatial distribution of the separate classes was calculated according to the number of pixels in every derived class as described below (Fig. 39).

2.2. Comparison of the remote sensing–derived classification map with a "ground truth" biotope map

In order to compare ground truth data with the supervised classification result, the 153 classes (Fig. 18) in the biotope map (NP Berchtesgaden) were combined into a new map with 7 classes. The initial map was reclassified and the names of the original land-cover categories were also changed to reflect the dominant plant growth forms at the study sites. They are grouped into functional classes selected for forest mask derivation and further extrapolation procedures (refer to appendix B). In this study the forest was separated into 3 main classes – deciduous, needle and mixed forest. At the beginning as the guiding principle for vegetation mapping, physiognomy and structure was used (Küchler, 1988). Each type is physiognomic in character and the classes are first distinguished by the species dominance. According to Küchler (1988), the woody vegetation can be separated on the basis of leaf characteristics, i.e., whether it is evergreen, deciduous broadleaf or needleleaf. In the Alps and in the National Park Berchtesgaden, respectively, the deciduous forest is described as the plants, which defoliate periodically so that they carry no green leaves during a part of the year (*Fagus*

sylvatica, Alnus viridis). The needleleaf forest can be described as the forest type with needle-like leaves (*Picea abies, Pinus mugo* and *Larix decidua*). In this study the term mixed forest is employed in a restricted way to a mixture of broadleaf deciduous, and needleleaf plants. Each of them occupies at least 25% of the area (Küchler, 1988).

Functional aspects are included into the definition of the forest classes. Many attempts have been made to classify biological systems according to functional criteria, e.g. vegetation functional types (Smith et al., 1997; Grime, 1993; Solomon, 1993). Differentiation into "types" assumes similarities in plant or ecosystem functions and structures (Falge et al., 2002a, Körner, 1994, Woodward and Kelly, 1997). Generalization of the seasonal patterns of net ecosystem carbon exchange might be used for vegetation grouping into functional classes. Very important "functional" differences in deciduous and coniferous forest were found from FLUXNET measurements related to annual patterns in net ecosystem exchange of CO_2 as well as CO_2 uptake capacity (Falge, 2002a, 2002b). For example, coniferous forests show lower maximum CO_2 uptake than deciduous forests (Falge, et al., 2002a). This "functional" aspect of the forest types was also taken into account with the forest classes that were assigned.

The third aspect of the forest type definition was the presence along the altitudinal gradient in the Alps. The vegetation is strongly affected by factors changing along the elevation gradient. Within the territory of the National Park Berchtesgaden and also in Stubai and Ötz Valleys, there is a strong differentiation in vegetation distribution according to elevation. (in the **submontane zone** (at 700 m a.s.l.) deciduous forests are dominant; **the montane zone** between 700 m a.s.l. and 1400 (1300) m a.s.l. is comprised of mixed forest; in the **subalpine zone** (1400 (1300) m a.s.l. – 2000 (1900) m a.s.l.) needleleaf forests dominate - refer to Chapter I). These special features in vegetation zonation along the elevation gradient were taken into consideration when forest classes were assigned.

In this study after derivation of the spectral signatures for the defined classes, forest types were separated according to their spectral response and using ground truth data for validation of the defined test areas.

The remote sensing-derived classification map was then compared to the ground truth biotope map (Fig. 38).
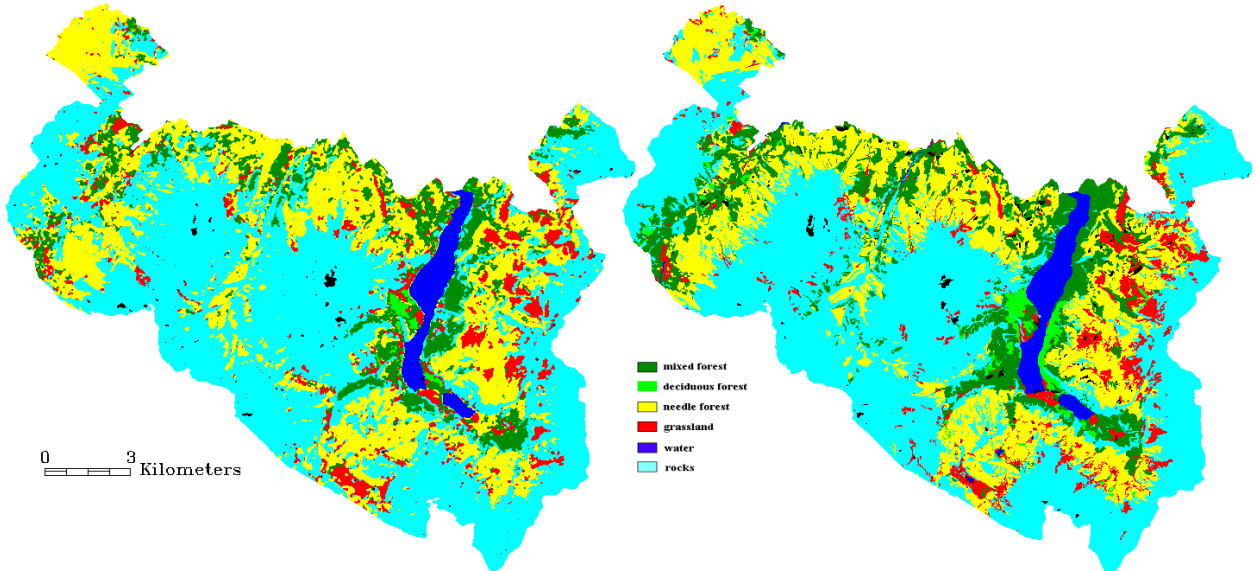
Fig. 38: Supervised classification (left) and ground truth biotope map (right)

The remote sensing-derived land cover map includes 7 classes – coniferous forest, deciduous forest, mixed forest, grassland, water, rocks and unclassified areas. Mixed forest are stands where neither deciduous nor coniferous trees cover more than 75% of the area, in accordance with the definition of UN-ECE/FAO (2000).
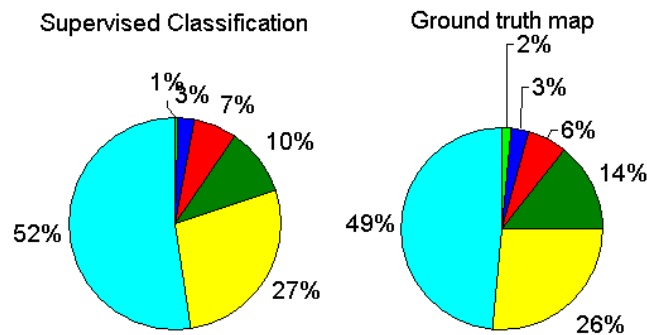
Fig. 39: Spatial distribution of the classes in both maps Percent cover of land surface within Berchtesgaden National Park

Vegetation data were examined with respect to topographic situation. The DEM was separated into four zones – submontane zone (at 600 -700 m a.s.l.); montane zone between 700 m a.s.l. and 1300 m a.s.l; subalpine zone (1300 m a.s.l. – 1900 m a.s.l.);

alpine zone (above 1900 m a.s.l.). The distribution of the vegetation classes along the elevation gradient was estimated (Fig. 40).
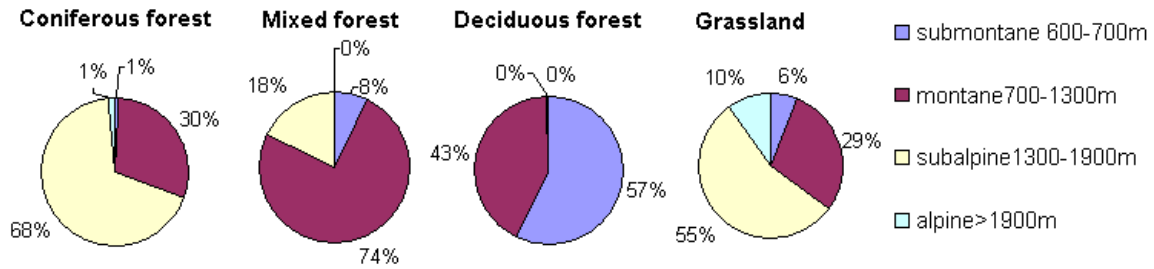
Fig. 40: Elevation distribution of vegetation classes – Berchtesgaden National Park supervised classification

The major part of coniferous forest (68%) is found in the subalpine elevation; 30% is distributed in the montane level. Mixed forest is distributed mainly (74%) as montane forest. Deciduous forest is present in both submontane and montane elevation zones (57% and 43%, respectively). Vegetation class grassland is present in all elevation levels, but mainly at the montane and subalpine levels. 10% of grassland is found at the alpine level.

The distribution of the vegetation classes along the elevation gradient from the "ground truth" map was also calculated (Fig. 41). The results were compared with those after supervised classification. Vegetation classes show similar distribution along the elevation gradient. No significant differences were found.
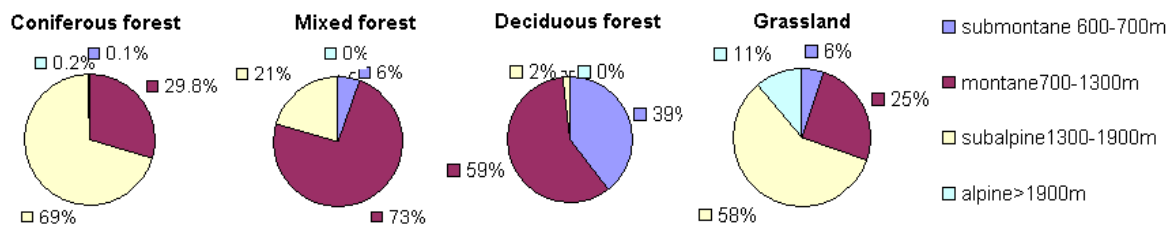
Fig. 41: Elevation distribution of vegetation classes – Berchtesgaden National Park "ground truth" map

In the "ground truth" map, the major part of deciduous forest (59%) is found at montane level. In the remote sensing map, only 43% was identified at this elevation level. 39% of the deciduous forest is distributed at submontane level in the "ground truth" map, while 57% occurs here in the remote sensing map. This class also shows the lowest degree of accuracy according to the confusion matrix report (refer to accuracy assessment). Grassland is present at all elevation levels, but more extensively at montane and subalpine levels.

A greater differentiation in the land cover classes was also considered. A new map with 10 classes was created (Fig. 42). Considering that needleleaf forests include not only evergreen needleleaves but also deciduous needleleaves (*Larix decidua*), the class needle forest can be separated in two distinct subgroups – 1) where *Picea abies* is dominant and 2) where mixed needleleaf forest occurs. The first class combines all pure spruce (*Picea abies*) communities, and the second includes stands where *Larix decidua* occurs simultaneously. Class *grassland* was separated into *pastures and meadows* vs. *dry grassland*. *Pastures and meadows* are intensively managed and include all the grassland except dry types at relatively higher elevation (ski slopes in the case study). Some part of the previous defined class *rocks* was determined as *rocks with alpine grasses*. These are areas at very high elevation (at subalpine level) where patches of alpine vegetation occur. (Schuttflur mit Bewuchs- Bundesamt Für Naturschutz, HRSG, 1995; Kias et al., 1994, 1996) This class shows the same spectral profile as class *rocks* but the values are lower in comparison (Fig. 36).
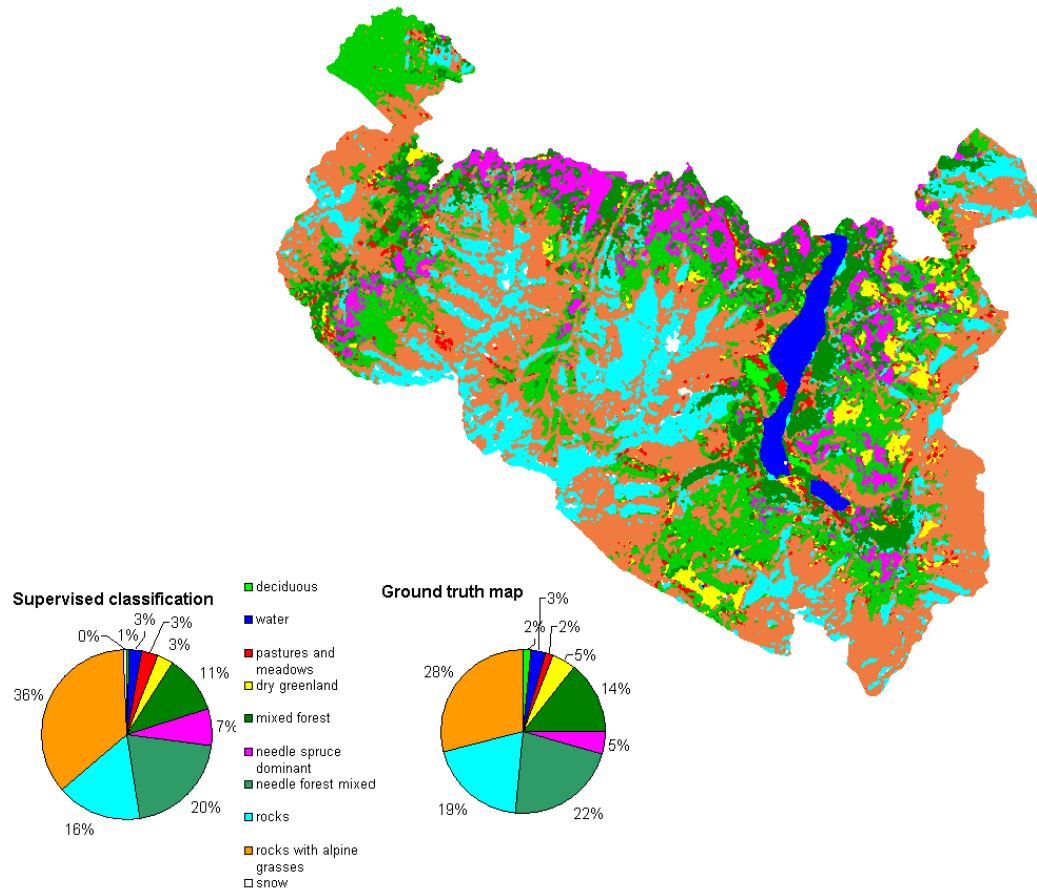
Fig. 42: Land cover map with 10 classes

2.3. Classification accuracy assessment

To show the accuracy of classification results that compares classification results with ground truth information a *Confusion Matrix* (ENVI) was used (refer to Chapter II). It shows the correspondance between the remote sensing-derived classification map and refererence test information ("ground truth map") (Fung and Ledrew, 1988).

To create a Confusion matrix, reference plots on the "ground truth" image were sampled. A method of random sampling (observations are randomly placed) was used (ENVI 3.4; ERDAS, 1994). Each column of the confusion matrix represents a ground truth class; reference data are assumed to be correct. The values in the column correspond to the classification image's labeling of the ground truth pixels. Diagonals represent sites classified correctly according to reference data; off-diagonals were misclassified (Table 9).

Table 9: Confusion matrix report

Class types determined from classified map (%)	Class types determined from reference source (ground truth) (%)						
	unclass.	Water	rocks	Deciduous forest	grassland	mixed forest	needle forest
unclass.	86.96	0	1.28	0	0	0	0
water	0	95.83	0.05	1.38	0	0.25	0
rocks	13.04	1.30	91.51	4.14	12.21	5.82	8.54
deciduous forest	0	0	0	58.62	0	1.52	0
grassland	0	0.26	1.09	8.28	78.8	1.77	0.93
mixed forest	0	0.52	0.2	21.38	1.84	76.2	5.82
needle forest	0	2.08	5.87	6.21	7.14	14.43	84.7
Overall Accuracy	86.0746%						
Kappa Coefficient	0.8051						

An overall accuracy of 86% (number of pixels are also shown) was achieved with a Kappa coefficient of 0.8. The overall classification accuracy is determined by dividing the number of test pixels correctly classified by the number of total test pixels.

A further confusion matrix for the remotely sensed map with 10 land cover classes was produced. The "ground truth" classes were compared with those from supervised classification map (Table 10). An overall accuracy of 86% with kappa coefficient of 0.84 was achieved.

Table 10: Confusion matrix report – Land cover map with 10 classes

Class types determined from classified map (%)	Class types determined from reference source (ground truth) (%)										
	unclass	water	rocks	rocks with alpine grasses	Deciduous forest	dry greenland	pastures and meadows	mixed forest	Needle forest spruce dominant	needle forest mixed	snow
unclass.	100	0	0	0	0	0	0	0	0	0	0
water	0	97.8	0	0	0	0	0	0	0	0	0
rocks	0	0.44	74.3	3.74	0	0	0	0	0.85	0	14.8
rocks with alpine grasses	0	0	24.3	95.3	4.4	6.1	5.9	1.6	0.85	3.05	3.7
deciduous forest	0	0	0	0	63.	0	0	2.4	0	0	0
dry greenland	0	1.3	0	0.47	0	90.2	5.9	0	0	0	0
pastures and meadows	0	0	0	0.47	4.4	3.7	88.2	1.6	0.85	0	0
mixed forest	0	0	0	0	17.4	0	0	79	5.1	0.76	0
needle forest spruce dominant	0	0	0	0	0	0	0	3.2	88	4.96	0
needle forest mixed	0	0	0	0	10.9	0	0	10.5	4.3	91.2	0
snow	0	0.44	1.38	0	0	0	0	0	0	0	81.5

Overall Accuracy	86.9118%
Kappa Coefficient	0.8481

3. Discussion and conclusion

The ability to identify land cover classes using satellite images offers the possibility of frequent monitoring over large areas. The analysis of land cover characteristics is an important aspect in the process of understanding high mountain ecology. The present study combines a GIS and remote sensing data to produce a remote-sensing-based land cover map for National Park Berchtesgaden.

The classification of land cover in Berchtesgaden National Park is based on Landsat TM data but includes information from other ancillary sources – DEM, ground truth map, field studies, etc. A number of color composite images were created for better recognition of land cover types. The definition of the training areas was based on all of these data. Satellite data together with ancillary information provides more accurate discrimination of land cover types. All methods used for land cover mapping depend on various parameters (e.g., number of classes, number of training areas, DEM, ground truth polygons, etc.) which directly influence the computational complexity and the classification performance.

An important preliminary step in the classification procedure was the topographic correction of the satellite scene. The influence of topography, especially in mountain areas, is very large and leads to errors in definition of land cover types. Spectral classification alone is not sufficient for extracting land cover data. Special problems encountered during classification due to illumination effects and topographic shading were resolved using a radiation model based on an approach by Parlow (1986). The model made use of the Digital Elevation Model, deriving additional layers (slope, aspect, horizon, sky view factor) for the calculation of a topographic correction matrix. The accuracy of the classification results was increased by using these topographic corrections.

The ground truth biotope map of Berchtesgaden National Park was used as a reference map for testing the classification accuracy. The estimates of the land cover types were mainly based on the previous classification (ground truth biotope map) for which the true class membership was known. This reduces possible errors by selection of the most appropriate training areas.

The digitized "ground truth" map was used together with the remotely-sensed land cover map to produce a matrix of correspondence (Confusion matrix – ENVI 3.4.) linking the two classifications. Comparing remote sensing and ground truth map a satisfactory overall accuracy (86%) was achieved. Best classification results are obtained for spectrally distinct classes like *water* or *rocks* with 95 and 91%, respectively. Highest inaccuracies occurred in the class *deciduous forest*. Only 58.6% of deciduous forest are correctly classified, the remaining 41.4% are classified either as *mixed forest* (21%) or as *needle forest* (6%) and *grassland* (8%), resulting from the low spatial resolution of the sensor data, which leads to many pixels with mixed spectral characteristics in areas with overlapping classes. The class *deciduous forest* is in confusion with all other classes perhaps because as well they cover a very small area in the park.

Some accuracy assessment errors in different classes are possible because of the nature of the classified objects. For example some of the pixels belonging to classes *needle forest* and *deciduous forest* are put into the class *mixed forest* and vice versa. Some pixels of class *grassland* fall into the class *rocks*. A part of the areas included in class *rocks* are covered with alpine grasses and have spectral signatures corresponding to class *rocks*, not to class *grassland* (and vice versa).

Other reasons for assessment error is the location of ground truth polygons in the reference biotope map produced by the National Park investigators. In reality the use of different criteria in the definition of land cover types in each classification means that satellite and "ground truth" cover types cannot be considered directly equivalent (Cherrill A.J. et al., 1995). The reference data are assumed to be correct, which is also relative (Congalton 1991, Congalton and Green 1999b; Jensen J. 1996). The ground data are just another classification which may contain error (Congalton R.G., 1999a; Khorram S., 1999; Lunetta R. S. et al., 2001; Zhou, Q. et al., 1998). The ground truth map is based on orthophotos, while the remote sensing map on satellite images. The ground truth map combines data obtained between 1995 and 2003, while the supervised classification considers the exact moment of time on 13.09.1999 during satellite overpass. Therefore, the accuracy assessment of the satellite-derived land cover map was deemed satisfactory. Considering the accuracy assessment of the 10 class map, one finds an improvement in the correspondence between "ground truth" and remote sensing classes (Table 11). The

differentiation of coniferous forest into two classes (*needle mixed* and *needle with spruce dominant*) lead to better correspondence with "ground truth" classes (91% and 88%, respectively).

The *deciduous forest* class shows 63% degree of correspondence in the new map compared to the first one (58%). *Mixed forest* shows 3% improvement. Separation of grassland into *pastures and meadows* and *dry grassland* also leads to better results.

Table 11: Accuracy assessment comparison

Class	% correspondence land cover map (6 classes)	% correspondence land cover map (10 classes)
unclass.	87	100
water	95.8	97.8
rocks	91.5	74.3
rocks with alpine grasses	-	95.3
deciduous forest	58.6	63
dry greenland		90.2
pastures and meadows	78.8	88.2
mixed forest	76.2	79
needle forest spruce dominant	84.7	88
needle forest mixed		91.2
snow	-	81

The derived spectral signatures of the defined test areas were further used in an extrapolation procedure to map land cover in Stubai and Ötz Valley. Extrapolation of the results to other test areas in the Alps (Stubai and Ötz Valleys) requires accurate remote-sensing-based mapping and interpretation of vegetation at the reference test site, i.e., the National Park Berchtesgaden. The derived classification map was used to create a forest mask, which was essential in the algorithm for prediction LAI at the investigated sites (refer to Chapter V).

IV. CONCEPT OF BUILDING AN EXTRAPOLATION TOOL FOR INTERPRETATION OF VEGETATION IN STUBAI AND ÖTZ VALLEYS

1. Summary

Satellite imagery allows the construction of maps for otherwise inaccessible or non-investigated regions, where other data sources do not exist.

Some particular areas in the Alps were used to test the possibility of extrapolating the land cover classification in Berchtesgaden National Park along elevation gradients. Stubai Valley is an area of study for the European ECOMONT and CARBOMONT projects, and the Ötz Valley is an area investigated in the GLOWA-DANUBE project. Both projects provide data such as Digital Elevation Models, LAI "ground truth" maps, land cover maps, etc., which could be used for further validation of procedures developed within this study. Also they are typical examples for land use in the Central Alps with strong elevation influences on the vegetation.

The classification map of National Park Berchtesgaden was a key element in extrapolation procedure. It was used as a primary reference map for the distribution of the vegetation in these other alpine regions. The specified spectral signatures of the training areas in Berchtesgaden were used together with maximum likelihood algorithm for classification of land cover in Stubai and Ötz Valleys, Austria. Land cover maps with the same number of classes as in Berchtesgaden were derived. The results were compared with ground truth maps (Stubai Valley).

2. Results

2.1. Extrapolation procedure

A vegetation map for the Stubai and Ötz Valleys in Austrian Alps based on vegetation classification techniques developed for the Berchtesgaden National Park was derived within this study. Before using satellite images for both regions (Stubai and Ötz Valleys) atmospheric correction (dark subtraction) and topographic correction (Parlow, 1996)

were applied as for correction of Berchtesgaden satellite data (refer to Chapter II, image preprocessing).

The extrapolation was based on the ground observation data collected at permanent test sites in the National Park Berchtesgaden and satellite remote sensing data – Landsat 5 TM and Landsat 7 ETM+ (Fig. 43).

Conception of building extrapolation tool

Endmember collection Extrapolation

Apply Maximum Likelihood Classifier

Vegetation interpretation and classification Stubaital and Ötztal
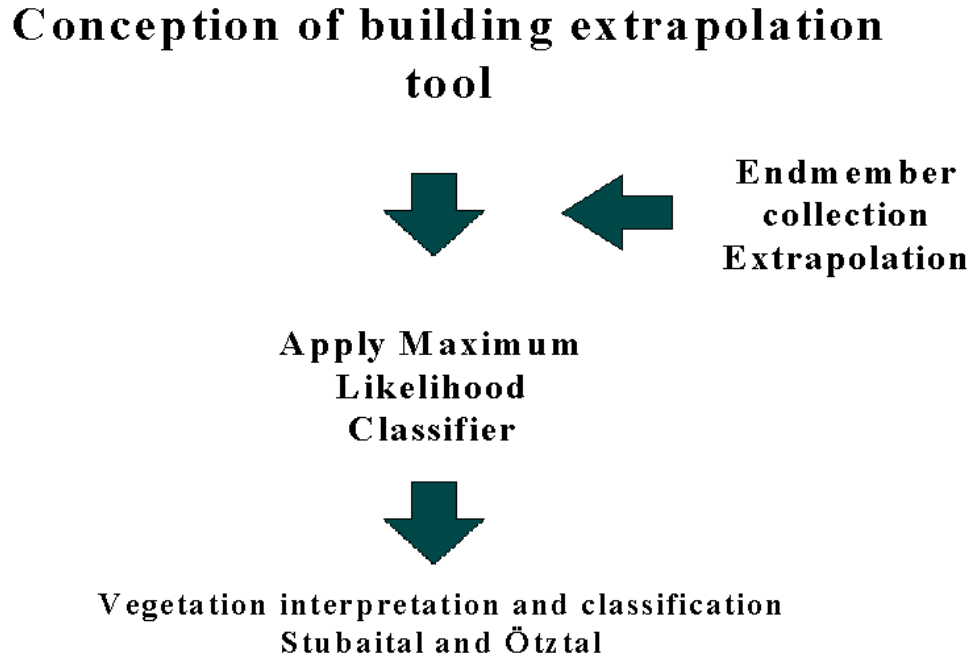
Fig. 43: Strategy for extrapolation of the Berchtesgaden classification

Both regions were masked and the valleys were isolated. For interpretation, a set of color composite images the same as in Berchtesgaden National Park were created. A maximum likelihood algorithm with training site data (Regions of interest) derived from the Berchtesgaden National Park map was applied. The ENVI routine *Endmember Collection* was used for the procedure, which extracts the reflectance values (spectral signatures) for all the classes in the Berchtesgaden map. Then the same spectral signatures were used as input for classification of the Stubai and Ötz valleys. Land cover maps for those areas were created (Fig. 44).
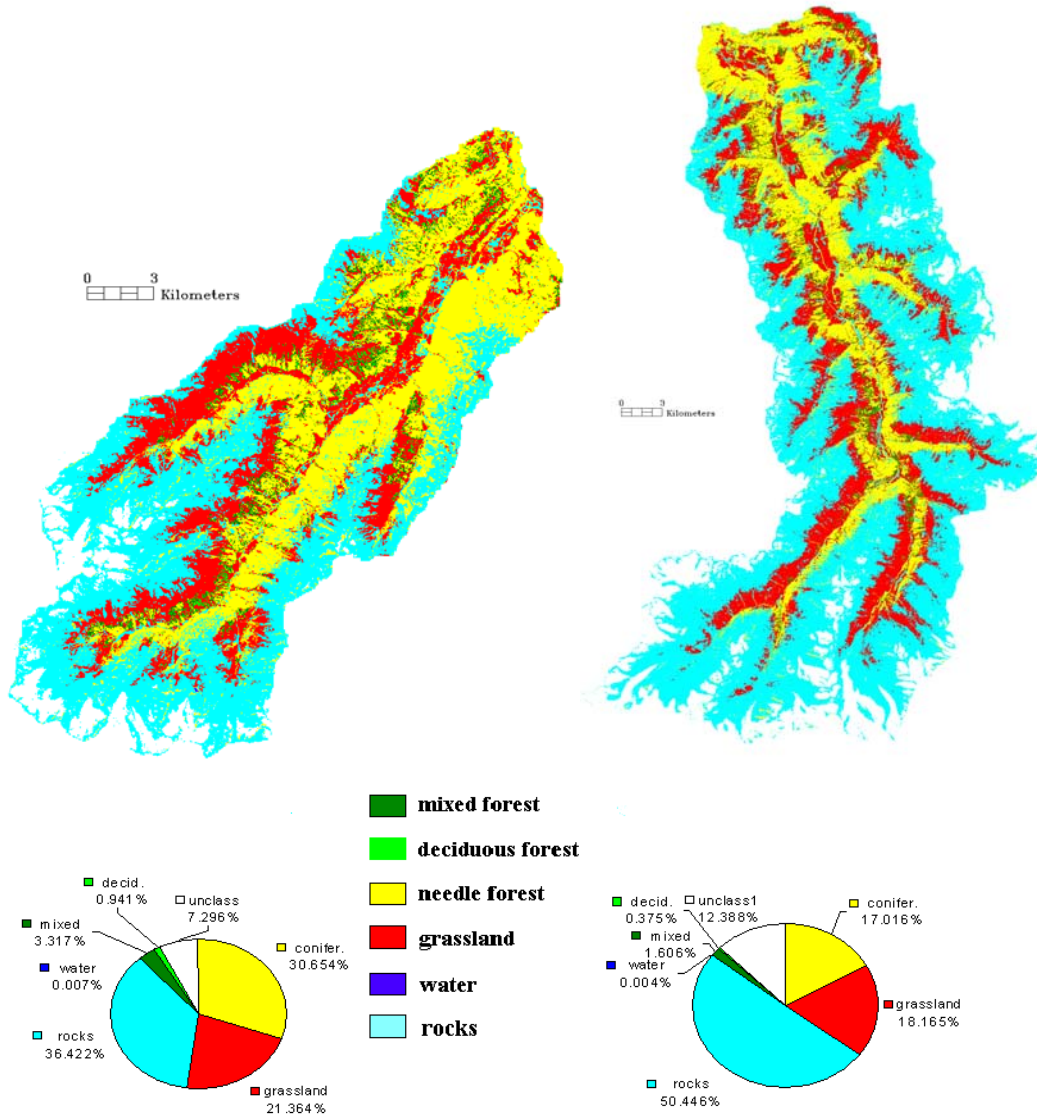
Spatial distribution of the classes– percent cover of land surface within Stubai and Ötz valley

Fig. 44: Classification map of Stubai and Ötz Valleys – after extrpolation

According to the supervised classification the percent cover of the derived classes was calculated. In both test sites on the unglaciated areas above 2300 m, the dominant natural surface types are moraine, bare rock, sedges, grasses and dwarf shrubs. Below 2300 m, coniferous forests and cultivated meadows are the main vegetation types.

Vegetation data were analyzed quantitatively using the digital elevation model. The DEM was separated into four zones – submontane zone (at 650 -1000 m a.s.l.); montane zone between 1000 m a.s.l. and 1750 m a.s.l; subalpine zone (1750 m a.s.l. – 2300 m a.s.l.);

alpine zone (above 2300 m a.s.l.) (Kilian, et. al.,1994). The distribution of the vegetation classes along the elevation gradient was calculated (Fig. 45).
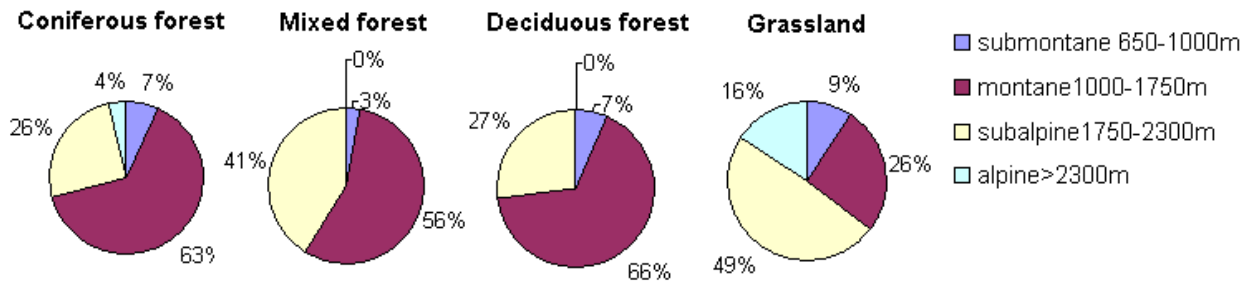
Fig.45: Elevation distribution of vegetation classes – Stubai Valley

In Stubai Valley the major part of coniferous forest (63%) is distributed at montane elevatation level. 26% are distributed at subalpine level. Mixed forest is distributed mainly at montane and subalpine levels (56% and 41%, respectively). Deciduous forest is present at montane and subalpine elevation levels (66% and 27%, respectively). Only 7% of deciduous forest is present at submontane level. The vegetation class grassland occurs at all levels, but mainly in the montane and subalpine. 16% of grassland is distributed at alpine level.
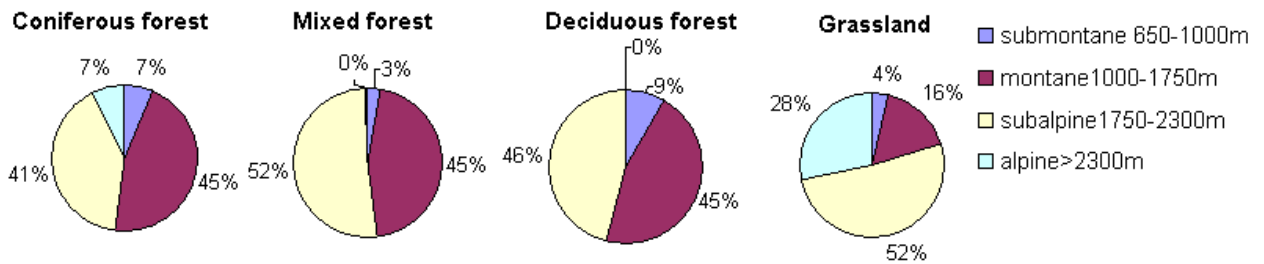
Fig. 46: Elevation distribution of vegetation classes – Ötz Valley

Similar distribution of vegetation classes can be found in the Ötz Valley (Fig. 46). 45% of conifeorus forest are distributed at montane elevation and 41% - at subalpine level. 45% of mixed and deciduous forest, respectively, are distributed at montane elevation, and 52% (mixed forest) and 46% (deciduous forest) at subalpine elevation. The vegetation class grassland is present at all elevations, but mainly at subalpine and alpine levels (52% and 28%, respectively). 16% of grassland is distributed at montane level.

2.2. Comparison with ground truth reference data

For validation of the results after extrapolation, a comparison between the supervised classification map and ground truth data was carried out. As a reference, a ground truth land use map for Stubai Valley was used. It is based on CIR – images and was created for investigating land-use changes in European terrestrial mountain ecosystems (as a part of ECOMONT project) (Fig. 47).

Lebensräume
- See
- Kies- und Schotterbank
- Latschengebüsch
- Nadelwald der subalpinen Stufe
- Nadelwald der montanen Stufe
- Gehölzbestände auf Felsflur
- Grünerlengebüsch
- Naß- und Feuchtwälder
- Mischbestand: Feuchtwald-Nadelwald
- Laubwald
- Laub-Nadel-Mischwald
- Gletscher, oder permanentes Schneefeld
- Felslebensraum des Hochgebirges
- Felslebensraum der planaren bis subalpinen Stufe
- Blockhalden oder Schuttflurgesellschaften des Hochgebirges
- Blockhalden oder Schuttflurgesellschaften der planaren bis subalpinen Stuf
- Natürliche alpine Rasen
- Verbrachte Wiesen und Weiden
- extensiv genutztes Grasland
- mäßig intensiv bewirtschaftetes Grünland
- intensiv genutztes Wirtschaftsgrünland
- Lärchwiese/ -weide
- Siedlungsraum
- Parkplätze
- Pilotprojektgebiet

Fig. 47: Land use map – Stubai Valley

The remote sensing derived map was cut to correspond to that from CIR, and then co-registered to the map. The ArcInfo shape file was converted into grid and resized to 30m resolution – the same as the supervised classification resolution. The land use categories of the CIR map were combined and organized into a new map with 7 distinct classes identical to the satellite based land cover classes (refer to appendix C) (Fig. 48).
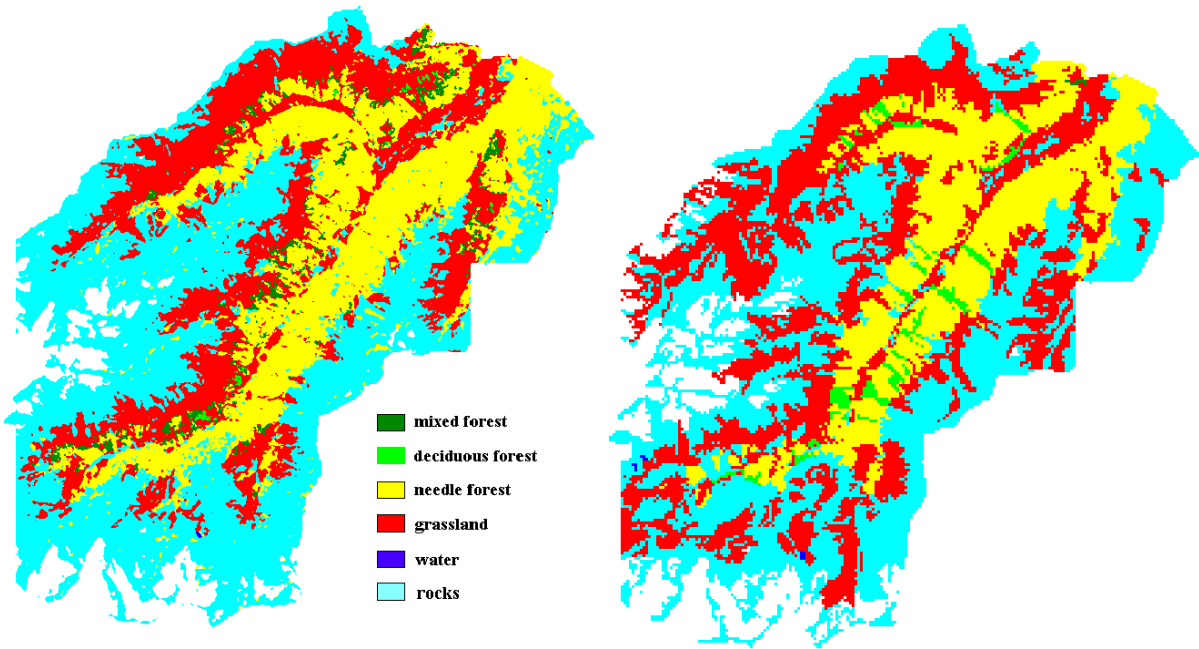
Fig. 48: Remote sensing map (left); ground truth map (right) with the same number of classes. The percent cover of classes was calculated (Fig.49).
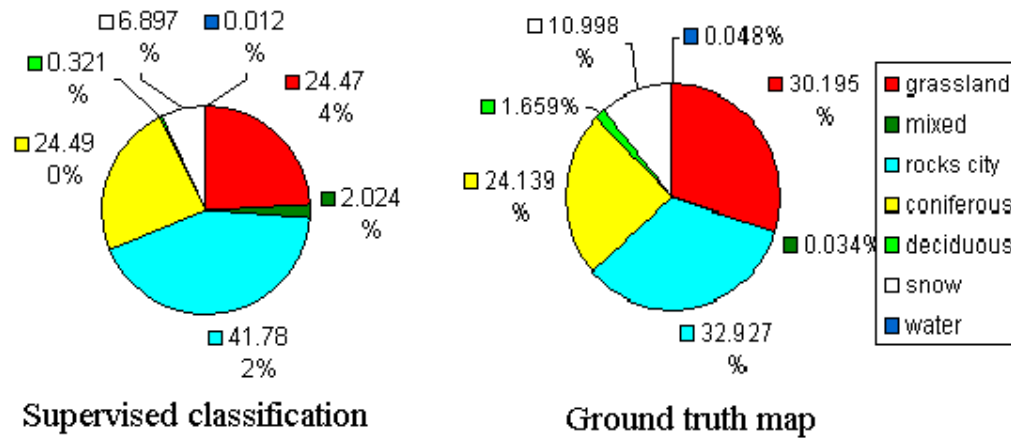
Fig. 49: Spatial distribution of land cover classes – Stubai Valley

Visual interpretation shows that there are not large differences between maps. One more class was required in the Stubai and Ötz Valleys, namely *snow*. The differences in percentage cover between the two maps depend on the nature of the land cover types. They are shown and explained in details in the confusion matrix report.

2.3. Classification accuracy assessment

For accuracy assessment of the derived maps, the same approach as in Berchtesgaden was used. For creation of the confusion matrix, an arbitrary number of reference plots on the ground truth image were sampled randomly (Congalton and Green, 1999b; ENVI, 2000; ERDAS, 1994). An overall accuracy of 81% was achieved with a Kappa coefficient of 0.82. Each column of the confusion matrix represents a ground truth class (reference data assumed to be correct). The values in the column correspond to the classification image's labeling of the ground truth pixels. Diagonals represent sites classified correctly according to reference data; off-diagonals were misclassified. The overall classification accuracy is determined by dividing the number of test pixels correctly classified by the number of total test pixels (Table 12).

Table 12: Confusion matrix report

Class types determined from classified map (%)	Class types determined from reference source (ground truth) (%)							
	unclass.	water	rocks	deciduous forest	grassland	mixed forest	needle forest	snow
unclass.	100	0	1.66	0	0	0	0	0
water	0	28.6	0	0	0	0	0	0
rocks	0	66.7	90.9	0	6.7	0	0.5	30.5
deciduous forest	0	0	0	48.2	0	0	0.22	0
grassland	0	0	4.15	1.9	91.9	25	3.5	0
mixed forest	0	0	0	20.4	0.08	37.5	2.7	0
needle forest	0	4.8	2.07	29.6	1.3	37.5	93	0
snow	0	0	1.24	0	0	0	0	69.5

Overall Accuracy	87%
Kappa Coefficient	0.8189

3. Discussion and conclusion

A remote sensing approach for extrapolating land cover information from the well known and investigated region to other test areas was appropriate, especially given the broad similarities of topography, climate and vegetation across this part of the Alps and the availability of similar satellite imagery. The methodology used in this study gives the possibility for comparison between field data and remote sensing data. Combining both data sets leads to improvement of the results in describing heterogeneity of the landscape. A remote sensing approach for extrapolation of the results from National Park Berchtesgaden to Stubai and Ötz Valleys was possible because of the following:

- the climate, physiography, substrates, vegetation, altitude in Berchtesgaden are similar to those in Stubai and Ötz Valleys

- all the regions belong to the Alps and are subject to the strong gradients in climate in the mountains and in the mountain-forelands

- both satellite scenes used in this study are Landsat scenes

- the same satellite bands are used for classifications – 1 to 7 except band 6 (the temperature band)

- the same classification algorithm was used – Maximum Likelihood algorithm

- there is just one day difference in the acquisition date of both scenes used in this study - 13.09.1999 and 14.09.1999 – variation in sun elevation and azimuth was minimized

- the model used for topographic and atmospheric correction was the same

- atmospheric correction normalized the atmospheric scattering and atmospheric absorption influences on NDVI

Some accuracy assessment errors in different classes are possible because of the nature of the classified objects and the algorithms and techniques used for producing both maps: 1) the reference data are assumed to be correct, which is also relative; (Congalton 1991, Congalton and Green 1999b; Jensen J., 1996); 2) the ground truth map is based on orthophotos, while the remote sensing map is based on satellite images; 3) the ground truth map combines data from different years and field studies, while supervised classification is done in exact moment of time on 13.09.1999;

For example, there are differences with respect to the class *snow*. The snow cover recorded by satellite is for the exact acquisition date and time. The ground truth snow cover class utilizes average data from different years. As seen from the pie diagram (Fig. 49), supervised classification shows about 4% less snow cover than the reference map. The confusion matrix shows that 30% of class *snow* from the reference map was classified as *rocks* in the remote sensing map. Some pixels of class *grassland* fall into the class *rocks*. A part of the areas included in class *rocks* are covered with sparse alpine grasses and have spectral signatures corresponding to class *rocks*, not to class *grassland* (and vice versa). About 20% of class *deciduous forest* are associated with class *mixed forest*, and about 29% with class *needle forest*. This is not a function of mixing of the reflectance values of the land cover classes. The dominant species in deciduous forest in Berchtesgaden is *Fagus sylvatica*, but in Stubai Valley *Alnus viridis*. Therefore, there are differences in spectral signature for deciduous forest. There are not significant differences in class coniferous forest. It covers 24% of the area and has 92% of accuracy according to the confusion matrix.

The elevation distribution of vegetation classes at the investigated sites shows some differences (Fig. 40, Fig. 45 and Fig. 46). 68% of the coniferous forests in Berchtesgaden National Park are distributed at subalpine level. These for Stubai and Ötz Valleys are respectively 26% and 41%. The major part of coniferous forest in Stubai and Ötz Valleys is distributed at montane elevation level (63% and 41%, respectively). In Berchtesgaden National Park, deciduous forest is distributed only at submontane and montane elevation level (57% and 43%, respectively). In Stubai and Ötz Valleys, it is mainly distributed at montane and subalpine level (66% and 27%, respectively in Stubai Valley; and 45% and 46%, respectively in Ötz Valley. Only 7% (Stubai Valley) and 9% (Ötz Valley) of deciduous forest is distributed at submontane level in comparison with Berchtesgaden where this is 52%. *Alnus viridis* and *Sorbus aucuparia* are the dominant species of deciduous forest in Stubai and Ötz Valley. This is a natural subalpine forest community with a mainly inner-alpine distribution. (Cernusca et.al., 1999) The dominant growth form in deciduous forest in Berchtesgaden is *Fagus sylvatica* with mainly submontane distribution (600-700m a.s.l.).

V. LANDSCAPE LAI VARIATIONS ALONG THE ELEVATION GRADIENTS IN THREE TEST AREAS IN THE ALPS – NATIONAL PARK BERCHTESGADEN, STUBAI VALLEY AND ÖTZ VALLEY

1. Summary

Leaf area index (LAI), the leaf area per unit ground area is one of the most important parameters determining gas exchange (water loss and carbon gain) of forests. Leaf area index is an important measure of forest productivity and a key variable for forest process models. Parameterization of these models could be improved if LAI estimates are reliably obtained by using remotely sensed imagery and terrain variables. The current investigation is directed to obtaining spatially distributed data on LAI in complex terrain. Leaf area index can be quantified using indirect satellite remote sensing methods. They provide a unique way to obtain the distributions of LAI over large areas. Green leaves absorb more visible radiation for photosynthesis and less near-infrared radiation. Reflectance in red and near-infrared wavebands is used to derive vegetation indices as indicators of vegetated surfaces. Mapping LAI from Landsat TM or ETM+ has largely depended on empirical relationships derived from single-date spectral vegetation indices. The most frequently used to derive LAI are Normalized Difference Vegetation Index (NDVI) and its counterpart, the Simple Ratio (SR) (Chen J.M. and Cihlar J., 1996; Fassnacht et al., 1997; White et al., 1997).

Empirical models are important tools for relating field measured (or allometric derived) biophysical variables to remote sensing data. A number of empirical algorithms, which relate LAI to spectral vegetation indexes derived from remote sensing data, were developed in this study. Landsat TM data with 30m resolution pixel size used in this study were suitable for comparison with the ground truth data. A thematic map of forest leaf area index was produced in National Park Berchtesgaden. The same empirical relationships derived for Berchtesgaden were used for extrapolation to Stubai and Ötz Valleys in the Alps. LAI maps for both regions were derived.

2. Results

2.1. Strategy for derivation of remotely sensed LAI map

In order to map LAI in the selected mountain region, a Landsat 5 TM scene from 14.09.1999, NDVI index and SR index were examined together with forest inventory data of the Berchtesgaden National Park. Before using the Landsat TM data, an atmospheric correction was applied. A method of dark subtraction was used (refer to Chapter II, image preprocessing). Both raster images (LAI map and Landsat scene) were co-registered using image-to-image registration procedures (ENVI 3.4). The strategy is based on establishing empirical relationships between both datasets, i.e., LAI „ground truth data" and remote sensing vegetaion indices (NDVI and SR) (Fig. 50). Some other ancillary data sources were included – DEM, forest mask, etc.
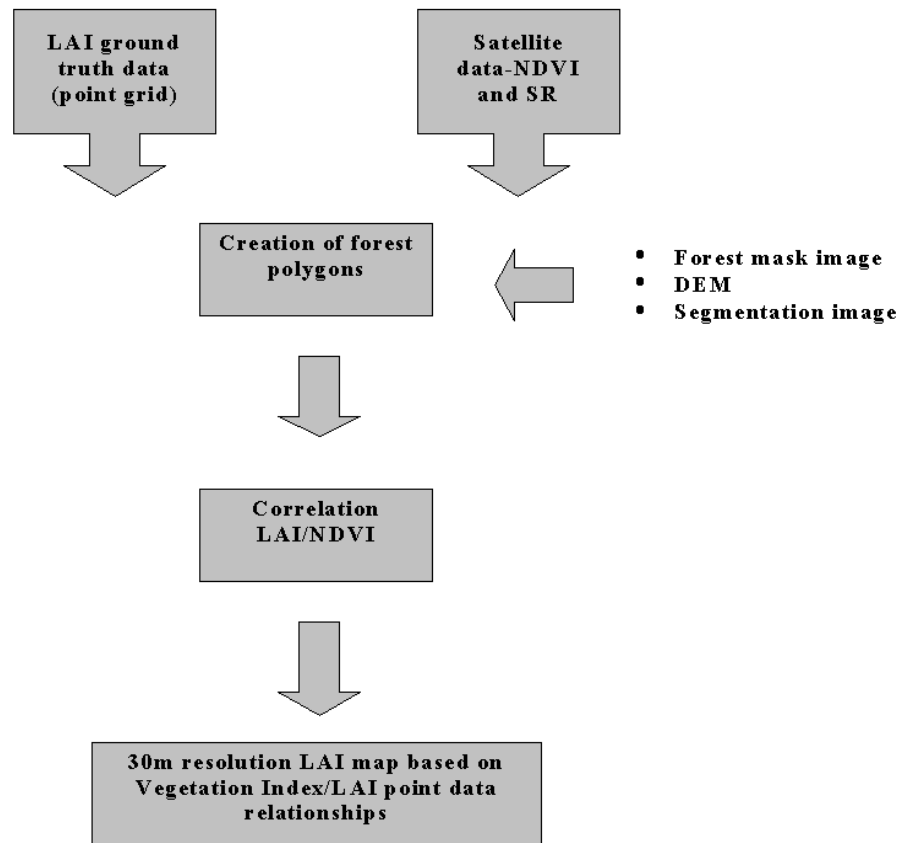

Fig. 50: Flow diagram of the research procedure

Extracting the forest mask

As a first step for supervised classification from the Landsat image, all of the areas covered with forest were separated. Coniferous, deciduous and mixed forests were masked and the extracted forest masks were used to develop correlations with ground truth data (Fig. 51).
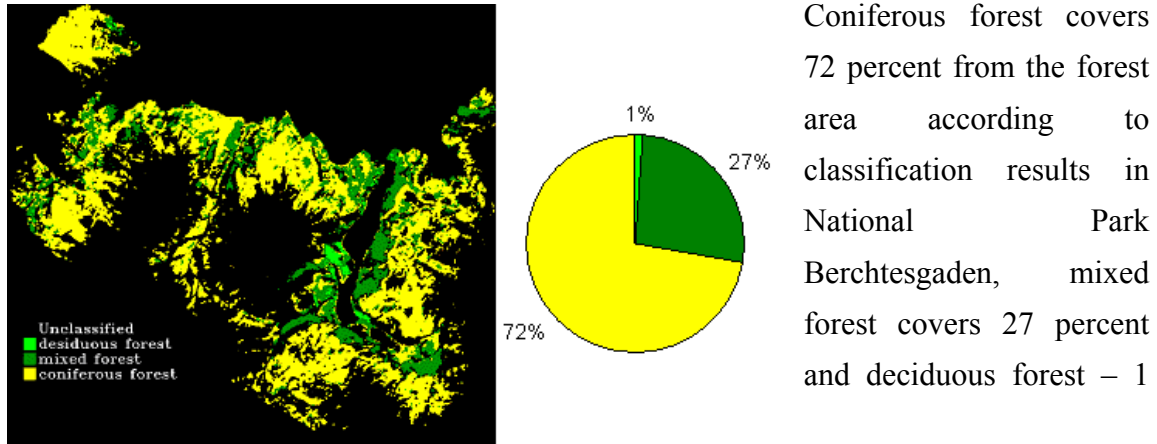

Coniferous forest covers 72 percent from the forest area according to classification results in National Park Berchtesgaden, mixed forest covers 27 percent and deciduous forest – 1

Fig. 51: Extraction of forest mask – deciduous, coniferous and mixed forest

Calculating NDVI and SR

For the forest area, both vegetation indices were calculated from bands 3 and 4 of Landsat TM. NDVI was calculated from the red portion of the visible and near infrared radiation (refer to Chapter II, vegetation indices) (Fig. 52):

$$NDVI=NIR-RED/NIR+RED=TM4-TM3/TM4+TM3$$

The Simple Ratio (SR) image, which is the ratio of near infrared to red reflectance, was also calculated (Fig. 52):

$$SR=NIR/RED=TM4/TM3$$

For forested sites, NDVI ranged from 0.45 to 0.85, while the SR varied from 2 to 9.
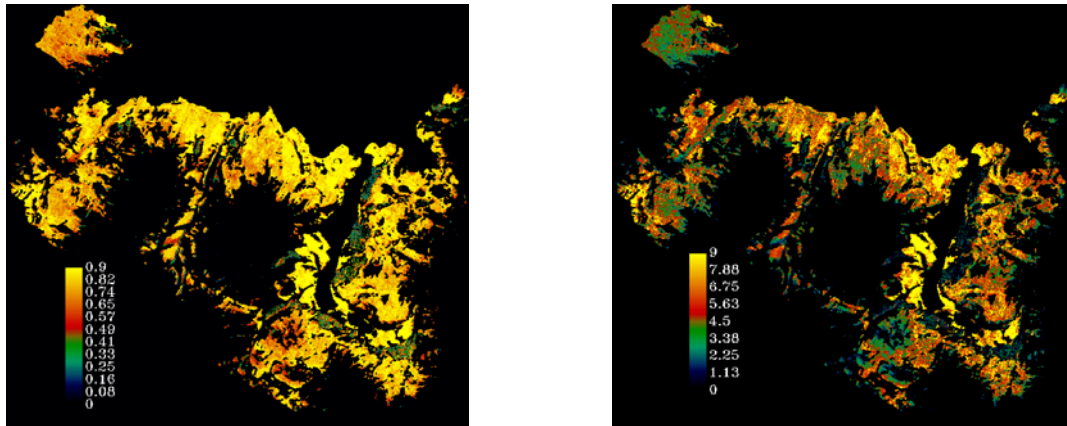
Fig. 52: NDVI (left) and Simple Ratio (right) – National Park Berchtesgaden

LAI data derived from forest inventory

Over the territory of the National Park Berchtesgaden a raster grid with 200 by 200 m squared cells was created. For each of the forest stands (grid cells), a number of stand parameters was measured - stand age, tree height, stand density, soil depth, DBH (diameter at breast height). The data were stored in a GIS (ArcInfo).

According to the forest type map (derived from CIR-biotop and -vegetation maps), leaf area index was calculated using allometric relationships (relating tree size and leaf area) as derived from tree harvests together with the forest inventory database. LAI was calculated separately for coniferous forest, deciduous forest and mixed forest using the following correlations (Fig. 53). Coniferous and deciduous trees are treated as spruce (*Picea abies*) and beech (*Fagus sylvatica*). For the mixed forest the mean value from both datasets was used. The ground truth LAI map in raster format was created with ArcInfo software.
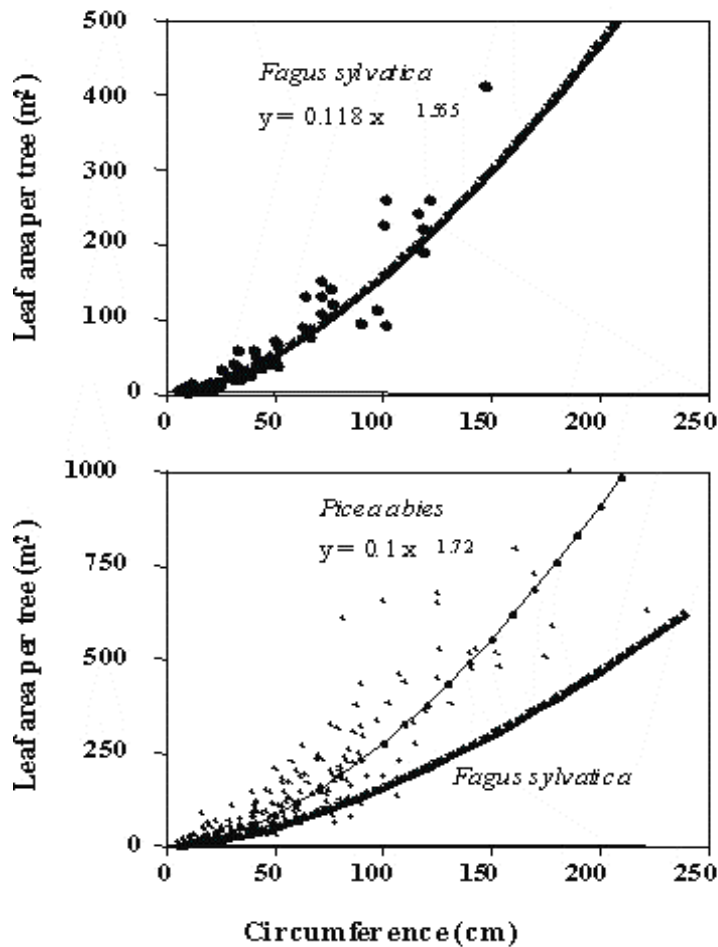
Fig. 53: Allometric relationships used for derivation of LAI Allometric relationships for *Picea abies* are after Alsheimer M. , 1997; Faltin W. (unpublished); Burger H., 1939; 1942, 1953; and for *Fagus sylvatica* – after Granier, A. (unpublished); Burger H., 1945; Bartelink HH., 1997; Pellinen P., 1986;

The LAI data were derived for every measured forest stand (grid cells respectively) (refer to Chapter II, data collection). This point grid map was used for further correlation with remote sensing vegetation indices.

Image segmentation and derivation of homogeneous forest polygons

Although a large effort was made to obtain high precision in the image to image registration between the „ground truth" and remote sensing maps, there is no guarantee that the sample point with LAI data on the ground corresponds exactly to specified satellite pixel. By co-registration of two digital images, there is always a geolocation error. Additionally, the LAI point grid data were obtained via allometric relationships and are extrapolated within the 200x200m grid, which also leads to registration error. LAI values represent leaf area not for a single tree but for the forest stand.

According to the principles of remote sensing, pixels from an image are assumed to be representative samples of objects (Lillesand and Kiefer, 2000). In reality, individual pixels often cover parts of two or more objects on the ground, resulting in mixed pixels. Thus the effectiveness of the analysis is undermined. Conversely, individual pixels could be small relative to the earth objects. Then the internal variance of the objects affects the analysis (Tian et al., 2002a, 2002b; Wang et al., 2003; Wang, 2002; Macdonald and Hall, 1980; Cushnie, 1987). Therefore, comparing single pixels of the satellite image with LAI point data can not be considered as representative. Single pixels NDVI values should not be correlated with the equivalent LAI value for that pixel. The ideal situation occurs when the analyzed elements on the ground correspond directly to homogeneous objects in the satellite scene (Tian et al., 2002a, 2002b; Wang et al., 2003; Woodcock and Harward, 1992).

Therefore, to avoid the above mentioned problems, satellite pixels were assumed to be samples of objects. The investigated area was regarded as a collection of smaller objects namely homogeneous forest polygons. For generating homogeneous forest polygons on the satellite scene, image segmentation (ENVI 3.4.) was used. Image segmentation is a partitioning of an image into segments or polygons. Polygons are defined separately for the three forest types derived from the forest mask. The base image for the segmentation procedure was the NDVI image with a minimum threshold value of 0.45 and maximum threshold value of 0.85 derived from the statistic for every forest type. A set of segmented images was calculated with a set of different threshold values (Table 13).

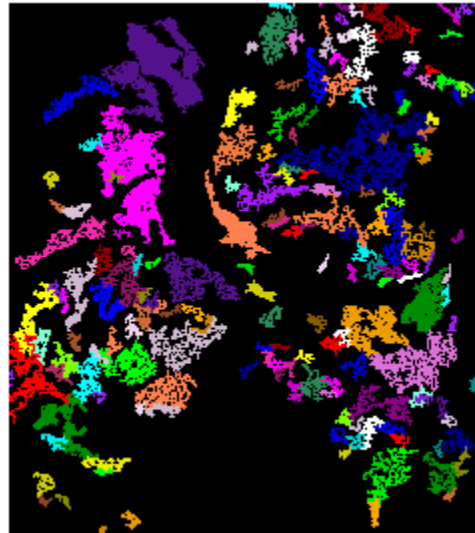| Segment image	NDVI values (min. and max. threshold)
1	0.45 – 0.55
2	0.55 – 0.6
3	0.6 – 0.65
4	0.65 - 0.7
5	0.7 – 0.85

Table 13: Threshold values for image segmentation

Fig. 54: Image segmentation and derivation of forest

As a result, every forest polygon consists of satellite pixels that have similar data feature values (NDVI values) and is associated with the corresponding forest type (Fig. 54). 183 forest polygons were derived: 120 – coniferous forest; 45 – mixed forest; 18 – deciduous forest. All of the created homogeneous forest polygons correspond to test areas on the ground with a different LAI value. Some of the polygons include more than one LAI value. The LAI values were grouped by polygons and the mean LAI value for every polygon was calculated, excluding LAI points located at polygon boundaries. Respectively, the mean vegetation index value was calculated for each forest polygon.

2.2. Correlation with remote sensing data

Polygon by polygon correlation of the mean LAI and vegetation index values was carried out. The relationships were derived for every forest type separately (Fig. 55 and Fig. 56).

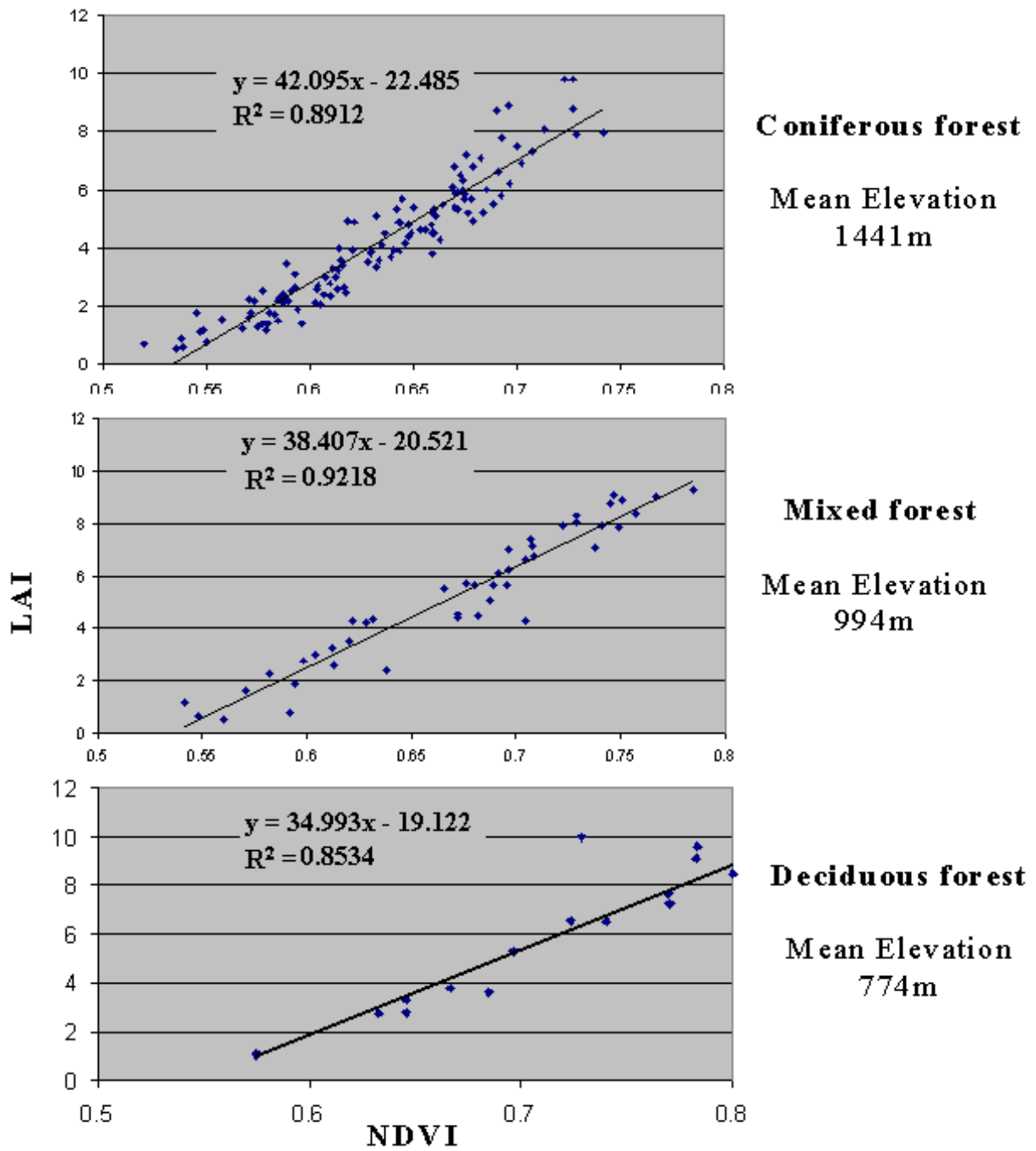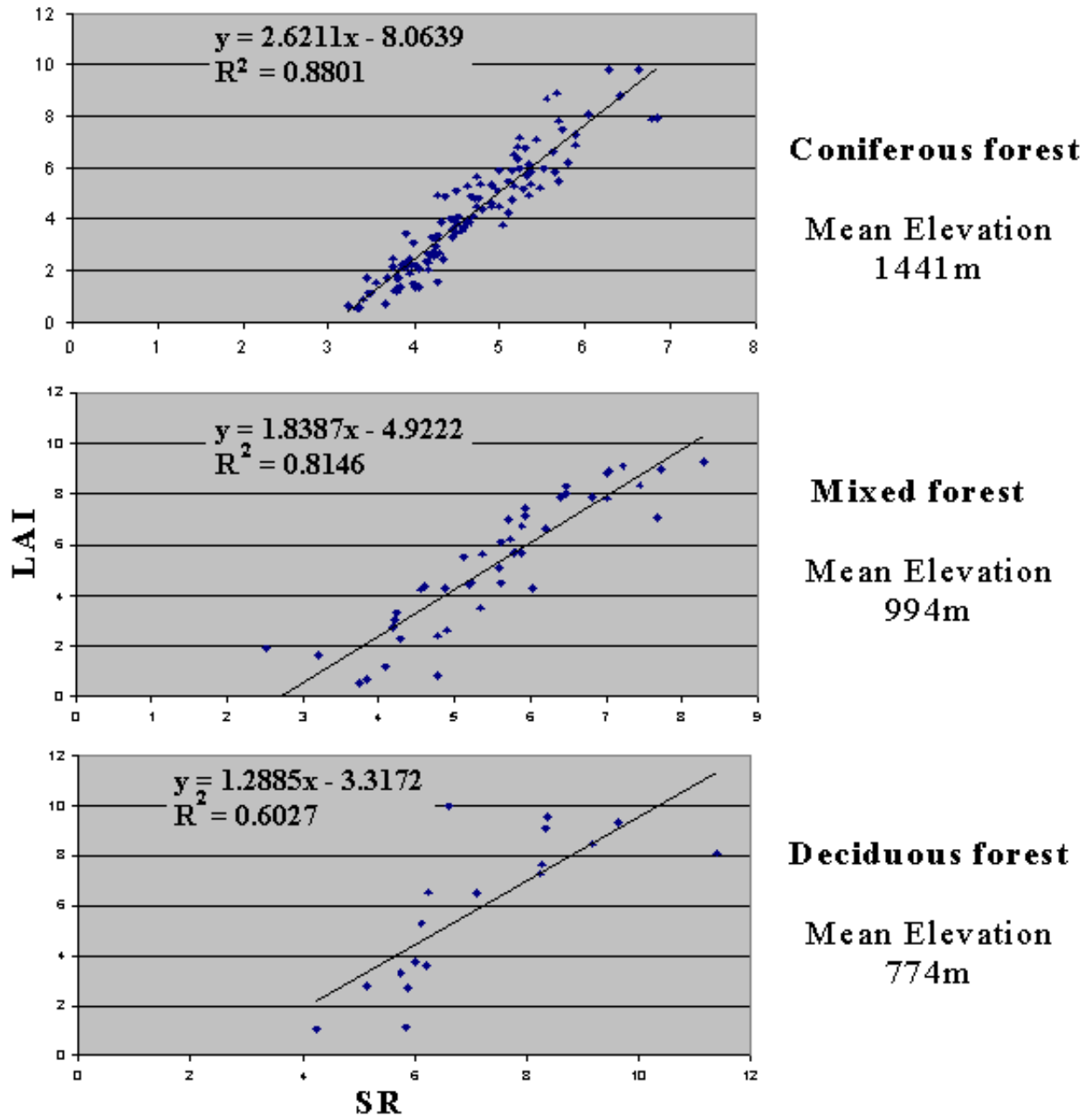**Fig. 55: Correlation LAI/NDVI**

Fig. 56: Correlation LAI/SR

NDVI shows better correlation than the Simple Ratio. Although a good correlation is found between LAI and NDVI the dynamic range in NDVI is small. The mean NDVI values are in the interval 0.45 and 0.85. The range of Simple Ratio is between 3.0 and 9.0. The NDVI relationships were used for derivation of a 30 m resolution LAI map

(*Band Math – ENVI 3.4*). Every forest type was separated in a mask image and the corresponding correlation was applied to the mask image:

Coniferous LAI = (42.095*NDVI) – 22.485

Mixed LAI = (38.407*NDVI) – 20.521

Deciduous LAI = (34.993*NDVI) – 19.122

The fit of the relationship between LAI and NDVI is:

- Coniferous forest R^2=0.89
- Mixed forest R^2=0.92
- Deciduous forest R^2=0.85

The predictive equations of LAI from Simple Ratio in this study are:

Coniferous LAI = (2.6211*SR) – 8.0639

Mixed LAI = (1.8387*SR) – 4.9222

Deciduous LAI = (1.2885*SR) – 3.3172

The fit for SR and LAI is:

- Coniferous forest R^2=0.88
- Mixed forest R^2=0.81
- Deciduous forest R^2=0.61

Then three forest masks were combined in final LAI map and LAI variations are shown (Fig. 57 and Fig. 58).

Coniferous forest shows better correlation results than other two types of vegetation. The reason for this is the higher number of training polygons created for this class. Deciduous

forest covers a small area in the park and just 20 homogeneous polygons were available. When more training sites are available the limitation on the accuracy of this estimate will be smaller.
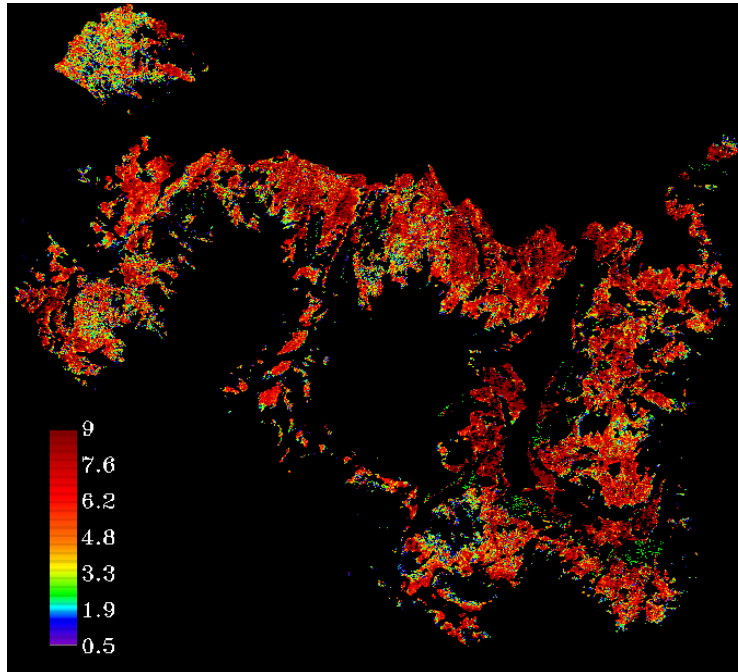

Fig. 57: LAI map derived from Landsat TM data – National Park Berchtesgaden
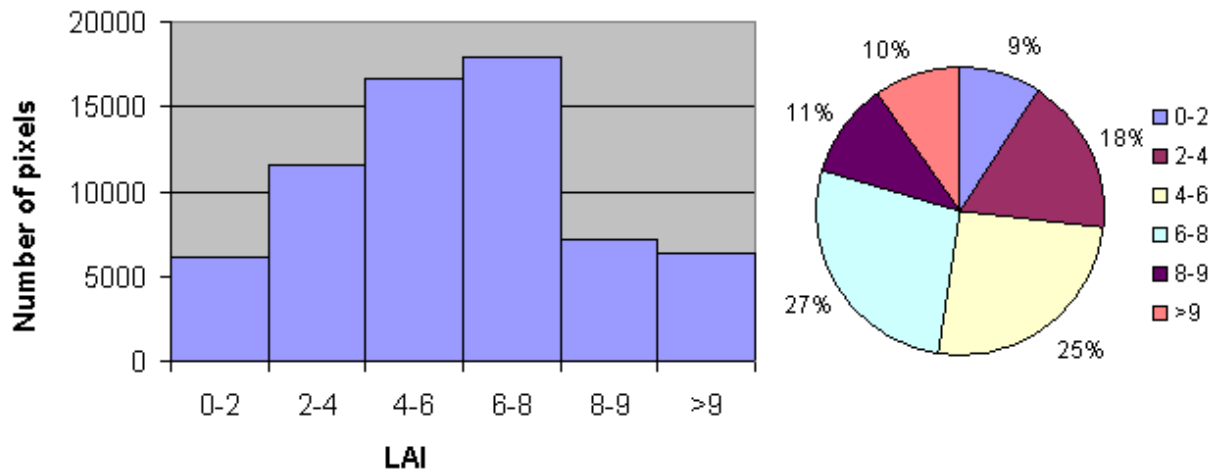

Fig. 58: LAI variations – National Park Berchtesgaden

As seen from the figure above for about 52% of the forest area LAI values vary from 4 to 8. The three forest classes show differences in LAI distribution. Needle forest shows maximum number of pixels with LAI values between 4 and 6. Mixed forest shows maximum number of pixels with LAI between 6 and 8. By deciduous forest, the maximum number of pixels is where the LAI values vary between 8 and 9 or are >9 (Fig. 59).
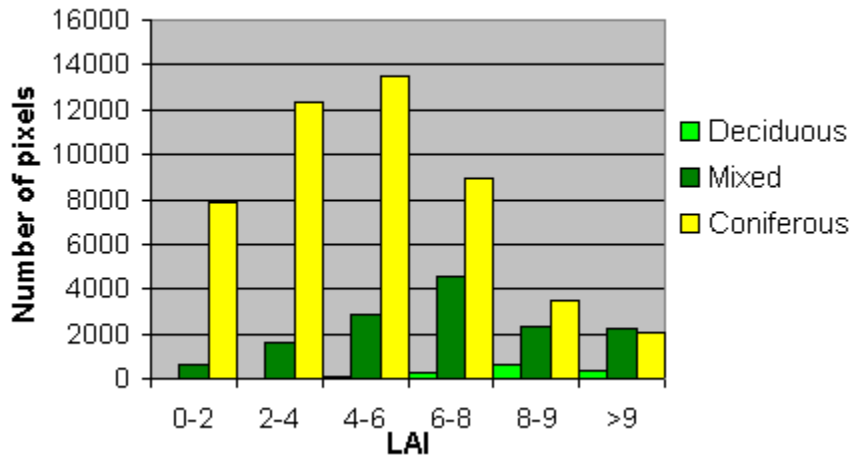
Fig. 59: LAI of deciduous, needle and mixed forest – National Park Berchtesgaden
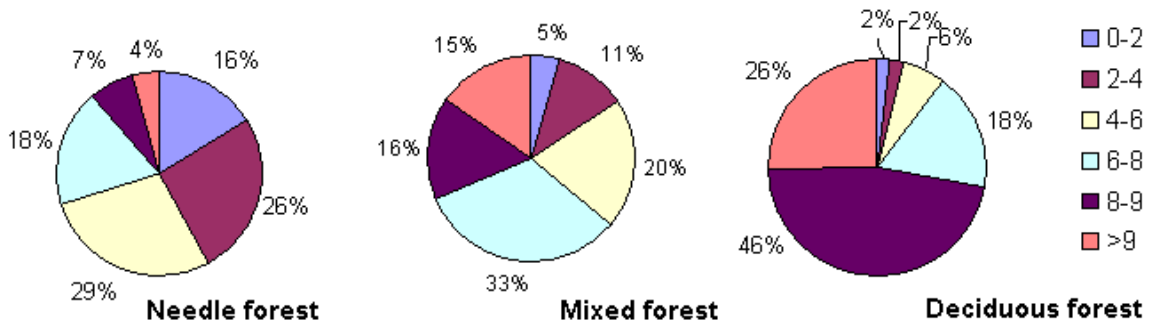
Fig. 60: LAI distribution – National Park Berchtesgaden

As seen from Fig. 60 the LAI values for 29% of needle forest vary between 4 and 6. By mixed forest, 33% of the area that they cover has LAI values between 6-8. LAI values vary between 8-9 for 46% of the deciduous forest area. The LAI values >9 for needle, mixed and deciduous forest are respectively 4%, 15% and 26%. Very small part of the needle forest has high LAI values (>9). Deciduous forests show higher LAI values than

needle and mixed forest. In comparison with needle forest (16%) by mixed and deciduous forest the area with LAI between 0 and 2 is respectively 5% and 2%.

The same correlations were used for extrapolation to Stubai and Ötz valeys in the Alps. Both vegetation indices were calculated for Stubai and Ötz Valleys. LAI maps for both regions were created (Fig. 61).
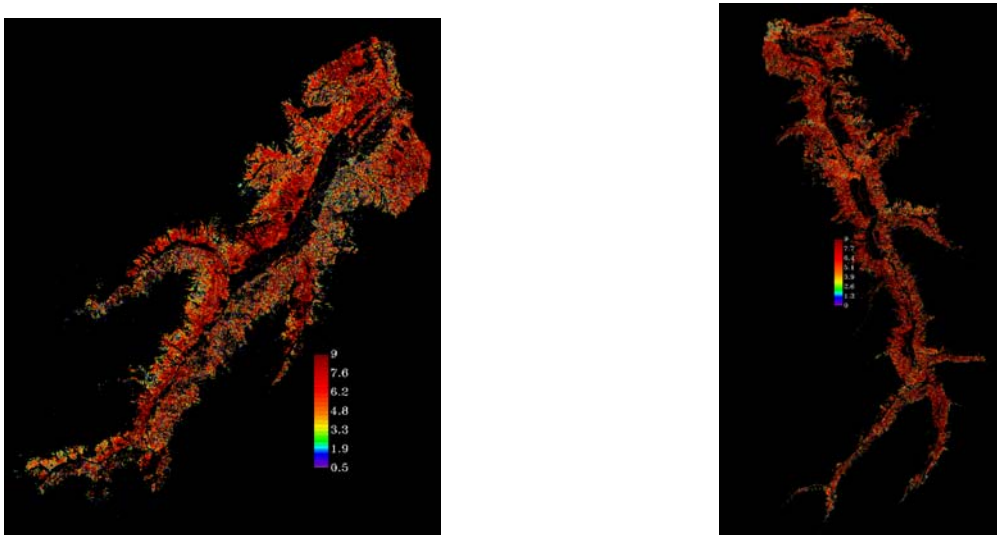
Fig. 61: LAI map derived from Landsat data – Stubai Valley (left) Ötz Valley (right)
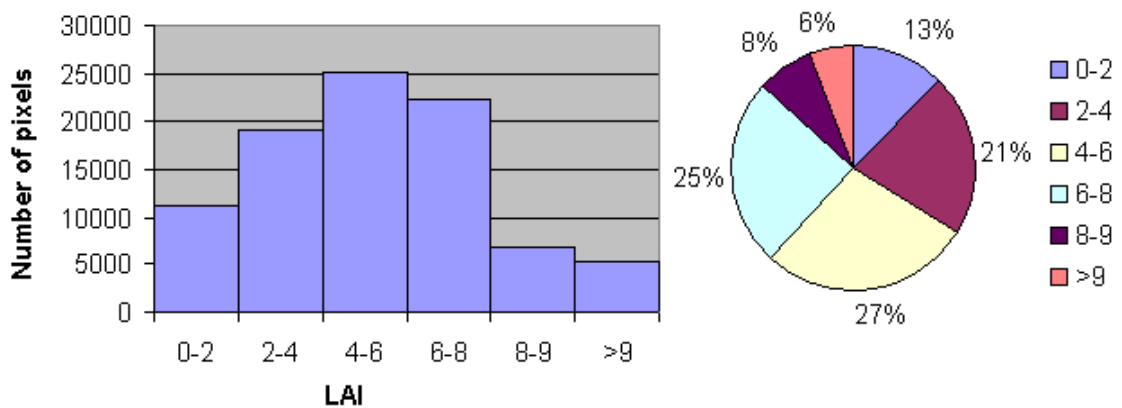
Fig. 62: LAI Variations – Stubai Valley

For 52% of the area LAI values vary between 4 and 8 (Fig. 62). The three forest types show differences in LAI distribution. In Stubai and Ötz Valleys coniferous forest cover

very large area and strongly predominate over other two forest classes. 87% of the forested area is covered by needle forest (Fig. 63).
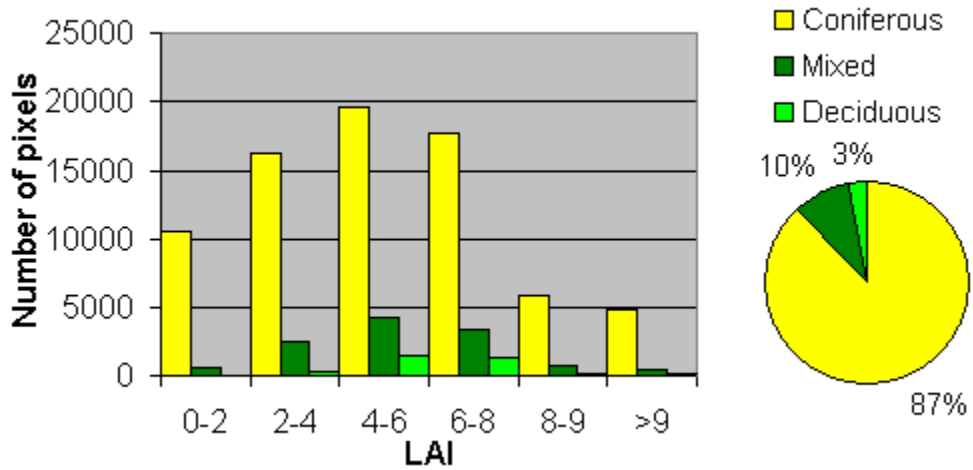
Fig. 63: LAI of deciduous, needle and mixed forest – Stubai Valley
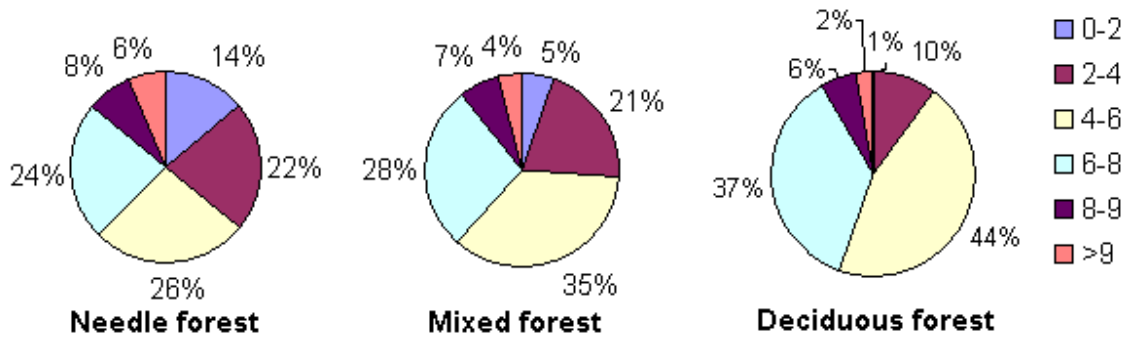
Fig. 64: LAI distribution – Stubai Valley

LAI values between 4 and 6 predominate in all forest types - 26% (needle forest), 35% (mixed forest) and 44% (deciduous forest). Very often LAI values vary between 6 and 8 – 24% (needle forest), 28% (mixed forest), 37% (deciduous forest). 14% of coniferous forest show LAI values between 0 and 2. Mixed and deciduous forests with LAI values between 0 and 2 are not very well represented (5% and 1% respectively) (Fig. 64).
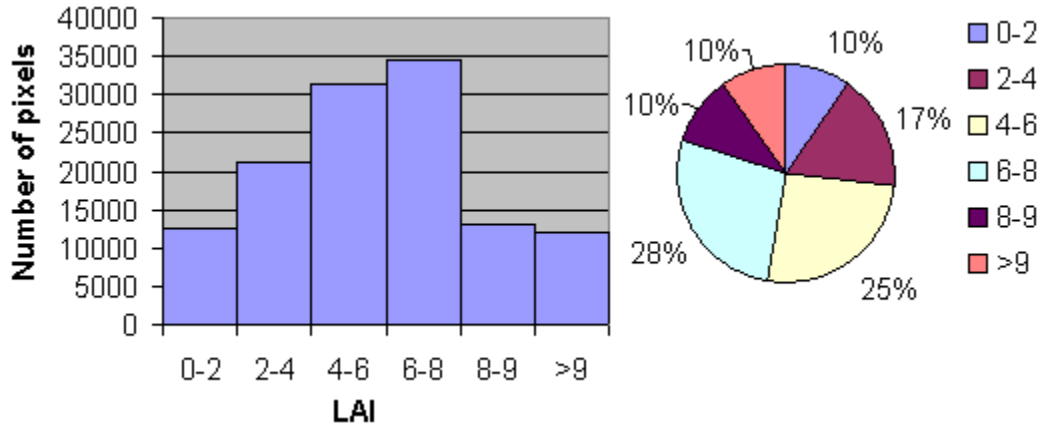
Fig. 65: LAI Variations - Ötz Valley

In comparison with Berchtesgaden and Stubai Valley, LAI values show similar distribution. In Ötz Valley, the most frequently LAI values are also between 4 and 8 (Fig. 65).
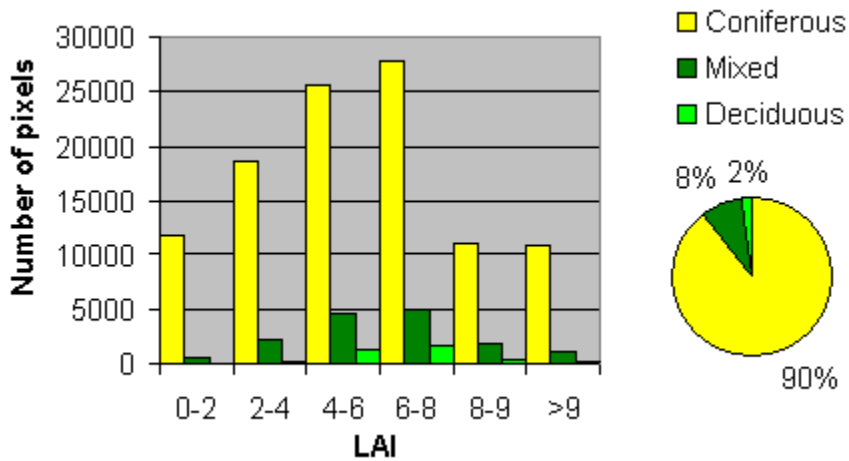
Fig. 66: LAI of deciduous, needle and mixed forest – Ötz Valley

Coniferous forest in Ötz Valley as in Stubai Valley strongly predominates. They cover 90% of the forested area in the Valley. Deciduous forests are not very good presented (2%). Mixed forest covers 8% of the forest area in the Valley (Fig. 66). By all the three forest types most frequently presented LAI values are in the interval 6 to 8 (Fig. 67).
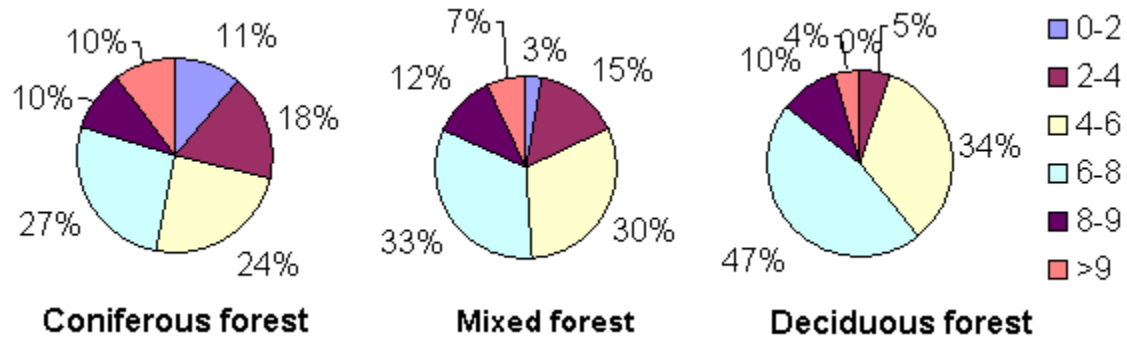
Fig. 67: LAI distribution – Ötz Valley

11% of coniferous forest show LAI values between 0 and 2. Mixed and deciduous forests with LAI values between 0 and 2 are not very well represented (3% and 0.4% respectively).

An effort to validate results was carried out in Stubai Valley. For accuracy assessment of the results, the digital LAI map of Stubai Valley was compared with LAI map derived from allometric relationships in Neustift (part of Stubai Valley). The research was part of ECOMONT and INTERREG II Projects (Fig. 68).

Fig. 68: Neustift-Stubai Valley–Color Composite Image (5, 4 and 3 Landsat bands)

The investigation sites of ECOMONT (Ecological Effects of Land-Use Changes on European Terrestrial Mountain Ecosystems) project are situated in the district Neustift im Stubaital. As a part of INTERREG II Project a forest structure analysis were carried out in Neustift.

Leaf Area Index of the coniferous forest (*Picea abies, Larix decidua*) was derived using allometric relatioships (relating DBH, tree height and leaf area) as derived from forest inventories. The data were stored in a GIS (ArcInfo) and the digital LAI map was available (Fig. 69).
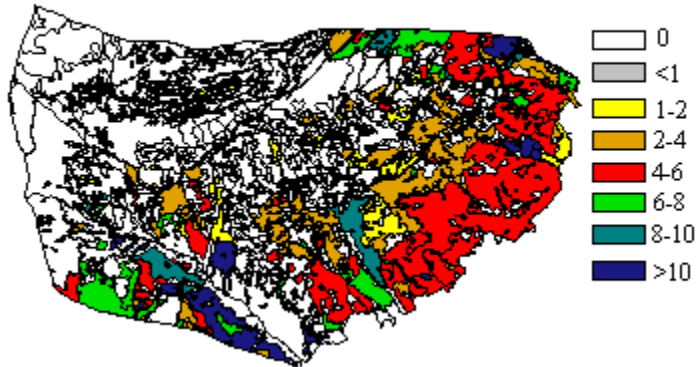
Fig. 69: LAI of needle forest in Neustift (part of Stubai Valley) – *Picea abies, Larix decidua* (after Aschauer M., 2001)

The data were organized in LAI polygons (vector extrapolation in ArcInfo). They were correlated with NDVI derived from Landsat image in Stubai Valley (Fig. 70). The predictive equation of LAI from NDVI for needle forest in Neustift is:

$$LAI = 45.08NDVI - 25.666$$
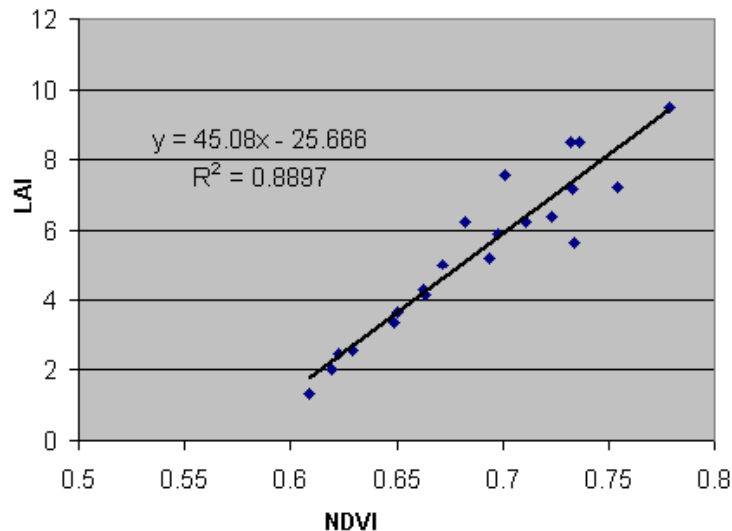
Fig. 70: Correlation LAI/NDVI in Neustift - Stubai Valley

A strong relationship between NDVI and LAI was found. The dynamic range in NDVI is small. The mean NDVI values are in the interval 0.6 and 0.8.

3. Discussion and conclusion

The proposed approach to estimating LAI using Landsat data was demonstrated to be reasonable. The National Park Berchtesgaden was used as a reference test area to derive a land cover map, define forest classes, establish a comparison of Landsat with ground truth data, and to obtain extrapolation relationships for related areas. The number of ground plots with LAI data available in the National Park was the motivation for selecting Berchtesgaden as a representative area for mapping and validation procedures. The number of data points was generally sufficient for each forest cover type (coniferous, mixed and deciduous forest) and the range of ground LAI data was large enough. Because of surface heterogeneity (cover type, density changes), it was necessary to separate the forest into three major cover types: coniferous, mixed and deciduous forest. The choice of NDVI for emphasis in the extrapolation was because NDVI provided a much better correlation with LAI than did SR.

Pixel by pixel comparison was not suitable because of the geolocation (co-registration) error when comparing both maps. The use of forest polygons for correlation between LAI and NDVI reduced registration error between both images. The averaged values of LAI and NDVI for one forest stand are better spatial estimates than provided by the pixel values. This approach leads to better results when comparing remote sensing and ground truth data (Wang Y., et. al., 2002, 2003; Wulder M.A., 1998;).

Coniferous and mixed forests show better correlation results than deciduous forest, which is caused by the number of investigated training polygons – 120 for coniferous-, 43 for mixed- and 18 for deciduous forest. The employed methodology depends on the area covered by every forest type and on the ground truth data available. For coniferous forests the relationships between LAI and NDVI and LAI and SR are essentially linear. There does not appear to be a saturation point at high LAI values (Fig. 55 and Fig. 56). For deciduous forest a linear relationship with the fit of 0.85 was found. Differences in canopy roughness (especially in deciduous forest at the scale of meters) affect the study of forests. These meter-sized shadows are not visible in the Landsat imagery, for which sensor resolution is 30x30m. Band ratios (NDVI, SR) tends to remove such variations in overall brightness (Jensen J.R., 1996). Thus resulting NDVI and SR values should not be affected by small shadows (Aber J., et al., 2002).

If an exponential relationship in the study of deciduous forest is used, a slightly better explanation of the overall data is achieved, while saturation is then predicted at high LAI values (>8) (Fig. 71). More cannot be said from the current data sets. Nevertheless, reflection characteristics exist that allow separation of forest LAI to values as high as 8 to 10.
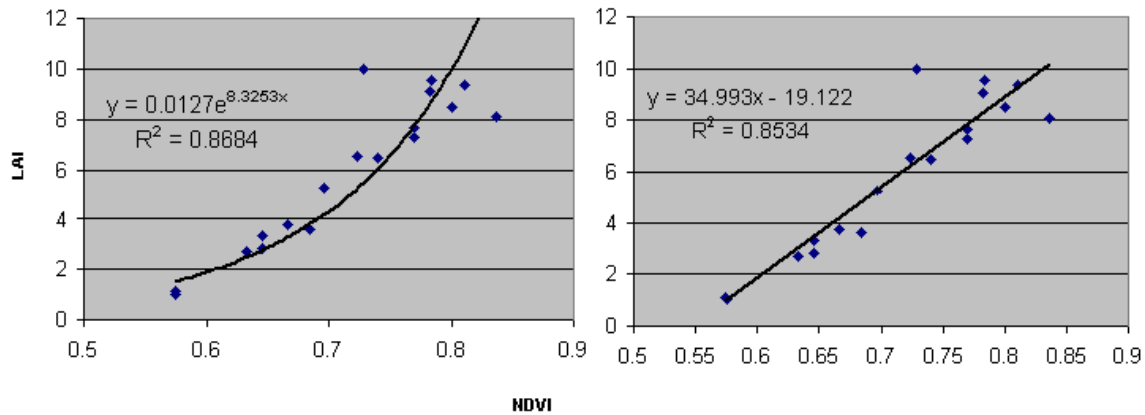
Fig. 71: Correlation LAI/NDVI – deciduous forest (National Park Berchtesgaden)

Results such as these have been reported in some other studies (Chen et. al., 2002). According to the simulations of the 4-scale bidirectional reflection model based on canopy architecture, shadow fractions in the deciduous stands in the red band are less dark than those in coniferous stands. This high red reflectance imposes limits in vegetation indices at high LAI values. (Chen J.M. and Leblanc S., 1997) Mixed forests are the intermediate case between conifer and deciduous and the relationship can also be nonlinear. In this study, an approximately linear relationship was found, which may depend on the percentages in the mixture.

The validation results derived for coniferous forest in Neustift (Stubai Valley) show good correspondence to the results derived in Berchtesgaden (refer to Chapter V, results, correlation with remote sensing data) (Fig. 72).
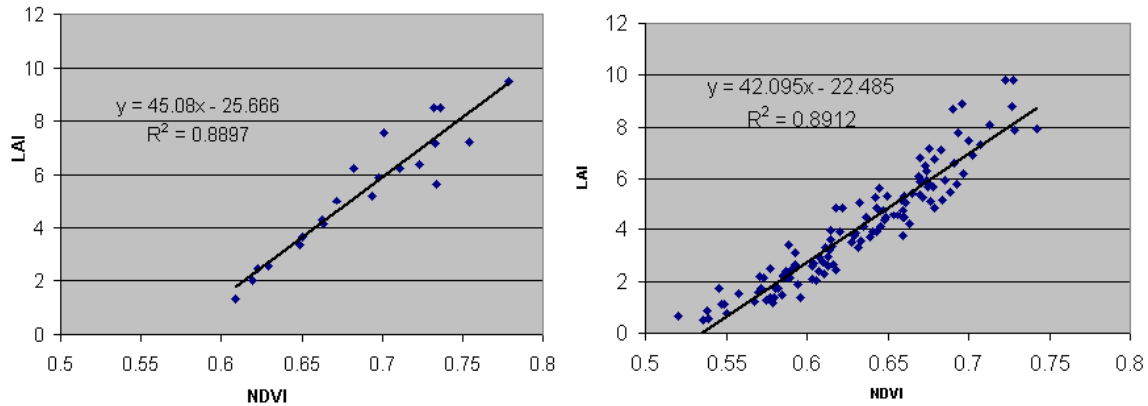
Fig. 72: Correlation LAI/NDVI (needle forest) in Neustift - Stubai Valley (left) and in Berchtesgaden (right)

For both investigated sites, LAI is successfully described with a simple and reasonable correlation with NDVI. Future studies of the forest LAI/NDVI relationship, especially in mountain areas, will require further field investigations of the spatial and temporal distribution of leaf area index. The sample size in Neustift was limited by practical considerations. All the relationships have only been tested on a single Landsat TM scene. Nevertheless, similar correlations were found in other studies, especially for coniferous forests (Wang Y., 2002; Chen and Cihlar, 1996; Running et. al. 1986; Nemani et.al. 1993; Curran et.al. 1992), or for the other forest classes (mixed and deciduous forest) (Fassnacht et.al. 1997; Eklundh L. et.al. 2003; Chen et. al. 2002)(refer toAppendix A).

Because the methodology of deriving digital LAI maps is dependent on vegetation type, it can be applied to images acquired over other areas of interests if they consist of the same vegetation types (e.g. Stubai and Ötz Valleys). This requires a previous study of vegetation distribution and creation of forest type maps. Therefore the derivation of land cover maps was a very important preliminary step in the current study. The major advantage of remote sensing methods is that estimates of LAI for large areas can be done without the need for extensive field measurements, especially in inaccessible or non-investigated regions, where other sources of data are often not available. The European Alps is a good example for such a research region in which logistic and practical problems are of frequent occurrence.

Using further Landsat scenes would allow additional extrapolation to other test areas beyond the Alps where similar conditions exist. Considering the various regression models used to estimate LAI from vegetation indices derived from Landsat data as reported in the literature (refer to Appendix A), however one can see that the regression models are highly site-specific. They depend on climate, physiography, substrates, altitude and vegetation at the investigated sites. Therefore the extrapolation of the results is possible only in regions with similar conditions and vegetation. The regression model can not be generalized to other geographic regions. Caution must even be used in extrapolating results temporally (time period of full leaf out) at the study locations.

VI. CONCLUDING DISCUSSION

<u>Land Cover Classification and Vegetation Interpretation</u>

The production of thematic maps, such as those depicting land cover, using image classification is one of the most common applications of remote sensing. The classification of land cover characteristics is an important aspect in the process of understanding high mountain ecology. Remote sensing data are useful in mapping land cover or for vegetation interpretation in mountainous areas, where accesibility is limited. Classification of remote sensing data in mountainous terrain is difficult because of variations in the sun illumination angle. Spectral classification alone is not sufficient for extracting land cover data. The main reasons are elevation differences, illumination variations and the effect of topographic shadow. In the case of steep or high relief energy areas both land cover and topography determine the spectral values in remote sensing imagery (Dorren K., et al., 2003).

Topographic correction reduced the shadow effect by decreasing the brightness values of surfaces facing the sun and increasing values of surfaces facing away from the sun (Parlow E., 1996a). Using the SWIM model for topographic correction, the topography-controlled illumination effects were reduced (refer to image preprocessing). The improvement of classification results in mountain terrain after correction of topographic effect can be found in several studies of Parlow, as for example, in the testsite Abisko Lappland or in Riviera Valley in the Alps (Parlow, 1996a; Imbery et al., 2001) or in other studies (Dorren, et al., 2003; Itten et al., 1991, 1992a, 1992b, 1995). Therefore, in this study, the correction of the influence of topography was an important and obligatory preliminary step in the analysis. The extrapolation procedure, especially in mountainous terrain, is not possible without correction of these illumination effects. Extrapolations of supervised classification results (spectral signature extrapolation) have previously been tried only in flat terrain (Muller, 1999). Rugged terrain always causes problems in extrapolation procedures. Therefore, the same methods for topographic correction were applied in Stubai and Ötz Valleys as well as using scenes that were obtained at essentially the same time (one day appart).

Another important step in image preprocessing was the atmospheric correction of the satellite scene. It was applied in order to remove the influence of the atmospheric scattering. The integration of field measurements, aerial photos and remote sensing data to create land cover maps and a forest mask was a challenging task in this study. Such data integration leads to better results in land cover classification, and subsequent applications of the information in ecosystem study. The use of reference test data (data set from National Park Berchtesgaden) was a very important point in the definition of test areas used for maximum likelihood classification. The derivation of land cover classes in the reference test area National Park Berchtesgaden was the starting point of this study. The remote sensing map was the basis for extraction of the forest mask used further in LAI estimates from the satellite image. The definition of spectral signatures of the derived classes was also important for extrapolation procedure and for derivation of land cover maps in Stubai and Ötz Valleys.

Extrapolation

A strong relationship was found between regional inventories and remote sensing supervised classification. Forest inventory data measured on the ground were used in combination with a classified image to provide the algorithm for extrapolation from known site information to where similar conditions exist. This technique can assist in focusing survey and field inventory.

A critical point in this study was the identification of the class deciduous forest because the dominant species in Berchtesgaden (*Fagus sylvatica*) and in Stubai and Ötz Valleys (*Alnus viridis*) showed differences in spectral response. This may have been the result of using a scene from September, and in addition that *Fagus sylvatica* and *Alnus viridis* occur at different elevations. Nevertheless, deciduous forest covers a very small area in the investigated sites in comparison with other forest classes. These results are specific to the mountainous region in the Alps, but they may be applicable to other regions where similar condition exists.

Building up a remote sensing dataset for different test areas will be very useful for long-term monitoring of changes in vegetation cover in the Alps. Because satellites provide a

regular return interval for change detection, studies applying extrapolation algorithms for supervised classification or LAI will allow seasonal and annual monitoring.

Accuracy assessment

Exact correspondence between land cover classifications detected by the two survey methods (aerial photography and field survey and remote sensing method) is not to be expected. Despite different methods for defining land cover categories in "ground truth" and remotely sensed maps, the overall accuracy achieved was 86% and 87% in National Park Berchtesgaden and in Stubai Valley, respectively. A remote sensing approach for extrapolating the classification results to the other alpine test areas was valid because: 1) the investigated sites are alpine Valleys where similar condition exist; 2) the imagery available for making the maps are Landsat scenes with just one day difference in the acquisition; 3) the same approaches were used for atmospheric and topographic correction and for supervised classification. Therefore, it is encouraging that the correspondence between remotely-sensed and ground cover maps was as close as in the present study.

Leaf Area Index Variations

Leaf area index is a key variable that describes the amount and potential functioning of vegetation and is required for modeling vegetation productivity (Gower et. al, 1999), land surface climatology (Sellers et. al., 1997), global carbon budgets and agricultural resource management (MacVicar and Jupp, 1998; Prince, 1991). For that reason the need for LAI information over large areas has prompted investigations of the relationship between ground-measured LAI and vegetation indices derived from satellite-measured reflectance. The common approach has been to correlate ground-measured or allometric derived LAI against the Simple Ratio (SR) or the Normalized Difference Vegetation Index (NDVI) (Franklin, 1986; Spanner et al., 1990, Nemani et al., 1993; Chen and Cihlar, 1996; Fassnacht et al., 1997). The proposed empirical approaches to LAI estimates from satellite data have been demonstrated to be reasonable. Although the empirical models are site-specific, similar correlations were found in other studies for

three forest types (coniferous, deciduous and mixed forest). (Wang, 2002; Chen and Cihlar, 1996; Running et. al. 1986; Nemani et.al. 1993; Curran et.al. 1992; Fassnacht et.al. 1997; Eklundh et.al. 2003; Chen et. al. 2002) (refer to Appendix A). For all three forest types close relationships between vegetation indices and LAI were obtained in this study, suggesting that predictive capability can be achieved. Validation requires a new independent data set. Such an effort was carried out in Neustift (Stubai Valley), where the validation results show correspondence with the relationships found for Berchtesgaden. Systematic shifts may relate either to actual differences or more likely to differences in the allometric equations used in upscalling local information to derive the LAI "ground truth" map.

The land cover maps of all investigated sites will be useful for a wide variety of modeling efforts relating vegetation to climate as well as disturbance. They will also be useful for defining regional relationships between alpine vegetation functional types and climate. An important application of land cover and LAI digital maps is in landscape modeling. They can be successfully used for model parameterization in a spatial context Fig. 73).
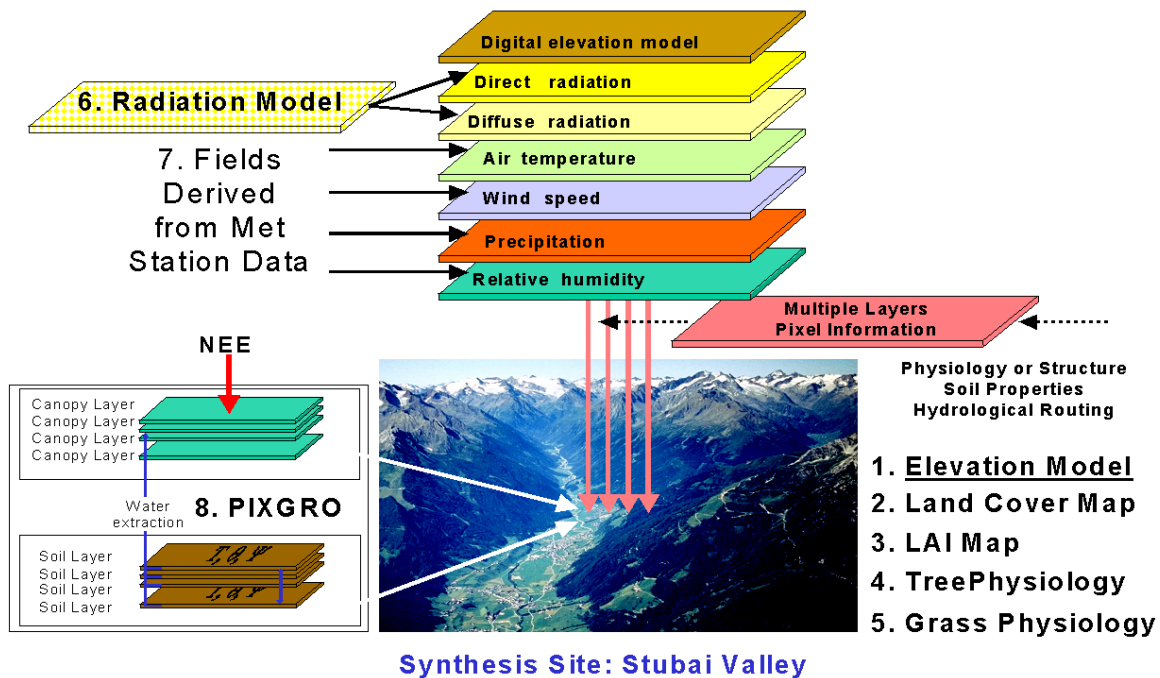
Fig. 73: Landscape model (Tenhunen et al., unpublished) – Stubai Valley test site

The methodology for supervised classification and for extrapolation can be used to develop a standardized classification procedure of land cover types in alpine areas using satellite data. The use of multitemporal satellite images and the ability to consistently apply classification techniques and algorithms of LAI derivation will allow a long term monitoring of vegetation cover, leaf area index, and vegetation change - key elements in the study of Global Change. The strategy can be related to those used by HABITALP Project (Alpine Habitat Diversity) – developing a method for long-term monitoring of protected areas using aerial photographs.

Integration of land cover or LAI maps and information from a digital elevation model allows definition of the distribution of vegetation types along the elevation gradients covering large areas.

For the needs of GLOWA-DANUBE Project the investigated sites can be used as a microscale reference test areas in the study of Global Change within the Upper Danube catchment. For modeling of land surface processes in the Decision-Support System DANUBIA, a proxel-area of 1 km^2 has been used. For that purpose, the data from the current study be upscaled to 1 km scale and used for modeling or other remote sensing data validation (Fig. 74 and Fig. 75).

Fig. 74: Forest LAI map derived from NDVI and subsequently aggregated to 1 km resolution

Fig. 75: Modis tile with LAI at 1 km resolution, coregistered to Landsat scene

A comparison of the MODIS LAI map and LAI map derived from Landsat data and aggregated to MODIS resolution can be done (Fig. 76).
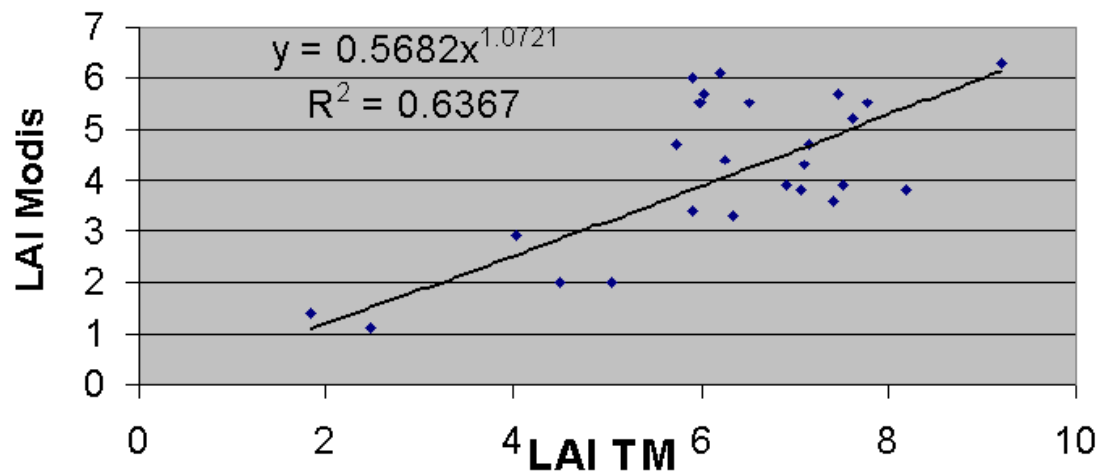
Fig. 76: Correlation between Modis LAI map and Landsat LAI map

In conclusion, the current work should stimulate further research in three different directions: 1) detailed study of land cover changes in the Alps using multitemporal satellite images; 2) further validation of LAI/NDVI (SR) relationships in other test areas or using different data sets; 3) further extrapolation to other test areas in the Alps and accuracy assessment of the results on the base of ground truth maps or field measurements. Further studies in this direction will include not only monitoring of ecosystem changes in spatial pattern but also in spectral one.

VII. SUMMARY

Land cover change is an important element of global environmental change processes. Most ecosystem processes strongly depend on land cover and its attributes. Mapping land cover, especially in mountain terrain is a difficult and challenging task. Remote sensing is an attractive source of thematic maps, such as those depicting land cover. Thematic mapping from remote sensing data is typically based on image classification. The image classification procedure synthesizes satellite data with field data and other ancillary data derived from a Geographic Information System (GIS - ArcInfo) coverage. The present study combines GIS and remote sensing data to produce a land cover map for the National Park Berchtesgaden and to build an extrapolation for other test areas in the Alps (Stubai and Ötz Valleys). Although a vast GIS data set had been assembled for the National Park, remote sensing was not previously used as a tool for land cover mapping and forest ecosystem analysis. For supervised classification, the maximum likelihood algorithm was used to sort and group data into discrete classes, which can be uniquely identified. Comparison and accuracy assessment with „ground truth" data was carried out. An overall accuracy of 86% and 87% of the classification results in the National Park Berchtesgaden and in Stubai Valley, respectively, was achieved.

Another important parameter determining gas exchange (water loss and carbon gain) of alpine forests is Leaf Area Index (LAI). Remote sensing provides a means to estimate LAI over large areas. To map LAI in mountain regions, Landsat TM NDVI index and SR index were examined together with forest inventory data of the Berchtesgaden National Park. "Ground truth" point grid maps for LAI were obtained through the use of allometric relationships (relating tree size and leaf area) as derived from tree harvests and together with the forest inventory database. On the basis of the forest mask derived from land classification and the Landsat vegetation indices, homogeneous forest polygons were identified. They were used for polygon by polygon correlation between LAI and vegetation indices. Mean forest polygon values were used to determine the relationships. With the derived equations, LAI was mapped at 30m resolution (Landsat data). Using the digital elevation model, the distribution of the vegetation types and LAI along elevation gradients was investigated.

The results in National Park Berchtesgaden were further used in an extrapolation to classify land cover in Stubai and Ötz Valleys. Except to detect the distribution of land cover classes, supervised classification was used as a part of the algorithm for predicting forest leaf area index at the investigated sites. The digital LAI map of Stubai Valley was compared with LAI map derived from allometric relationships in Neustift (part of Stubai Valley). A correlation between NDVI and LAI in Neustift was derived. The validation results derived for coniferous forest in Neustift (Stubai Valley) show good correspondence to the results derived in Berchtesgaden. For both investigated sites, leaf area index can successfully be described with simple and reasonable correlation with NDVI.

VIII. DEUTSCHE ZUSAMMENFASSUNG

Landnutzungsänderung ist ein wichtiges Element der globalen Klimaänderungsprozesse, da die meisten Ökosystemprozesse stark von der Landnutzung und von ihren Attributen abhängen. Landnutzung, besonders im Gebirgsgelände, abzubilden ist dabei eine schwierige und lockende Aufgabe. In diesem Zusammenhang ist die Fernerkundung eine attraktive Quelle thematischer Karten. Die thematischen Karten der Fernerkundung basieren gewöhnlich auf der Methode der Bildklassifikation. Das Bildklassifikationsverfahren synthetisiert Satellitendaten mit Felddaten und anderen zusätzlichen Daten, die von Geographischen Informationssystemen (GIS) abgeleitet werden. Die vorliegende Untersuchung kombiniert GIS und Fernerkundung, um Landnutzungskarten für den Nationalpark Berchtesgaden zu produzieren und Nutzungskarten auf andere Testgebiete in den Alpen (Stubaital und Ötztal) zu extrapolieren.

Obwohl eine ausgedehnte GIS Datenbank für den Nationalpark zusammengestellt worden war, wurde die Fernerkundung vorher nicht zur Erstellung von Landnutzungskarten und für die Waldökosystemanalyse verwendet. Während der „supervised classification" wurde der Maximum Likelihood Algorithmus verwendet, um Daten in getrennte Kategorien zu sortieren und zu gruppieren. Ein Vergleich und eine Genauigkeitseinschätzung mit "ground truth" Daten wurden durchgeführt. Es wurde eine gesamte Genauigkeit der Klassifikationresultate von 86% im Nationalpark Berchtesgaden und 87% im Stubaital erzielt.

Ein anderer wichtiger Parameter für den Gasaustausch (Wasserverlust und Kohlenstoffgewinn) der alpinen Wälder ist der Blattflächenindex (LAI). Die Fernerkundung liefert Mittel, den LAI für große Gebiete zu schätzen. Um den LAI in den Gebirgsregionen abzubilden, wurden Landsat TM NDVI-Index und SR-Index zusammen mit Waldinventurdaten des Nationalpark Berchtesgaden überprüft. „Ground truth" Punktrasterdaten für LAI wurden über allometrischen Beziehungen aus Baumernten, die Baumgröße und Blattfläche verknüpfen, und der Waldinventurdatenbank abgeleitet. Mit Hilfe einer Maske, die Koniferen, Mischwald und Laubwald unterscheidet, und die von der Landklassifikation und von den Landsat-Vegetationindizes abgeleitet wurde, wurden

homogene Waldpolygone identifiziert. Auf der Basis dieser Polygone wurde für jeden Waldtyp ein mathematischer Zusammenhang zwischen LAI und Vegetationindex bestimmt. Mit den abgeleiteten Gleichungen wurde der LAI in der Landsat Daten Auflösung (30m) abgebildet. Mittels eines digitalen Geländemodell wurde die Verteilung der Vegetationstypen und des LAI entlang den Höhengradienten untersucht.

Die Resultate im Nationalpark Berchtesgaden wurden in einer weiteren Extrapolation verwendet, um die Landnutzung im gesamten Stubaital und im Ötztal zu klassifizieren. Außer für die Verteilung der Landnutzungsklassen wurde in der Arbeit stets „supervised classification" als Teil des Algorithmus zur Vorhersage des LAI in den Untersuchungsgebieten verwendet. Die digitale LAI-Karte des Stubaital wurde aus allometrischen Beziehungen in Neustift im Stubaital abgeleitet und anhand von „ground truth" Daten validiert. Dafür wurde ein mathematischer Zusammenhang zwischen NDVI und LAI in Neustift wurde abgeleitet. Der Korrelationskoeffizient für Koniferenwald im Neustift (Stubaital) ist ähnlich wie die für Berchtesgaden erhaltenen Werte. Für beide Untersuchungsgebiete konnte der LAI mit einer einfachen Beziehung aus dem NDVI berechnet werden.

IX. REFERENCES

Aber, J.S., Wallace, J. and Nowak, M.C. (2002) Response of forest to climatic events and human management at Fort Leavenworth, Kansas. Kansas Geological Survey, Current Research in Earth Sciences, Bulletin 248, part 1

Albertz, J. (1991) Grundlagen der Interpretation von Luft- und Satellitenbildern. Eine Einführung in die Fernerkundung, Wissenschaftliche Buchgesellschaft (Darmstadt)

Alsheimer, M. (1997) Charakterisierung räumöicher und zeitlicher Heterogenität der Transpiration unterschiedlicher montaner Fichtenbestände (Picea abies (L.) Karst.) durch Xylemflussmessungen. Bitök, Bayreuth

Aschauer M. (2001) Strukturanalyse der Wälder im INTERREG II-Projektgebiet Kaserstattalm (Neustift im Stubaital), Diplomarbeit an der naturwissenschaftlichen Fakultät der Leopold-Franzens-Universität Innsbruck, Institut für Botanik, Abteilung Ökologie

Avery, T. E., and Berlin, L. B. (1992) Fundamentals of remote sensing and airphoto interpretation: New York, Macmillan, 472 p.

Band, L.E., Peterson, D.L., Running, S.W., Dungan, J., Lathrop, R., Coughlan, J., Lammers, L., and Pierce, L.L. (1991) Forest ecosystem processes at the watershed scale: basis for distributed simulation, Ecological Modeling, Vol. 56, pp. 171–196.

Bartelink HH. (1997) Allometric relationships for biomass and leaf area of beech (*Fagus sylvatica L.*) Ann Sci for 54: 39-50

Bebi, P., Kienast, F., Schönenberger, W. (2001) Assessing structures in mountain forests as a basis for investigating the forests dynamics and protective function. Forest ecology and management, special issue on structure of mountain forests 145, 1-2: 3-14.

Bonan, G.B. (1995) Land-atmospheric interactions for climate system models: coupling biophysical, biogeochemical and ecosystem dynamical processes, Remote Sensing of Environment, Vol. 51, pp. 57–73.

Bonan, G.B. (1993) Importance of leaf area index and forest type when estimating photosynthesis in boreal forests. Remote Sensing of Environment, Vol. 43, pp. 303–314.

Bundesamt für Naturschutz (1995) Systematik der Biotoptypen- und Nutzungstypenkartierung (Kartieranleitung). Schriftenreihe für Landschaftspflege und Naturschutz, Heft 45

Burger H. (1939) Kronenaufbau gleichartiger Nadelholzbestände. Mitt. Schweiz.Anst.f.d. forstl. Versuchswesen 21, 5-56

Burger H. (1942) Holz, Blattmenge und Zuwachs. V. Mitteilung: Fichten und Föhren verschiedener Herkunft auf verschiedenen Kulturorten. Mitt. Schweiz.Anst.f.d. forstl. Versuchswesen 22, 10-62

Burger H. (1945) Holz, Blattmenge und Zuwachs – Die Buche. Mitt. Schweiz.Anst.f.d. forstl. Versuchswesen 26: 419-468

Burger H. (1953) Holz, Blattmenge und Zuwachs. XIII. Mitteilung: Fichten im gleichaltrigen Hochwald. Mitt. Schweiz. Anst. f. d. forstl. Versuchswesen 29, 38-130

Cayrol, P., Chehbouni, A., Kergoat, L., Dedieu, G., Mordelet, P., and Nouvellon, Y. (2000) Grassland modeling and monitoring with SPOT4 VEGETATION instrument during the 1999 SALSA experiment, Agricultural and Forest Meteorology, Vol. 105, No.1-3, pp. 91–115.

Cernusca, A., M. Bahn, Chemini C., Grabe W., Siegwolf R., Tappeiner U., Tenhunen J. (1998)"ECOMONT: a combined approach of field measurements and process-based modelling for assessing effects of land-use changes in mountain landscapes." Ecological Modelling 113(1-3): 167-178.

Cernusca, A., Tappeiner U. and Bayfield N. (Eds.) (1999) Land-use changes in European Mountain Ecosystems, Blackwell Wissenschafts-Verlag, Berlin, Wien etc.

Chapin, F. S., E. S. Zavaleta, V. T. Eviner, R. L. Naylor, P. M. Vitousek, H. L. Reynolds, D. U. Hooper, S. Lavorel, O. E. Sala, S. E. Hobbie, M. C. Mack, and S. Díaz. (2000) Consequences of Changing Biodiversity, Nature 405:234-242.

Chavez, P. S. (1988) An Improved Dark-Object Subtraction Technique for Atmospheric Scattering Correction of Multispectral Data. Remote Sensing of Environment 24:459-479.

Chen J.M. and Cihlar J. (1996) Retrieving leaf area index of boreal conifer forests using Landsat TM images, Remote Sensing of Environment 55, pp. 153–162.

Chen, J. M., G. Pavlic , L. Brown, J. Cihlar, S.G. Leblanc, H. P. White, R. J. Hall, D. Peddle, D.J. King, J. A. Trofymow, E. Swift, J. Van der Sanden, and P. Pellikka (2002) Derivation and Validation of Canada-wide coarse-resolution leaf area index maps using high-resolution satellite imagery and ground measurements. Remote Sensing of Environment 80:165-184

Chen, J. M. and Leblanc S. (1997) A 4-scale bidirectional reflection model based on canopy architecture, IEEE Transactions on Geoscience and Remote Sensing, 35:1316-1337.

Cherrill A.J., McClean C., Fuller RM (1995) A comparison of land cover types recognised in an ecological field survey of Northern England and in the first remotely sensed Land Cover Map of Great Britain, Biological Conservation, 71: 313-323

Cihlar J. (1999) A new methodology of land cover mapping, International Journal of Remote Sensing, Vol. 20, pp. 1457-1459

Cihlar J. (2000) Land cover mapping of large areas from satellites: status and research priorities, International Journal of Remote Sensing, Vol. 21, pp. 1093-1114

Cihlar J., B. Guindon, J. Beaubien, R. Latifovic, D. Peddle, M. Wulder, R. Fernandes, and J. Kerr (2003a) From the need to product: a methodology for completing a land cover map of Canada with Landsat data, Can. J. Remote Sensing, Vol. 29, No. 2, pp. 171-186

Cihlar J., R. Latifovic, J. Beaubien, B. Guindon, and M. Palmer (2003b) Thematic mapper (TM) based accuracy assessment of a land cover product for Canada derived from SPOT VEGETATION (VGT) data, Can. J. Remote Sensing, Vol. 29, No. 2, pp. 154–170

Congalton R.G. (1991) A review of assessing the accuracy of classification of remotely sensed data. Remote Sensing of Environment 37:35-46

Congalton R.G. (1996) Accuracy Assessment: A Critical Component of Land Cover Mapping Gap Analysis: A landscape approach to biodiversity planning, American Society for Photogrammetry and Remote Sensing, p. 119 – 131

Congalton R. G. (1999a) Sampling Issues for Assessing the Accuracy of Remotely Sensed Data, 4th Annual GLOBE Conference, University of New Hampshire, July 18-23, 1999

Congalton R. G. and K. Green (1999b) Assessing the accuracy of remotely sensed data: Principles and practices, Lewis Publishers, Boca Raton

Coops, N.C., Waring, R.H., and Landsberg, J.J. (2001) Estimation of potential forest productivity across the Oregon transect using satellite data and monthly weather records, International Journal of Remote Sensing, Vol. 22, No. 18, pp. 3797–3812

Curran, P. J., Dungan, J. L., Gholz H. L. (1992) Seasonal LAI in slash pine estimated with Landsat TM, Remote Sensing of the Environment, 39, 3-13.

Cushnie, J. L. (1987) The interactive effect of spatial resolution and degree of internal variability within land-cover types on classification accuracies. International Journal of Remote Sensing, 8(1), 15– 29.

DeFries, R., Hansen, M., Townshend, J. R. G. and Sohlberg, R. (1998) Global land cover classifications at 8 km spatial resolution: The use of training data derived from Landsat imagery in decision tree classifiers, International Journal of Remote Sensing; 19 (16): 3141-3168

Dickinson, R.E. (1995) Land processes in climate models, Remote Sensing of the Environment, 51:1:27-38.

Dorren, L. K., Maier B., Seijmonsbergen, A.C. (2003) Improved Landsat-based forest mapping in steep mountainous terrain using object-based classification, Forest Ecology and Management, V. 183, 31-46pp.

Estes, J. E., E. J. Hajic, and L. R. Tinney (1983) Fundamentals of image analysis: Analysis of visible and thermal infrared data, In Manual of Remote Sensing, R. N. Colwell, (editor) American Society of Photogrammetry 1:987-1124.

Eklundh, L., Harrie, L., and Kuusk, A. (2001) Investigating relationships between Landsat ETM+ sensor data and leaf area index in a boreal conifer forest, Remote Sensing of Environment, 78(3): 239-251

Eklundh, L., Hall K., Eriksson H., Ardö J., Pilesjö P. (2003) Investigating the use of Landsat thematic mapper data for estimation of forest leaf area index in southern Sweden, Canadian Journal of remote Sensing, Vol.29, No3, pp. 349-362

ENVI User's Guide (2000) Version 3.4, Research Systems Inc.

ERDAS, Inc., Atlanta, GA. ERDAS Field Guide (1994)

EURIMAGE, Products and Services (2001) Multi-mission satellite data, Eurimage S.p.A., Italy

Falge, E., Tenhunen, J., Baldocchi, D., Aubinet, M., Bakwin, P., Berbigier, P., Bernhofer, C., Bonnefond, J-M., Burba, G., Clement, R., Davis, J.D., Elbers, J.A., Falk, M., Goldstein, A.H., Grelle, A., Granier, A., Grünwald, T., Gudmundsson, J., Hollinger, D., Janssens, I.A., Keronen, P., Kowalski, A.S., Katul, G., Law, B.E., Malhi, Y., Meyers, T., Monson, R.K., Moors, E., Munger, J.W., Oechel, W., Paw, U., Pilegaard, K., Rannik, Ü., Rebmann, C., Suyker, A., Thorgeirsson, H., Tirone, G., Turnipseed, A., Wilson, K. & Wofsy, S. (2002a)Phase and amplitude of ecosystem carbon release and uptake potentials as derived from FLUXNET measurements. Agricultural and Forest Meteorology 113: 75-95.

Falge, E., Baldocchi, D., Tenhunen, J., Aubinet, M., Bakwin, P., Berbigier, P., Bernhofer, C., Burba, G., Clement, R., Davis, J.D., Elbers, J.A., Goldstein, A.H., Grelle, A., Granier, A. Gudmundsson, J., Hollinger, D., Kowalski, A.S., Katul, G., Law, B.E., Malhi, Y., Meyers, T., Monson, R.K., Munger, J.W., Oechel, W., Paw, U., Pilegaard, K., Rannik, Ü., Rebmann, C., Suyker, A., Valentini, R. & Wofsy, S. (2002b) Seasonality of ecosystem respiration and gross primary production as derived from FLUXNET measurements. Agricultural and Forest Meteorology 113: 53-74.

Fassnacht K., S. Gower, M. MacKenzie, E. Nordheim and T. Lillesand (1997) Estimating the leaf area index of north central Wisconsin forests using the Landsat Thematic Mapper. Remote Sensing of Environment 61, pp. 229–245

Friedl, M.A. and C.E. Brodley (1997) Decision tree classification of land cover from remotely sensed data, Remote Sensing of Environment, vol. 61, pp. 399-409.

Foody, G.M. (2002) Status of land cover classification accuracy assessment, Remote Sensing of Environment 80, 185-201

Franklin, J. (1986) Thematic Mapper Analysis of Coniferous Forest Structure and Composition, International Journal of Remote Sensing. Vol. 7. No. 10. pp. 1287-1301.

Frank, A.B. (2002) Carbon dioxide fluxes over a grazed prairie and seeded pasture in the Northern Great Plains, Environmental Pollution, Vol. 116, No. 3, pp. 397–403.

Franz H. (2000) Landscape monitoring using infrared aerial photos, EUROPARC Expertise Exchange, Topical Workshop: Organisation of Monitoring in Protected Areas, April 12 - 16

Fung, T. and E. LeDrew (1988) The determination of optimal threshold levels for change detection using various accuracy indices, American Society for Photogrammetry and Remote Sensing. 54(10): 1449-1454.

Gemmell, F.M. (1995) Effects of Forest Cover, Terrain, and Scale on Timber Volume Estimation with Thematic Mapper Data in a Rocky Mountain Site, Remote Sensing of Envirnonment, Vol. 51, pp. 291–305.

Grime, J.P. (1993) Vegetation functional classification systems as approaches to predicting and quantifying global vegetation change. In: Solomon, A.M., Shugart, H.H. (Eds.), Vegetation Dynamics and Global Change, Chapman & Hall, London, pp. 293–305.

Gower, S. T., Kucharik, C. J., and Norman, J. M. (1999) Direct and indirect estimation of leaf area index, fAPAR and net primary production of terrestrial ecosystems. Remote Sens. Environ., 70:29-51

Hall, F.G., J.R. Townshend, E.T. Engman (1995) Status of Remote Sensing Algorithms for Estimation of Land Surface State Parameters, Remote Sensing of Environment, vol. 51, no. 1, pp. 138-156.

Hall R.J., D.P. Davidson, and D.R. Peddle (2003) Ground and remote estimation of leaf area index in Rocky Mountain forest stands, Kananaskis, Alberta, Can. J. Remote Sensing, Vol. 29, No. 3, pp. 411–427

Hansen, M., DeFries, R., Townshend, J. R. G. and Sohlberg, R. (2000) Global land cover classification at 1km resolution using a decision tree classifier, International Journal of Remote Sensing. 21: 1331-1365

Hoffer, R.M. (1978) Biological and physical considerations in applying computer-aided analysis techniques to remote sensor data. In: Remote sensing: The quantitative approach. (eds.) Swain, P. H., and Davis S.M. McGraw- Hill Inc., pp. 227-289.

Imbery F., E.Parlow, and R.Vogt (2001) Satellite-based land-use classification of the MAP-Riviera area, MAP-meeting 2001, Poster presentation

Itten, K.I.; Meyer, P.; Kellenberger, T.; Leu, R.; Sandmeier, St.; Bitter, P.; Seidel, K. (1991) Assessment of the impact of topography on remote sensing forest mapping of alpine regions; Final Report ESA Study Nr. 90/ E56, Zurich , pp. 48

Itten, K.I.; Meyer, P.; Kellenberger, T.; Sandmeier, St.; Leu, R.; Bitter, P. ; Seidel, K. (1992a) Assessment and Correction of the Impact of Topography and Atmosphere on Remote Sensing Forest Mapping of Alpine Regions; European ISY Conference, Munich, ESA ISY-1, pp. 1369-1372

Itten, K.I.; Meyer, P.; Kellenberger, T.; Leu, R.; Sandmeier, St.; Bitter, P.; Seidel, K. (1992b) Correction of the Impact of Topography and Atmosphere on Landsat - TM Forest Mapping of Alpine Regions; Remote Sensing Series Vol. 18, Geographisches Institut der Universität Zürich, pp. 50

Itten, K.I., P. Meyer, T. Kellenberger, R. Leu, St. Sandmeier, P. Bitter and K. Seidel (1995) Digital Forest Mapping of Alpine Regions - Correction of the Impact of Topography and Atmosphere; in: Beckel, L.: Satellite Remote Sensing Forest Atlas of Europe, Justus Perthes Gotha, pp. 60 - 61

Jensen, J. R. (1996) Introductory Digital Image Processing: A Remote Sensing Perspective (2nd. Ed.), Prentice Hall, Englewood Cliffs, NJ, 316-318p.

Jensen, J.R. (2000) Remote Sensing of the Environment - An Earth Resource Perspective, 544 pp., Prentice Hall, Upper Saddle River, NJ

Johnson, R.L. (2000) Airborne remote sensing of forest leaf area index in mountainous terrain. M.A. thesis, Department of Geography, University of Lethbridge, Lethbridge, Alta.

Kalliola R. and Syrjänen K. (1991) To what extent are vegetation types visible in satellite imagery? Ann Bot Fenn 28: 45–57.

Kerner, H. F., Spandau, L. & J. G. Kiöppel (1991) Methoden zur angewandten Ökosystemforschung, entwickelt im MaB-Projekt 6 ”Ökosystemforschung Berchtesgaden”. Abschlussbericht, herausgegeben von der Projektsteuereungsgruppe. MaB - Mitteilungen 35.

Kerr J. T., Ostrovsky M. (2003) From space to species: ecological applications for remote sensing. Trends in ecology and Evolution, Review, Article in Press, Elsevier

Keuchel J., S. Naumann, M. Heiler, A. Siegmund (2003) Automatic Land Cover Analysis for Tenerife by Supervised Classification using Remotely Sensed Data Remote Sensing of Environment, Vol. 84(4), pp. 530-541.

Khorram S. (Ed.) (1999) Accuracy assessment of remote sensing-derived change detection, American Society for Photogrammetry and Remote Sensing, Bethesda, MD

Kias U., Demel W., Reiter K., Richter C.H. (1994) Ökosystemforschung Berchtesgaden, Nachführung von digitalisierten räumlichen Daten im Nationalpark Berchtesgaden, Bericht über den Projektzeitraum August 1993 bis März 1994. Nationalpark Berchtesgaden Berchtesgaden

Kias U., Demel W., Reiter K., Richter C.H. (1996) Ökosystemforschung Berchtesgaden - Nachführung von digitalisierten räumlichen Daten im Nationalpark Berchtesgaden - Schlußbericht August. Nationalparkverwaltung Berchtesgaden

Kias, U., Demel, W., Funck, W., Schäfer D. and E. Rausch (1999) Erstellung eines Orthophotokataloges und Nachführung der Biotop- und Nutzungstypen für das Biosphärenreservat Berchtesgaden. Ein Forschungsvorhaben am Landschaftsinformatikzentrum der Fachhochschule Weihenstephan im Auftrag der Nationalparkverwaltung Berchtesgaden.

Kilian, W., Müller, F. and F. Starlinger (1994) Die forstlichen Wuchsgebiete Österreichs. Eine Naturraumgliederung nach waldökologischen Gesichtspunkten. FBVA-Bericht Nr. 83, Forstliche Bundesversuchsanstalt Wien, 60 S.

Konnert, V. (2000) Gemeinsame Auswertung der ersten und zweiten permanenten Stichproben-Inventur.-Forschungsbericht 43, Nationalpark Berchtesgaden: 3 - 92.

Konnert, V. (2001) Mapping site characteristics in the National Park Berhtesgaden – Project in coorperation with Technical University of Munich, Dept. of Ecology,

the Faculty of Forest Science and Resource Management, Dept. of Geobotany (Prof. Dr. Anton Fischer), and the Administration of the National Park Berchtesgaden

Körner, C. (1994) Scaling from species to vegetation: the usefulness of functional groups. In: Schulze, E.-D., Mooney, H.A. (Eds.), Biodiversity and Ecosystem Function. Springer, New York, pp. 117–140.

Küchler W.A. and I.S. Zonneveld, eds (1988) Vegetation mapping. Kluwer Academic, Norwell, MA

Liang, S., H. Fang, J. Morisette, M. Chen, C. Walthall, C. Daughtry, and C. Shuey (2001) Atmospheric Correction of Landsat ETM+ Land Surface Imagery: II. Validation and Applications, IEEE Transactions on Geosciences and Remote Sensing

Lillesand, T. M. and R. W. Kiefer. (2000) Remote Sensing and Image Interpretation. Wiley & Sons, New York

Liu, J., Chen, J.M., Cihlar, J., and Park, W.M. (1997) A process-based boreal ecosystem productivity simulator using remote sensing inputs. Remote Sensing of Environment, Vol. 62, pp. 158–175.

Loveland TR, Belward A.S. (1997) The IGBP-DIS global 1 km land-cover data set, DISCOVER-first results. Int. J. Remote Sensing 18, 3291-3295.

Loveland, T.R., J.W. Merchant, J.F. Brown, D.O. Ohlen, B. Reed and P. Olsen (1995) Seasonal Land Cover Regions of the United States, Annals of the Association of American Geographers. 85: 339-355.

Loveland, T., B. Reed, J. Brown, D. Ohlen, Z. Zhu, L. Yang and J. Merchant (2000) Development of a Global Land Cover Characteristics Database and IGBP DISCover from 1-km AVHRR Data. International Journal of Remote Sensing, 21: 1303-1330.

Lunetta, R.S., Iiames, J., Knight, J., Congalton, R.G. and Mace, T.H. (2001) An assessment of reference data variability using a "virtual field reference database", Photogrammetric Engineering and Remote Sensing 63, pp. 707–715.

MacVicar, T. R., and Jupp, D. L. B. (1998) The current and potential operational use of remote sensing to aid decision on drought exceptional circumstances in Australia: a review. Agric. Systems, 57(3): 299-468

Maingi J. K., Marsh St. E., Kepner W. G., Edmonds C. M. (2002) An Accuracy Assessment of 1992 Landsat-MSS Derived Land Cover for the Upper San Pedro Watershed (U.S./Mexico), EPA/600/R-02/040, June 2002

Marcus, W.A., Legleiter, Carl J., Aspinall, R.J., Boardman, J.W., and Crabtree R.L. (2003) In Press, High spatial resolution, hyperspectral (HSRH) mapping of in-stream habitats, depths, and woody debris mountain streams: Geomorphology.

Mauser, W., Tenhunen, J.D., Schneider, K., Ludwig, R., Stolz, R., Geyer, R., and E. Falge (2001) Remote Sensing, GIS and Modelling: Assessing Spatially Distributed Water, Carbon, and Nutrient Balances in the Ammer River Catchment in Southern Bavaria. In: J. Tenhunen, R. Lenz, and R. Hantschel (eds), Ecosystem Approaches to Landscape Management in Central Europe, Ecological Studies, Springer Verlag, Heidelberg, pp.583-619.

Myneni, R. B., and Williams, D. L. (1994) On the relationship between FAPAR and NDVI. Remote Sens. Environ., 49:200-211.

Muller, S. V., Racoviteanu, A. E., and Walker, D. A. (1999) Landsat MSS-derived land-cover map of northern Alaska: extrapolation methods and a comparison with photo-interpreted and AVHRR-derived maps. International Journal of Remote Sensing 20 (15&16): 2921-2946

Nemani, R., Pierce, L., Running, S., and Band, L.E. (1993) Forest Ecosystem Processes at the Watershed Scale: Sensitivity to Remotely-Sensed Leaf Area Index Measurements, International Journal of Remote Sensing, 14:2519-2534.

Nouvellon, Y., Rambal, S., Lo Seen, D., Moran, M.S., Lhomme, J.P., Bégué, A., Chehbouni, A.G., and Kerr, Y. (2000) Modelling of daily fluxes of water and carbon from shortgrass steppes, Agricultural and Forest Meteorology, Vol. 100, No. 2-3, pp. 137–153.

Parlow E. (1986) Landschaftsökologische Inhalte von Landsat-TM Aufnahmen. In: W. Endlicher and H. Goßmann, Editors, Fernerkundung und Raumanalyse: Klimatologische und Landschaftsökologische Auswertung von Fernerkundungsdaten, Wichmann-Verlag, Karlsruhe, pp. 129–145.

Parlow, E. (1991) Einstrahlungskorrekturen - eine Anwendung für digitale Geländemodelle in der Satellitenfernerkundung. Freiburger Geographische Hefte, H. 34, 1991, S. 111- 118.

Parlow, E. (1996a) Correction of Terrain Controlled Illumination Effects in Satellite Data, In: Parlow, E.: Progress in Environmental Remote Sensing Research and Applications, Balkema Rotterdam, S. 139-145.

Parlow, E. (1996b) Determination and intercomparison of radiation fluxes and net radiation using Landsat-TM data of Liefdefjorden/NW-Spitsbergen. ESA SP 391, P. 27 - 32

Peddle, D.R., Hall, F.G., and LeDrew, E.F. (1999) Spectral mixture analysis and geometric optical reflectance modeling of boreal forest biophysical structure. Remote Sensing of Environment, Vol. 67, pp. 288–297.

Peddle, D.R., and Johnson, R.L. (2000) Spectral mixture analysis of airborne remote sensing imagery for improved prediction of leaf area index in mountainous terrain, Kananaskis, Alberta. Canadian Journal of Remote Sensing, Vol. 26, pp. 176–187.

Pellinen P. (1986) Biomasseuntersuchungen im Kalkbuchenwald. Ph.D. Dissertation, Universität Göttingen

Peterson, D. L., Spanner, M. A., Running, R. W. and Band, L. (1987) Relationship of thematic mapper simulator data to leaf area index of temperate coniferous forest. Remote Sens. Environment, 22:323-341.

Pfeffer K., Theo W.J. van Asch, Peter A. Burrough, Andrea G. Fabbri (2000) Integration of modeling approaches in the assessment of environmental impact of ski pistes in alpine areas, 4th International Conference on Integrating GIS and Environmental Modeling (GIS/EM4): Problems, Prospects and Research Needs. Banff, Alberta, Canada, September 2 - 8

Prince, S. D. (1991) Satellite remote sensing of primary production: comparison of results for Sahelian grassland 1981-1988. . Int. J. Remote Sens., 12:1301-1311.

Richards J.A. (1994) Remote Sensing Digital Image Analysis, Springer-Verlag, Berlin, p. 340.

Rosenfield, G.H. and K. Fitzpatrick-Lins (1986) A coefficient of agreement as a measure of thematic classification accuracy, Photogrammetric Engineering and Remote Sensing, 52(2), pp. 223-227.

Running S.W., Peterson, D.L., Spanner, M.A. and Teuber, K.B. (1986) Remote Sensing of coniferous forest leaf area, Ecology, 67, pp. 273-276.

Running, S. and J. C. Coughlan (1988) A general model of forest ecosystem processes for regional applications: I. Hydrologic balance, canopy gas exchange and primary production processes. Ecological Modeling 42:125–154.

Running, S. W. and S. T. Gower (1991) FOREST-BGC, A general model of forest ecosystem processes for regional applications. II. Dynamic carbon allocation and nitrogen budgets. Tree Physiology 9, 147-160.

Running, S.W. (1992) A bottom-up evolution of terrestrial ecosystem modeling theory; and ideas toward global vegetation modeling. Pp 263-280. In: Modeling the Earth System. D. Ojima (ed.)Univ. Corp for Atmospheric Research, Office for Interdisciplinary Earth Studies, Global Change Institute Vol 3. Boulder, CO.

Running, S.W., and Hunt, E.R. (1993) Generalization of a forest ecosystem process model for other biomes, BIOME-BGC, and an application for global-scale models. In Scaling physiological processes: leaf to globe. Edited by J. Ehleringer. Academic Press, New York. pp. 141–158. 29 041.

Running S.W., Hunt E. R., Nemani R., Glassy J. (1994) MODIS LAI (leaf area index) and FPAR (fraction photosyntheticalyy active radiation), MODIS algorithm document, NASA, 19pp.

Sabins, F. F. (1986) Remote Sensing: Principles and Interpretation. Freeman, San Francisco, CA, 449pp.

Schowengerdt, R.A. (1983) Digital image classification, chapter 3 of Techniques for image processing and classification in remote sensing: Academic Press, Orlando, Florida, p. 129-207.

Sellers, P.J., Mintz, Y., Sud, Y.C., and Dalcher, A. (1986) A simple biosphere model (SiB) for use within general circulation models. Atmospheric Science, Vol. 43, No. 505–531.

Sellers, P. (1991a) Canopy reflectance, photosynthesis and transpiration. International Journal of Remote Sensing 6:1335–1372.

Sellers, P. (1991b) Modeling and observing land-surface-atmosphere interactions on large scales. Surveys of Geophysics 12:85–114

Sellers, P.J. and Schimel, D. (1993) Remote sensing of the land biosphere and biochemistry in the EOS era: science priorities, methods and implementation - EOS land biosphere and biogeochemical panels. Global and Planetary Change, Vol.7. 279-297.

Sellers, P.J., S.O. Los, C.J. Tucker, C.O. Justice, D.A. Dazlich, G.J. Collatz, and D.A. Randall (1994) A global 1 deg. x 1 deg. NDVI data set for climate studies. Part 2: The generation of global fields of terrestrial biophysical parameters from the NDVI. I. J. Remote Sensing. 15:7:3519-3545.

Sellers, P. J., Randall D. A., Betts A. K., Hall F. G., Berry J. A.,Collatz G. J., Denning A. S., Mooney H. A., Nobre C. A., Sato N., Field C. B., Henderson-sellers A.(1997) Modeling the exchanges of energy, water, and carbon between continents and the atmosphere. Science, 275:502-509.

Singhroy, V.H. (1992) Remote sensing in global geoscience processes: Introductory remarks. Episodes 15:3-6.

Shrestha D.B. and J Alfred Zinck (2001) Land use classification in mountainous areas: integration of image processing, digital elevation data and field knowledge (application to Nepal), International Journal of Applied Earth Observation and Geoinformation, Volume 3, Issue 1, 2001, Pages 78-85

Smith, T.M., Shugart, H.H., Woodward, F.I. (Eds.) (1997) Plant Functional Types. Cambridge University Press, New York.

Solomon, A.M., Shugart, H.H. (Eds.) (1993) Vegetation Dynamics and Global Change. Chapman & Hall, New York, pp. 338

Spanner, M.A., L.L. Pierce, D.L. Peterson and S.W. Running (1990) Remote sensing of temperate coniferous forest leaf area index. The influence of canopy closure, understory vegetation and background reflectance, International Journal of Remote Sensing, 11, pp. 95-111.

Stolz, R., Strasser, G. and Mauser W. (1999) A knowledge based multisensoral and multitemporal approach for landuse classification in rugged terrain using LANDSAT TM and ERS SAR. SPIE Proceeding Series, 3868, pp. 195-206

Storch M. (1993) Untersuchung der Waldvegetation im Nationalpark Berchtesgaden, Nationalpark Berchtesgaden. FEG 202

Strahler, A., J. Townshend, D. Muchoney, J. Borak, M. Friedl, S. Gopal A. Hyman, A. Moody and E. Lambin. (1996) MODIS Land Cover and Land-Cover Change Algorithm Theoretical Basis Document (ATBD), Version 4.1. Boston: Boston University, 102 pp.

Swain, P. H. and Davis, S. M. (1978) Remote Sensing: The Quantitative Approach. McGraw-Hill, New York, 396 pp.

Tenhunen, J.D., R. Siegwolf, and S.F. Oberbauer (1994) Effects of phenology, physiology, and gradients in community composition, structure, and microclimate on tundra ecosystem CO2 exchange. In: E.-D. Schulze and M.M. Caldwell (eds), Ecophysiology of Photosynthesis, Springer Verlag, Ecological Studies Series, Vol. 100, Heidelberg, pp 431-460

Tenhunen, J.D. (1999) Model hierarchies for relating vegetation structure, ecosystem physiology, and plant community distribution to landscape water use. In: A. Cernusca, U. Tappeiner, and N. Bayfield (eds.), Land-Use Changes in European Mountain Ecosystems. Blackwell Wissenschafts-Verlag, Berlin, pp 199-204.

Tian, Y., Woodcock, C. E., Wang, Y., Privette, J. L., Shabanov, N. V., Zhou, L., Zhang, Y., Buermann, W., Dong, J., Veikkanen, B., Häme, T., Ozdogan, M., Knyazikhin, Y., and Myneni, R. B. (2002) Multiscale Analysis and Validation of the MODIS LAI Product. I. Uncertainty Assessment. Remote Sens. Environ., 83:414-430.

Tian, Y., Woodcock, C. E., Wang, Y., Privette, J. L., Shabanov, N. V., Zhou, L., Zhang, Y., Buermann, W., Dong, J., Veikkanen, B., Häme, T., Ozdogan, M., Knyazikhin, Y., and Myneni, R. B. (2002) Multiscale Analysis and Validation of the MODIS LAI Product. II. Sampling Strategy. Remote Sens. Environ., 83:431-441

Townshend, J. R. G., C. Justice, W. Li, C. Gurney, and J. McManus (1991) Global land cover classification by remote sensing: Present capabilities and future possibilities. Remote Sensing of Environment 35:243–255.

Tucker, C. J., and Sellers, P. J., 1986, Satellite remote sensing of primary production. Int. J. Remote Sens., 7:1395-1416.

Tueller P. T. (1989) Remote sensing technology for rangeland management applications, Journal of range management 42(6)

Turner, D.P., W.B. Cohen, R.E. Kennedy, K.S. Fassnacht, and J.M. Briggs (1999) Relationships between leaf area index and Landsat TM spectral vegetation indices across three temperate zone sites. Remote Sensing of Environment 70:52-68.

UN-ECE/FAO (2000) Forest Resources of Europe, CIS, North America, Australia, Japan and New Zealand (industrialized temperate/boreal countries). UN-ECE/FAO Contribution to the Global Forest Resources Assessment 2000. Geneva Timber and Forest Study Papers, No. 17, United Nations, New York and Geneva

Verbyla, D.L. and T.O. Hammond (1995) Conservative bias in classification accuracy assessment due to pixel-by-pixel of classified images with reference grids. International Journal of Remote Sensing, 16: 581-587.

Verma, S. B., Sellers, P. J., Walthall, C. L., Hall, F. G., Kim, J., and Goetz, S. J. (1993) Photosynthesis and stomatal conductance related to reflectance on the canopy scale.Remote Sens. Environ., 44:103-116.

Wang Y. (2002) Assessment of the MODIS LAI and FPAR Algorithm: Retrieval Quality, Theoretical Basis and Validation, PhD Dissertation, Apr 2002., Boston University, Climate and Vegetation research group.

Wang Y., Curtis E. Woodcock, Wolfgang Buermann, Pauline Stenberg, Pekka Voipio, Heikki Smolander, Tuomas Häme, Yuhong Tian, Jiannan Hu, Yuri Knyazikhin, Ranga B. Myneni (2003) Validation of the MODIS LAI product in coniferous forests of Ruokolahti, Finland. Remote Sens. Environ. (submitted June 2003).

Waring, R.H., and Running, S.W. (2000) Forest ecosystems analysis at multiple scales. 2nd ed. Academic Press, Seattle, Wash.

White J., S. Running, R. Nemani, R. Keane and K. Ryan (1997) Measurement and remote sensing of LAI in Rocky Mountain montane ecosystems. Canadian Journal of Forest Research 27, pp. 1714–1727.

Woodcock, C. E., & Harward, V. J. (1992) Nested-hierarchical scene models and image segmentation. International Journal of Remote Sensing, 13(16), 3167– 3187.

Wulder, M. A. (1998) The prediction of leaf area index from forest polygons decomposed through the integration of remote sensing, GIS, UNIX, and C, Computers & Geosciences, vol. 24, N° 2, pp. 151 - 157.

Woodward, F.I., Kelly, C.K. (1997) Plant functional types: towards a definition by environmental constraints. In: Smith, T.M., Shugart, H.H., Woodward, F.I. (Eds.), Plant Functional Types. Cambridge University Press, New York, pp. 47–65.

Yamagata Y. (1997) "Advanced Remote Sensing Techniques for Monitoring Complex Ecosystems: Spectral Indices, Unmixing, and Classification of Wetlands" Phd thesis, University of Tokyo

Zeller, V., Bahn, M., Aichner, M., Tappeiner, U. (2000) Impact of land-use change on nitrogen mineralization in the Southern Alps. In: Biol. Fertil. Soils 31 p. 441-448

Zeller, V., Bardgett, R.D., Tappeiner, U. (2001) Site and management effects on soil microbial properties of subalpine meadows: a study of land abandonment along a north-south gradient in the European Alps. In: Soil Biology. & Biochemistry 33, p.639-649

Zhou, Q., Robson, M. and Pilesjo, P. (1998) On the ground estimation of vegetation cover in Australian rangelands. International Journal of Remote Sensing 19, pp. 1815–1820.

Zhu, Z., Yang, L., Stehman, S., and Czaplewski, R. (1999) Designing an accuracy assessment for USGS regional land cover mapping program: (In review) Photogrammetric Engineering and Remote Sensing.

Appendix A

The folowing relationships reported in literature relate to correlation between forest leaf area index (LAI) and vegetation indices derived from Landsat TM data (Table 14).

Table 14: LAI/NDVI or SR relationships found in literature

LAI/NDVI (SR) relationship (Landsat satellite data)	R^2	Author
NDVI= 0.0377LAI+0.607	0.72	Fassnacht et al. (1997)
SR= 0.9357LAI+3.552 0.71	0.71	Fassnacht et al. (1997)
SR=1.92LAI$^{0.583}$	0.91	Peterson et al. (1987)
SR=1.92+0.532LAI	0.83	Peterson et al. (1987)
NDVI=0.032LAI+0.635	0.42	Chen and Cihlar, (1996)
SR=1.014LAI+3.637	0.49	Chen and Cihlar, (1996)
SR=1.153LAI+2.56	0.66	Chen et. al. (2002)
LAI=33.99NDVI-14.21	0.75	Curran et. al. (1992)
SR=0.614LAI+1.23	0.82	Running et. al. (1986)
NDVI=0.03LAI+0.6	0.32	Nemani et. al. (1993)
LAI=13.26NDVI-8.2822	0.75	Wang Y., et. al., (2002)
LAI=0.5368SR-2.2025	0.81	Wang Y., et. al., (2002)
SR=8.20+1.039LAI	0.66	Eklundh L. et al., (2003)
LAI=1.2565SR+0.069	0.74	White J.D., (1997)
LAI=0.2273e$^{4.9721(ndvi)}$	0.9	White J.D., (1997)

Appendix B

The reference biotope map, based on CIR – images was reclassified and the names of the original land-cover categories were also changed to reflect the dominant plant growth forms at the study site. The land use categories were combined and organized into a new map with 7 distinct classes corresponding to the training areas for satellite-based land cover classes (Table 15).

Table 15: Combining „ground truth" classes for comparison with remote sensing supervised classification

"Ground truth" classes	Combined classes
Bach	Water
Fluss	Water
Wehr, Sohlabsturz	Unclassified
Uferbereich, Verlandungsbereich von Fliessgewaessern, Ufergehoelz/Weidengebuesch	Water
Auenstillgewaesser/Altwasser	Water
Kleine Stillgewaesser	Water
Fischteiche, intensiv genutzt	Water
temporaeres Stillgewaesser	Water
groessere Stillgewaesser	Water
groessere Stillgewaesser, strukturarm	Water
Ufer- und Verlandungsbereich von Stillgewaessern	Water
Hoch- (Regen)moor oder Uebergangsmoor	Water
Nieder-(Flach)moor, Anmoor, Sumpf (gehoelzfrei)	Water
Großseggen-Ried	Unclassified
Anbauflaeche	Grassland

Ackerland mit Sonderkulturen, Enzian	Grassland
Wiesen und Weiden, Grünland, Streuwiese	Grassland
Wiesen und Weiden, (Grünland), Maehweide mittlerer Intensitaet	Grassland
Wiesen und Weiden, (Grünland), Maehweide starker Intensitaet	Grassland
Wiesen und Weiden, (Grünland), Dauerweide	Grassland
Wiesen und Weiden, (Grünland), Maehweide mittlerer Intensitaet mit Skibetrieb	Grassland
Wiesen und Weiden, (Grünland), extensiv bewirtschaftete Maehweide, Weide mit Skibetrieb	Grassland
Wiesen und Weiden, (Grünland), Magerrasen, u.a. auf Buckelwiesen	Grassland
Wiesen und Weiden, (Grünland), beweidete Buckelwiese	Grassland
Wiesen und Weiden, (Grünland), Hutung	Grassland
Wiesen und Weiden, (Grünland), extensiv bewirtschaftete Wiese, Maehweide	Grassland
Wiesen und Weiden, (Gruenland), Schafweide	Grassland
Trockenes/Mageres Gruenland	Grassland
Trockenes/Mageres Gruenland, zugleich Skipiste	Grassland
Weideflaeche,stark veraendert/Laegerfluren	Grassland
Grünlandbrachen	Grassland
Erwerbsgartenbau	Grassland

Hochstaudenflur des alpinen und subalpinen Bereichs	Rocks
Fels- und Schotterrasen	Rocks
Kiesbank/Sandbank	Rocks
Steinriegel, freistehende Mauer, Stuetzmauer	Unclassified
Zwergstrauchheide	Grassland
Schuttflur ohne Bewuchs	Rocks
Schuttflur mit Bewuchs	Rocks
Schuttflur mit Bewuchs, Latsche	Rocks
Fels/Steilwand mit Bewuchs, Bäume	Rocks
Fels/Steilwand mit Bewuchs, Bäume	Rocks
Fels/Steilwand mit Bewuchs, Bäume	Rocks
Fels/Steilwand mit Bewuchs, Bäume	Rocks
Fels/Steilwand mit Bewuchs, Bäume	Rocks
Gletscher	Unclassified
Firnfeld	Unclassified
Feldhecke	Unclassified
Feldgehoelz	Unclassified
Gebüsch, Strauchgruppe, Weide	Grassland
Gebüsch, Strauchgruppe, Grünerle	Deciduous forest
Gebüsch, Strauchgruppe, Latsche	Needle forest
Gebüsch, Strauchgruppe, Latsche	Needle forest
Baumreihe	Mixed forest
Baumgruppe, Laubholz-Reinbestand	Deciduous forest
Baumgruppe, Nadelholz-Reinbestand	Needle forest
Baumgruppe, Mischbestand Laubdominanz	Mixed forest
Baumgruppe, Mischbestand, Nadeldominanz	Mixed forest
Baumgruppe, Laubmischbestand	Deciduous forest

Baumgruppe, Nadelmischbestand	Needle forest
Laubwald	Deciduous forest
Mischwald Laub-Nadel	Mixed forest
Mischwald Laub-Nadel	Mixed forest
Mischwald Laub-Nadel	Mixed forest
Mischwald Laub-Nadel, Aufforstung	Mixed forest
Wald, Jungwuchs (Aufforstung)	Mixed forest
Wald, Mittelwaelder (Ober- und Unterholz)	Mixed forest
Laubwald, Reinbestand	Deciduous forest
Laubwald, Reinbestand	Deciduous forest
Laubwald, Reinbestand, Dickung	Deciduous forest
Nadelwald, Reinbestand	Needle forest
Nadelwald, Reinbestand	Needle forest
Nadelwald, Reinbestand, Fichte	Needle forest
Nadelwald, Reinbestand, Kiefer	Needle forest
Nadelwald, Reinbestand, Laerche	Needle forest
Nadelwald, Reinbestand, Laerche	Needle forest
Nadelwald, Reinbestand, Dickung	Needle forest
Mischwald, Laub-Nadel, (Laubholz dominant)	Mixed forest
Mischwald, Laub-Nadel, (Laubholz dominant)	Mixed forest
Mischwald, Laub-Nadel, (Laubholz dominant)	Mixed forest
Mischwald, Laub-Nadel, (Laubholz dominant), Edellaubholz	Mixed forest
Mischwald, Nadel-Laub, (Nadelholz dominant)	Mixed forest
Mischwald, Nadel-Laub, (Nadelholz dominant)	Mixed forest

Mischwald, Nadel-Laub, (Nadelholz dominant)	Mixed forest
Mischwald, Nadel-Laub, (Nadelholz dominant), Kiefer	Mixed forest
Laubmischwald	Deciduous forest
Laubmischwald	Deciduous forest
Laubmischwald	Deciduous forest
Laubmischwald	Deciduous forest
Laubmischwald, Dickung	Deciduous forest
Nadelmischwald	Needle forest
Nadelmischwald	Needle forest
Nadelmischwald	Needle forest
Nadelmischwald	Needle forest
Nadelmischwald, Fichte, Laerche, Fichte dominant	Needle forest
Nadelmischwald	Needle forest
Nadelmischwald, Zirben, Laerchen, Zirben dominant	Needle forest
Nadelmischwald, Laerchen, Zirben, Laerchen dominant	Needle forest
Nadelmischwald, Laerche dominant, andere Nadelart: Latsche	Needle forest
Nadelmischwald, Dickung	Needle forest
Kahlschlag-, Windwurf-, Schneebruchfläche	Rocks
Schadfläche	Unclassified
Waldrand im engeren Sinne	Grassland
Kiesgrube	Rocks
Steinbruch	Rocks
Aufschüttungsflächen	Rocks

Recyclinghof	Unclassified
Wasserbehälter	Unclassified
Kläranlage	Unclassified
Sonstige Ver- und Entsorgungsflächen für Fernwärme	Unclassified
niedrige, offene Bauweise,ohne/mit Gehoelz	Unclassified
niedrige, offene Bauweise,ohne/mit Gehoelz	Unclassified
niedrige, offene Bauweise,ohne/mit Gehoelz	Unclassified
niedrige, geschlossene Bauweise	Unclassified
niedrige, geschlossene Bauweise	Unclassified
niedrige, geschlossene Bauweise	Unclassified
niedrige, geschlossene Bauweise	Unclassified
hohe, geschlossene Bauweise	Unclassified
Flächen mit gemischter Nutzung, ländliche Prägung, mit Gehölz	Unclassified
Flächen mit gemischter Nutzung, ländliche Prägung, mit Gehölz	Unclassified
Einzelgebäude und -anwesen, mit Gehölz	Unclassified
Einzelgebäude und -anwesen, mit Gehölz	Unclassified
Einzelgebäude und -anwesen, ohne Gehölz	Unclassified
Industrie- und Gewerbeflächen	Unclassified
andere Gewerbeflächen	Unclassified
Flächen mit besonderer baulicher Prägung	Unclassified
Land-/Hauptstrasse	Rocks
Parkplaetze, Wiese	Grassland
Parkplätze, Wiese, Versiegelungsgrad gering	Grassland

Parkplätze, Wiese, Versiegelungsgrad gering	Grassland
Parkplätze, Bitumen, Asphalt, Versiegelungsgrad hoch	Rocks
Parkplätze, Bitumen, Asphalt, Versiegelungsgrad mässig hoch, Teilversiegelung	Rocks
Bahngelände	Unclassified
Schiffverkehrsflächen	Unclassified
Verkehrsbegleitgrün	Grassland
Fußgaengerflächen	Unclassified
Seilbahnanlage	Unclassified
Park- und Grünanlage, Freizeitpark	Grassland
Sportplatz	Grassland
Bolzplatz	Grassland
Minigolfplatz	Grassland
Sporthalle	Unclassified
Reitplatz	Grassland
sonstiger Sportplatz	Grassland
Golfplatz	Grassland
Skipiste	Grassland
Stadion	Grassland
Zeltplatz, Campingplatz	Grassland
Freibad	Grassland
Friedhof	Unclassified

Appendix C

The initial map, based on CIR – images and created for investigating land-use changes in European Terrestrial Mountain Ecosystems (as a part of ECOMONT project) was reclassified and the names of the original land-cover categories were also changed to reflect the dominant plant growth forms at the study site. The land use categories were combined and organized in a new map with 6 distinct corresponding to the training areas for satellite-based land cover classes (Table 16).

Table 16: Combining „ground truth" classes for comparison with remote sensing supervised classification

"Ground truth" classes	Combined classes
See	Water
Kies- und Schotterbank	Rocks
Latschen	Needle forest
Nadelwald der subalpinen Stufe	Needle forest
Nadelwald der montanen Stufe	Needle forest
Grünerlengebüsch	Deciduous forest
Naß- und Feuchtwälder	Deciduous forest
Mischbestand: Feuchtwald-Nadelwald	Mixed forest
Laubwald	Deciduous forest
Laub-Nadel-Mischwald	Mixed forest
Gletscher, oder permanentes Schneefeld	Snow
Felslebensraum des Hochgebirges	Rocks
Felslebensraum der planaren bis subalpinen Stufe	Rocks
Blockhalden oder Schuttflurgesellschaften des Hochgebirges	Rocks
Blockhalden oder Schuttflurgesellschaften der planaren bis subalpinen Stufe	Rocks
Natürliche alpine Rasen	Grassland
Verbrachte Wiesen und Weiden	Grassland
extensiv genutztes Grasland	Grassland
mäßig intensiv bewirtschaftetes Grünland	Grassland
intensiv genutztes Wirtschaftsgrünland	Grassland
Wiese/ Weide	Grassland
Siedlungsraum	Grassland
Parkplätze	Rocks

ACKNOWLEDGEMENTS